

**An Evaluation of the Bendix Smolt Counter used to Estimate Outmigrating Sockeye Salmon Smolt in the Kvichak River, Alaska, and the Development of a Replacement Sonar, 2000–2001**

by

**Suzanne Maxwell,**

**Anna-Maria Mueller,**

**Don Degan,**

**Drew Crawford,**

**Lee McKinley,**

**and**

**Nick Hughes**

April 2009

---

---

Alaska Department of Fish and Game

Divisions of Sport Fish and Commercial Fisheries



## Symbols and Abbreviations

The following symbols and abbreviations, and others approved for the *Système International d'Unités* (SI), are used without definition in the following reports by the Divisions of Sport Fish and of Commercial Fisheries: Fishery Manuscripts, Fishery Data Series Reports, Fishery Management Reports, and Special Publications. All others, including deviations from definitions listed below, are noted in the text at first mention, as well as in the titles or footnotes of tables, and in figure or figure captions.

<b>Weights and measures (metric)</b>		<b>General</b>		<b>Measures (fisheries)</b>	
centimeter	cm	Alaska Administrative Code	AAC	fork length	FL
deciliter	dL	all commonly accepted abbreviations	e.g., Mr., Mrs., AM, PM, etc.	mid-eye to fork	MEF
gram	g	all commonly accepted professional titles	e.g., Dr., Ph.D., R.N., etc.	mid-eye to tail fork	METF
hectare	ha	at	@	standard length	SL
kilogram	kg	compass directions:		total length	TL
kilometer	km	east	E		
liter	L	north	N	<b>Mathematics, statistics</b>	
meter	m	south	S	<i>all standard mathematical signs, symbols and abbreviations</i>	
milliliter	mL	west	W	alternate hypothesis	H <sub>A</sub>
millimeter	mm	copyright	©	base of natural logarithm	<i>e</i>
		corporate suffixes:		catch per unit effort	CPUE
<b>Weights and measures (English)</b>		Company	Co.	coefficient of variation	CV
cubic feet per second	ft <sup>3</sup> /s	Corporation	Corp.	common test statistics	(F, t, $\chi^2$ , etc.)
foot	ft	Incorporated	Inc.	confidence interval	CI
gallon	gal	Limited	Ltd.	correlation coefficient (multiple)	R
inch	in	District of Columbia	D.C.	correlation coefficient (simple)	r
mile	mi	et alii (and others)	et al.	covariance	cov
nautical mile	nmi	et cetera (and so forth)	etc.	degree (angular)	°
ounce	oz	exempli gratia	e.g.	degrees of freedom	df
pound	lb	(for example)		expected value	<i>E</i>
quart	qt	Federal Information Code	FIC	greater than	>
yard	yd	id est (that is)	i.e.	greater than or equal to	≥
		latitude or longitude	lat. or long.	harvest per unit effort	HPUE
<b>Time and temperature</b>		monetary symbols		less than	<
day	d	(U.S.)	\$, ¢	less than or equal to	≤
degrees Celsius	°C	months (tables and figures): first three letters	Jan, ..., Dec	logarithm (natural)	ln
degrees Fahrenheit	°F	registered trademark	®	logarithm (base 10)	log
degrees kelvin	K	trademark	™	logarithm (specify base)	log <sub>2</sub> , etc.
hour	h	United States (adjective)	U.S.	minute (angular)	'
minute	min	United States of America (noun)	USA	not significant	NS
second	s	U.S.C.	United States Code	null hypothesis	H <sub>0</sub>
		U.S. state	use two-letter abbreviations (e.g., AK, WA)	percent	%
<b>Physics and chemistry</b>				probability	P
all atomic symbols				probability of a type I error (rejection of the null hypothesis when true)	α
alternating current	AC			probability of a type II error (acceptance of the null hypothesis when false)	β
ampere	A			second (angular)	"
calorie	cal			standard deviation	SD
direct current	DC			standard error	SE
hertz	Hz			variance	
horsepower	hp			population	Var
hydrogen ion activity (negative log of)	pH			sample	var
parts per million	ppm				
parts per thousand	ppt, ‰				
volts	V				
watts	W				

***FISHERY MANUSCRIPT NO. 09-02***

**AN EVALUATION OF THE BENDIX SMOLT COUNTER USED TO  
ESTIMATE OUTMIGRATING SOCKEYE SALMON SMOLT IN THE  
KVICHAK RIVER, ALASKA, AND THE DEVELOPMENT OF A  
REPLACEMENT SONAR, 2000–2001**

by

Suzanne Maxwell,

Alaska Department of Fish and Game, Division of Commercial Fisheries, Soldotna

Anna-Maria Mueller and Don Degan,

Aquacoustics, Inc., Sterling, Alaska

Drew Crawford and Lee McKinley,

Alaska Department of Fish and Game, Division of Commercial Fisheries, Anchorage

and

Nick Hughes

University of Alaska, School of Ocean and Fisheries, Fairbanks

Alaska Department of Fish and Game  
Division of Sport Fish, Research and Technical Services  
333 Raspberry Road, Anchorage, Alaska, 99518-1565

April 2009

This project was partially funded by Western Alaska Disaster Grant No. NA96FW0196. In 1998, the U.S. Congress funded an initiative for "... the State of Alaska to develop disaster research and prevention relative to the 1998 Bristol Bay, Kuskokwim and Yukon fishery resource disaster." The intent was to provide funds for research to mitigate unexpectedly low returns of salmon. A total of \$450,000 was appropriated for the Alaska Department of Fish and Game to evaluate the Bendix smolt counter and develop a side-looking acoustic system to estimate sockeye salmon passage rates in the Kvichak River.

The Fishery Manuscript series was established in 1987 by the Division of Sport Fish for the publication of technically-oriented results of several years' work undertaken on a project to address common objectives, provide an overview of work undertaken through multiple projects to address specific research or management goal(s), or new and/or highly technical methods, and became a joint divisional series in 2004 with the Division of Commercial Fisheries. Fishery Manuscripts are intended for fishery and other technical professionals. Fishery Manuscripts are available through the Alaska State Library and on the Internet: <http://www.sf.adfg.state.ak.us/statewide/divreports/html/intersearch.cfm> This publication has undergone editorial and peer review.

*Suzanne Maxwell,  
Alaska Department of Fish and Game, Division of Commercial Fisheries,  
43961 Kalifornsky Beach Rd., Suite B, Soldotna, AK 99669-8367, USA*

*Anna-Maria Mueller and Don Degan,  
Aquacoustics, Inc.  
P.O. Box 1473, Sterling, AK 99672-1473, USA*

*Drew Crawford and Lee McKinley,  
Alaska Department of Fish and Game, Division of Commercial Fisheries,  
333 Raspberry Rd., Anchorage, AK 99518-1599, USA*

*and  
Nick Hughes  
University of Alaska Fairbanks, School of Ocean and Fisheries,  
204 Arctic Health, Fairbanks, AK 99775-7220, USA*

*This document should be cited as:*

*Maxwell, S., A. Mueller, D. Degan, D. Crawford, L. McKinley, and N. Hughes. 2009. An evaluation of the Bendix smolt counter used to estimate outmigrating sockeye salmon smolt in the Kvichak River, Alaska, and the development of a replacement sonar, 2000–2001. Alaska Department of Fish and Game, Fishery Manuscript No. 09-02, Anchorage.*

The Alaska Department of Fish and Game (ADF&G) administers all programs and activities free from discrimination based on race, color, national origin, age, sex, religion, marital status, pregnancy, parenthood, or disability. The department administers all programs and activities in compliance with Title VI of the Civil Rights Act of 1964, Section 504 of the Rehabilitation Act of 1973, Title II of the Americans with Disabilities Act (ADA) of 1990, the Age Discrimination Act of 1975, and Title IX of the Education Amendments of 1972.

**If you believe you have been discriminated against in any program, activity, or facility please write:**

ADF&G ADA Coordinator, P.O. Box 115526, Juneau, AK 99811-5526

U.S. Fish and Wildlife Service, 4401 N. Fairfax Drive, MS 2042, Arlington, VA 22203

Office of Equal Opportunity, U.S. Department of the Interior, 1849 C Street NW MS 5230, Washington DC 20240

**The department's ADA Coordinator can be reached via phone at the following numbers:**

(VOICE) 907-465-6077, (Statewide Telecommunication Device for the Deaf) 1-800-478-3648, (Juneau TDD) 907-465-3646, or (FAX) 907-465-6078

**For information on alternative formats and questions on this publication, please contact:**

ADF&G Division of Sport Fish, Research and Technical Services, 333 Raspberry Road, Anchorage AK 99518 (907) 267-2375.

# TABLE OF CONTENTS

	<b>Page</b>
LIST OF TABLES.....	ii
LIST OF FIGURES.....	ii
LIST OF APPENDICES.....	iii
ABSTRACT.....	1
INTRODUCTION.....	1
OBJECTIVES.....	3
MATERIALS AND METHODS.....	4
Evaluation of the Bendix Smolt Counter.....	4
Smolt Behavior.....	4
Video Data Collection.....	5
Video Data Analyses.....	5
Smolt Passage Estimates.....	6
HTI Multiple Transducer System.....	7
BioSonics' and Video Systems.....	8
Comparison of the Bendix and New Systems.....	15
RESULTS.....	15
Evaluation of the Bendix Smolt Counter.....	15
Smolt Behavior.....	15
HTI Target Strength Comparisons.....	16
Smolt Passage Estimates.....	17
Acoustic and Video Scalers.....	18
Estimates of Outmigrating Smolt Passage.....	18
Comparison of the Bendix and New Systems.....	19
DISCUSSION.....	19
Evaluation of the Bendix Smolt Counter.....	19
Evaluating Sonar Assumptions.....	21
Problems Encountered.....	22
Acoustic-Video Comparison.....	23
Future Studies.....	24
ACKNOWLEDGMENTS.....	25
REFERENCES CITED.....	26
TABLES AND FIGURES.....	27
APPENDIX A.....	55
APPENDIX B.....	59
APPENDIX C.....	81

## LIST OF TABLES

<b>Table</b>	<b>Page</b>
1. Average target strength and sigma values of individual sockeye smolt from up-looking and side-looking split-beam HTI transducers, Kvichak River, May 27–28, 2000.....	17
2. The percentage of smolt in range increments for the 3 depth distributions used in the adjustment of the equivalent beam angle, Kvichak River, 2001.....	17
3. Estimates of smolt passage using the 3 depth distributions and 2 scalars. ....	18

## LIST OF FIGURES

<b>Figure</b>	<b>Page</b>
1. Aerial photo of the Kvichak River showing the outlet of Lake Illiamna and the locations of each sonar site. ....	28
2. An up-looking sonar (top) showing cross sections of the upstream-downstream plane of the sonar beam (top left) and the cross-river plane of the beam (top right) at 2 ranges (R1 and R2), and a side-looking sonar showing cross sections of the upstream-downstream plane of the beam (center) and the cross-river plane of the beam (bottom) at 2 ranges (R1 and R2). ....	29
3. The sampling locations used in 2000 based on bathymetry data collected in June 2000. ....	30
4. Diagram of the video sled and cameras used in the Kvichak River, 2000. ....	31
5. Synchronous images of quadrat nodes in 2 camera views from the Kvichak River in 2000.....	32
6. Synchronous images of a smolt school passing over the upstream camera (left) and downstream camera (right) with clouds visible through the water's surface and Snell's window appearing on the inside of both images, Kvichak River, 2000. ....	33
7. Kvichak River bottom profile (thick line) from 2000 bathymetry data and the 2001 setup including the BioSonics' side-looking transducer (large rectangle at 5 m), up-looking transducer arrays (short horizontal lines), video cameras (small square at 100 m) and approximate sampling areas of the cameras and transducers. ....	33
8. Simulated smolt depth distributions at a range of 97.5 m from the transducer based on video observations and two modeled distributions. ....	34
9. A cross-river slice of the side-looking acoustic beam diagramming parameters needed to calculate the vertical split-beam angles of the upper and lower boundaries of the 0.1 m depth strata shown in Figure 8.....	34
10. A hypothetical smolt distribution uniformly distributed in the top 1.2 m of the water column shown against the acoustic beam, and the expected behavior of the equivalent beam angle (EBA) correction factor across the sampled range.....	35
11. A conical beam shown with its bounding polyhedron.....	36
12. A diagram of the procedure used to obtain smolt estimates from a single camera (2-D techniques) rather than 2 cameras in stereo.....	37
13. The 2001 sampling locations of the side-looking BioSonics' system and the up-looking Bendix arrays overlaid on river bathymetry from June, 2000. ....	38
14. Diel depth distribution of outmigrating smolt, Kvichak River, 2000. ....	39
15. Diel velocity of outmigrating smolt relative to current flow, Kvichak River, 2000. ....	40
16. Diel body orientation of outmigrating smolt, with 0° as the nose-upstream direction, Kvichak River, 2000.....	41
17. School structure of outmigrating smolt, Kvichak River, 2000. ....	42
18. Video length measures of outmigrating smolt, Kvichak River, 2000.....	43
19. Side-looking sonar echograms of outmigrating smolt during the late evening (top) and early morning (bottom), Kvichak River, 2001.....	44
20. Side-looking sonar echograms of outmigrating smolt during the night (top) and day (bottom), Kvichak River, 2001.....	45

## LIST OF FIGURES (Continued)

<b>Figure</b>	<b>Page</b>
21. Target strength frequency distribution for the side-looking and up-looking split-beam transducers (top) and side-looking target strength values by range (bottom) with a linear regression (line) and standard deviation (short bars), Kvichak River, May 27–28, 2000. ....	46
22. Estimated depth distributions of migrating smolts, Kvichak River 2001. ....	47
23. Mean acoustic size of single targets by range (top), hour of the day (center), and date (bottom) from the side-looking Biosonics’ system, Kvichak River sonar, 2001. ....	48
24. Acoustic and video estimates of smolt density by time showing the similarity in peaks between the two assessment methods (top), and the linear regression (bottom) with the regression line (solid black line) compared against a slope of 1 (dotted line), 0600 May 22–1800 May 24, 2001. ....	49
25. Bendix and BioSonics’ acoustic smolt passage estimates during the day (top) and night (bottom), defined as 2200–0600, plotted on separate axes because of the wide spread between the two estimates, Kvichak River, 2001. ....	50
26. The ratio of day/night smolt passage estimates using the Bendix and BioSonics’ sonars, Kvichak River, 2001. ....	51
27. The cross-river smolt distribution from the BioSonics’ sonar estimates using the video scaler and video distribution (VS Video), the current velocity, and the percentage of the Bendix count for each of the three arrays (note: the first value is arbitrary), Kvichak River 2001. ....	52
28. Reverberation caused by a boat passing through the side-looking BioSonics’ beam with a threshold of -65 dB (top) and -55 dB (bottom), Kvichak River, 2001. ....	53

## LIST OF APPENDICES

<b>Appendix</b>	<b>Page</b>
A1. A summary of major changes to the Bendix counter and methodology used to estimate migrating smolt passage at the Kvichak River sonar site, 1976–2001. ....	56
B1. Summary of hydroacoustics test services for ITC Mode 5095 transducers. ....	60
B2. Calibrations and beam pattern plots for the Bendix smolt counter transducers. ....	62
C1. A functional description of the Bendix smolt counter. ....	82



## ABSTRACT

Smolt abundance estimates are useful in predicting adult salmon returns, setting escapement goals, and partitioning freshwater and ocean survival. Within the Bristol Bay area, several riverine sonar systems, Bendix smolt counters, have provided reasonable abundance estimates of sockeye salmon smolt for many years, but recently, the estimates appeared inflated. The Bendix system was initially validated, but not retested after substantive changes were made. We evaluated potential reasons for the failure, tested a new acoustic-video system, and compared estimates from the new and old systems. We combined a side-looking sonar to estimate smolt passage and up-looking video cameras to study behavior. The video data showed that smolt migrated primarily in the top 0.3 m of the river, their velocity was similar to current velocity, their body aspect varied considerably, and the majority migrated between late evening and early morning. The side-looking sonar defied a basic echo integration assumption, which assumes a uniform distribution, so it was necessary to modify the equivalent beam angle formula used in echo integration to account for the actual smolt distribution. We expected the inconsistencies in body aspect to reduce the smolts' target strength; however, the acoustic scaler ( $-46.4 \pm 2.3$  dB) was similar to a scaler derived from video methods ( $-47.3$  dB). Paired video and acoustic counts were strongly correlated, but linear regression results were not statistically equal to one (95% confidence interval 0.68–0.80). The acoustic-video abundance estimate was 15.3 M, considerably lower than the Bendix estimate of 325.9 M. The greatest differences occurred during daytime passage. Comparison and behavioral information from the video data gave us confidence in the side-looking acoustic estimates. However, processing the video data was time-intensive. A single up-looking sonar might efficiently provide similar information. We were unable to correct the historical Bendix estimates, but suggest studies that may provide a means.

Key words: Bendix, hydroacoustic, Kvichak River, *Oncorhynchus nerka*, salmon, smolt, sockeye salmon, sonar, split beam, underwater acoustics, underwater video

## INTRODUCTION

The outmigrating abundance of sockeye salmon smolt (*Oncorhynchus nerka*) has been estimated in Bristol Bay area rivers of Alaska for many years using Bendix<sup>1</sup> smolt counters. Bendix smolt counters are single-beam, echo integration sonars composed of a series of up-looking transducer arrays (Crawford and Fair 2003). We re-evaluated the smolt counter and developed a new counting system composed of a side-looking, split-beam sonar and up-looking video array. Sockeye salmon smolts outmigrate from their nursery lakes in early summer within the Bristol Bay watershed. The Bendix smolt counter, developed on the Kvichak River in 1969 (McCurdy and Paulus 1972; Paulus and Parker 1974), was run annually from 1976–2001 by the Alaska Department of Fish and Game (ADF&G). The Kvichak River was selected for this study because the outmigration occurs within a contracted time period, typically from mid May through mid June. Smolt data from the Kvichak River are used in conjunction with other data sources to predict future adult returns, set escapement goals, partition freshwater from ocean survival, and combined with age, length, and weight measures collected from fyke net catches, provide information on lake productivity and the rearing capacity of nursery lakes where juvenile salmon develop.

In recent years, ADF&G began to question the reliability of the smolt estimates. Forecasts using smolt data from the Kvichak River appeared reliable from the project's inception until 1992 (Crawford and Fair 2003). In 1993, because of problems with the counter, a newer model was substituted. This change in counters may have compromised the estimates. The counts of outmigrating smolt were an order of magnitude higher than expected based on the historical relationship between smolt and subsequent adult returns. From 1991–1995, the smolt-adult

---

<sup>1</sup> Product names used in this report are included for scientific completeness, but do not constitute a product endorsement.

forecast model was more reliable than either sibling or spawner-return forecasting models for age-1.2 fish, and comparable to other models for the other major age classes (age-1.3, age-2.2, and age-2.3). Subsequent forecasts proved unreliable and forced us to re-evaluate the Bendix smolt counter. High forecasts combined with unexpected poor returns created an economic disaster that brought in federal funds targeting disaster-related research and funding for this project.

Through the years, a series of modifications were made to the Kvichak River counter (Appendix A). The most significant modifications included a change in frequency (118 kHz to 235 kHz) and beam width (18° to 9°, both circular), an increase in cable length, moving the site 1 km downstream because of changes in the river channel (Figure 1, Site 2), and changes in the placement of the arrays. These changes created many potential sources for error to be introduced. The higher frequency transducers have the potential of detecting more environmental noise from entrained air bubbles, boats, rain, or wind, potentially amplifying the count. The Bendix smolt counter was initially tested by positioning a fyke net below a transducer array and calibrating the sonar to match the fyke net counts (personal communications, Al Menin, Bendix designer). No ground truthing was performed following modifications to the system, so the effects of the changes on smolt estimates are unknown. Additionally, relocating the site and changing the array placements may have altered the relationship between the transducers and cross-river smolt distribution, violating the linear assumption used in the spatial expansion of the counts.

In past years, the cross-river smolt distribution has been examined using side-looking sonars. At the first Kvichak River site, a Lowrance Model X-16 sonar (192 kHz, 8° transducer) was positioned near the left bank (facing downriver) at a fixed location with the beam directed perpendicular to the river current (side-looking) (Bue et al. 1988). Most smolt were observed between 6 and 74 m from the transducer in the 100 m wide river. In a later study conducted at the second site, a BioSonics' dual-beam sonar was deployed side-looking near the right shore ensonifying 88–90% of the 134 m wide river (Huttunen and Skvorc 1991, 1992). Although the total estimate from the BioSonics' system compared favorably with the Bendix smolt counter, there was no significant relationship between the hourly estimates from the 2 methods. The nightly cross-river distribution of smolts was highly dynamic with peaks observed beyond the range of the outermost Bendix array. During this same time period, the highest Bendix counts came from the nearshore array. Huttunen and Skvorc (1992) concluded the BioSonics' system may provide better estimates of smolt abundance. However, because of the similarity between the total estimates and the concerns with using a side-looking sonar in a shallow river to assess fish near the river's surface, use of the Bendix smolt counter continued.

These early side-looking sonar studies encouraged us to explore the use of a side-looking system to estimate smolt abundance. But there were obstacles that had to be considered. According to Bendix data and direct observations, smolt outmigrate predominately near the river's surface. Standard echo integration procedures assume targets are distributed uniformly across the sonar beam. Traditionally, echo integration techniques are used with the sonar beam directed either down or up, and we assume smolt to be randomly distributed across the beam. In an up-looking system with the sonar transducer placed on the river bottom, the xy plane of the beam is the upstream-downstream and cross-river dimensions. In this configuration, as long as the sonar beam is narrow compared to the scale of the cross-river smolt distribution, and the smolt density is approximately constant across the depth of a single pulse length, a long enough sampling period will smooth the smolt density in the downstream dimension. In a side-looking setup, the

xy plane is the upstream-downstream and depth dimensions (Figure 2). As the beam diameter widens with increasing range, the majority of smolts travel closer to the beam's top edge resulting in a greater proportion of off-axis targets, which reflect less energy and if uncorrected, underestimate smolt density. For a side-looking system, smolt density must be constant in the vertical dimension, which is not the case. It was therefore necessary to develop new methods to echo integrate under these special circumstances.

The nonuniform depth distribution of smolt also becomes an issue in the conversion between density (smolts/m<sup>3</sup>) and flux (smolts/s), i.e., passage rate. With standard echo integration, density is calculated as the mean density in the cross section of the beam, which is a circular region if the 2 axes of the beam are equivalent or oblong if they are not equivalent. When time is added to calculate flux (smolt passage downstream), the sampling region becomes rectangular, now defined by upstream-downstream, depth, and time dimensions. If the depth distribution is nonuniform, the mean density in the beam cross section will differ from the mean density in the rectangular cross section.

To estimate smolt-passage rates, the new sonar methods require knowledge of the smolt depth distribution. Although theoretically, the split-beam sonar provides the horizontal and vertical position of individual echoes, this positional information is poor near the river's surface. The position of individual echoes is corrupted if echoes from the surface mix with smolt echoes or if echoes from multiple smolt simultaneously present in the beam mix. The second effect becomes more pronounced as the size of the beam expands with range. Because of these inaccuracies, we used 3-dimensional (3-D) video technology to obtain a vertical (or depth) distribution for smolt.

To set up a new sonar system, we needed information on the smolts' aspect, depth distribution, velocity, diel patterns, and school structure. Smolt velocity is needed to expand density estimates to passage rates. Smolt detection with a side-looking system depends on the aspect angle, which was unknown. Limited information about the smolt depth distribution was available from combining oscilloscope measurements of smolt depth from the Bendix transducers with river depth measures over each array (Crawford and West 2001). According to historical Bendix data, smolts migrate primarily at night, although occasional periods of high passage have been observed during the day. For this study, we used an up-looking video system to gain information on smolt behavior and test the beam pattern adjustments needed to echo-integrate the side-looking sonar data. We deployed the side-looking sonar along one bank of the Kvichak River and the up-looking video array offshore near the sonar beam in a region where high smolt passage has been observed.

## OBJECTIVES

1. Describe and document the functional operation of the Bendix smolt counter.
2. Identify the potential sources of bias and variability in the current estimation method and mechanisms by which the Bendix counter may have failed in prior years.
3. Evaluate the assumptions about outmigrating smolt behavior at the current site.
4. Evaluate the hypothesis that smolt density estimates from the video and side-looking sonar are similar.

5. Compare smolt estimates from the new system and Bendix smolt counter to determine if the historical smolt abundance estimates are valid and if not, whether they can be corrected.
6. Select a new smolt counting system and identify a methodology that improves upon weaknesses identified in the Bendix smolt counter.

## **MATERIALS AND METHODS**

### **EVALUATION OF THE BENDIX SMOLT COUNTER**

The Bendix smolt counter (Model 1982) consisted of 3 arrays, each with 10 single-beam transducers spaced 30 cm apart mounted on the rungs of ladder-like plastic tubes. The counter summed the echo energy from each array of transducers and converted the energy to counts. The arrays were deployed perpendicular to the river's current inshore, mid-river, and offshore along the river bottom with the transducers pointed up, ensonifying approximately 7.5% of the river (Figure 3, dark or red dots). Unsampled regions were interpolated assuming a smooth distribution of smolt between each array and a linear drop-off from the edge of the outermost nearshore and offshore transducer to shore. Technicians operated the Bendix system 24 h daily except during brief periods when it was shut down due to passing boats or large surface disturbances (i.e., wind and rain events which produce counts unrelated to smolt passage, or false counts). The vertical range of the Bendix transducers was extended toward the river's surface until false counts from the surface remained just below threshold. Wind and rain events that did not shut down the system required reducing the vertical range. Additional information on sampling techniques and the Bendix setup can be found in Crawford and Tilly (1995), Crawford and West (2001), and Crawford (2001).

To better understand the Bendix smolt counter, we developed a functional description of the counter through interviews and telephone conversations with the counter's designer, Al Menin, calibrated the transducers, and tested their near-surface detection limits. During calibration, the system's sensitivity was measured and beam pattern plots were produced by comparing the output of each Bendix transducer to a standard transducer. In river, we measured the near-surface detection limits of the smolt counter's half arrays using a 38.1 mm calibration sphere, a relatively small target with a known target strength (TS),  $-38.8$  dB for a 235 kHz sonar (Faran 1951). Although the calibration sphere was acoustically larger than smolt, the target provided a reasonable smolt substitute because the edges of the Bendix transducer beams drop off sharply.

### **SMOLT BEHAVIOR**

Our primary analyses of sockeye salmon smolt behavior was derived from 3-D video techniques but the printed and electronic echograms from the side-looking sonars also provided information on smolt behavior. From the sonar system, we visually interpreted echograms and obtained quantitative analyses by exporting single target echoes. The 3-D video techniques were used to derive the smolts' depth, their velocity relative to the shoreline, body length, body orientation, and school structure.

## **Video Data Collection**

Deep Sea Power and Light (Model SC-5000) low-light cameras were selected for videotaping the outmigrating smolt to allow the best possible images of smolt schools traveling at the far range of the camera, near the river's surface. Sony (Model GVD-900) digital recorders were used to record the video data. We mounted 2 cameras on an aluminum sled that placed the cameras 1.5–2 m below the surface in 4 m of water and positioned them along the upstream-downstream axis with their fields of view overlapped (Figure 4), which is required for 3-D analysis. In 2000, we mounted an infrared light between the 2 cameras to illuminate smolt during the period when it was too dark to obtain detectable images without illumination (approximately 0100–0300 hours). The video cables were attached to a buoy about 25 m downstream of the video sled and accessed from a boat tied to the buoy. In 2001, we obtained longer cables that ran to the bank. To minimize potential smolt avoidance, we painted the cameras and sled with olive drab paint. Maneuvering the cameras into the desired position required dropping a large anchor upstream of the desired deployment, attaching a line from the anchor to the sled, and using a boat to tow the sled off the beach and into the river. The anchor line prevented the sled from being swept downstream as the boat moved the sled laterally. On June 1, 2000, we positioned the sled in the middle of the river well downstream of the sonar equipment. To obtain paired data with the side-looking sonar, we positioned the mount immediately downstream of the sonar beam in 2001 and registered the approximate range of the sled by panning the sonar beam downstream until echoes from the cameras appeared on the echogram. For our analyses, we divided the sampling into 4 groups: late evening (0000–0100 hours), mid-night (0215–0245 hours), early morning (0400–0430 hours), and day (2034–2045 hours). For all periods except mid-night, we obtained digitized data from enough schools to give us approximately 100 fish to analyze.

## **Video Data Analyses**

To create a coordinate system for 3-D video analyses, we recorded the image of a 3-D quadrat floating on the surface of the river as it appeared simultaneously in the view of both cameras. In 2000, we used a 0.5×0.5×0.3 m quadrat, in 2001 a 1×2×1 m quadrat. Both quadrats had visible nodes at 0.1 m intervals along the upstream-downstream (x) and cross-river (y) axes of its upper and lower faces. The upper face of the quadrat was level with the water surface. For each camera and each quadrat face, we used the correspondence between the screen and quadrat x- and y-coordinates to estimate 9 parameters in a 3×3 transformation matrix; a matrix capable of converting screen coordinates into quadrat x- and y-coordinates. The line of sight from a camera to a point of interest is defined by the coordinates at which that line intersects the 2 horizontal planes occupying the near and far faces of the quadrat. When a smolt is visible in both camera views, each camera provides a line of sight. The smolts' location was estimated using 3-D geometry to calculate the coordinates where the 2 lines of sight intersected or came closest together. Information from the synchronous views of the calibration quadrat provided by the 2 cameras determined 3-D coordinates of points simultaneously visible in both camera views (Figure 5). This technique is similar to one described by Hughes and Kelly (1996), but is more accurate than their use of a polynomial regression.

Synchronous images of the quadrat from the 2 cameras were paired by recording a flashlight turned on and off above the cameras just after videotaping the quadrat. The current velocity was determined by videotaping small pieces of orange peel as they floated over the cameras. Because

the camera's field of view expands with increasing range, including all visible smolts would overestimate the abundance of smolts near the surface. We used 3-D geometry to select only those smolts that crossed the cameras within a range bin defined by 2 vertical planes parallel to the current and separated by 1 m. In most cases, the full width of the 1 m range bin was visible at the depth of the deepest smolts. In the one case where smolts were deeper and the 1 m range bin was too wide for the camera view (May 22, 2001, 0500–0600 hours), we used a narrower 0.75 m range bin to determine depth distribution. This selection of smolts was used to analyze each of the following behaviors.

1. Smolt depth was estimated by digitizing the 2-dimensional (2-D) screen coordinates of the nose and tail of individual smolt as they passed over the cameras (Figure 6), and then using the 3x3 transformation matrix to convert the 2-D points into 3-D points. The depth distribution was created by sorting the 3-D smolt data into 0.1 m depth bins.
2. Smolt velocity was estimated by calculating the velocity of individual smolt relative to the shore from 3-D coordinates at 0.1 s intervals, and then subtracting the current velocity. Multiple estimates for individual smolt were used in the calculation.
3. Smolt length was determined by measuring the distance between nose and tail of smolts in the center of the volume of water imaged by both cameras.
4. Smolt orientation was determined by calculating their bearing relative to a nose-upstream orientation.
5. Smolt school structure was constructed from a combination of the smolts' time and location coordinates as they crossed the center of the volume imaged by both cameras, and the current velocity. By collecting this information for each smolt that passed over the cameras, we were able to back-calculate the approximate position of smolts at the moment the first smolt in the school became visible in the field of view. This reconstruction technique assumed that smolts were carried passively downstream by the current, which is often not the case. Nonetheless, the technique provided a useful picture of the smolt schools.

The 3-D video analyses on which these data are based appeared generally sound. We have identified biases and sources of variability, but in general these are small and it is unlikely that they introduce significant errors into the analyses. Nonetheless, some of the results should be treated with more confidence than others. Data on depth distribution, mean velocity, and body orientation are reliable for late evening, early morning, and day periods. They are less reliable for the middle of the night period because the image quality was poor. Data on fish length are less reliable overall because the poor image quality made it difficult to see where the tail ended, and smolt were often flexed, which made our measurements of the straight-line distance between the nose and the tip of tail less accurate. Synchronization errors between paired images will also have a larger impact on length estimates than the other types of data.

## **SMOLT PASSAGE ESTIMATES**

We began this study in 2000 with an Hydroacoustics Technologies Inc. (HTI) multiple transducer system. The system was comprised of one transducer positioned at a fixed location nearshore with the beam directed perpendicular to the current flow (side-looking) and 6 transducers set in an array and placed on the river bottom with the beams directed up (up-

looking). The HTI system was not available prior to the field season, so preseason testing was not possible. In the field, we discovered that the software for echo integrating the 20 Log R (range) data included a simplistic viewing program with no editing features, and since the software was proprietary, the file structure was not made available to us. We were unable to process the data to obtain smolt estimates. In addition, the HTI system was unreliable. A continuing string of printer jams and system crashes caused us to lose data throughout the field season. We were able to process the 40 Log R data and used the dataset to contrast the differences in smolt target strength between the side-looking and up-looking transducers. The printed charts provided qualitative information on smolt behavior.

Because of our inability to echo integrate the data and with no software improvements forthcoming, we replaced the system in 2001 with a single BioSonics' side-looking transducer. The system was not capable of multiplexing more than 2 transducers, so the up-looking sonar array was resigned. The BioSonics' software (Visual Analyzer V4.02) was capable of editing and integrating the data; however, the processing speed was incredibly slow. The software was used in the field, but postseason we gained access to Echoview software (SonarData's Echoview V3.00), and used it for processing all remaining data.

To estimate smolt passage, the BioSonics' data was echo integrated and scaled using acoustic and video scalars. Prior to scaling the data, the echo integration data were corrected by using an equivalent beam angle adjustment based on the smolt depth distribution. The estimates were converted from density to flux estimates and expanded for unsampled range and time. Finally, the resulting smolt estimates from the new system were compared with the Bendix estimates. Details of these methods are included below.

### **HTI Multiple Transducer System**

The 200 kHz HTI sonar system included the following components: a Model 244 Digital Echosounder, one nearshore, side-looking transducer ( $2.3^{\circ} \times 10^{\circ}$  split-beam) attached to an HTI Model 661H automated rotator; 6 up-looking transducers (five  $15^{\circ}$  single beam, one  $4^{\circ} \times 10^{\circ}$  split-beam); a data collection computer; and a digital chart recorder coupled to a black and white dot matrix printer. The system was deployed off the right bank (facing downstream) of the Kvichak River at Site 2 (Figure 1). The 6 up-looking transducers were mounted on 2 separate arrays on the rungs of a ladder-like plastic tube mount (similar to the Bendix mount). The 2 arrays were deployed on the river bottom approximately 15 m downstream of the inshore and center Bendix arrays. Initially, we tested a  $3^{\circ}$  circular transducer for the side-looking system, but interference with the surface and river bottom within our desired sampling range forced us to switch to the  $2.3^{\circ} \times 10^{\circ}$  transducer. The side-looking transducer was set up nearshore approximately 40 m downstream of the Bendix array and 7.5 m offshore, 0.3 m below the water surface, and aimed perpendicular to current flow as close to the water's surface as noise allowed (Figure 3). The maximum sampling range was set at 100 m for the printed charts and 120 m for the electronic data. The river width at the time of sampling was 132.6 m. Thresholds for the side-looking transducer were set at -48 dB for data collection and -40 dB for printing and -60 dB for both thresholds for all up-looking transducers.

Preseason, each transducer was calibrated by HTI against a standard hydrophone and with a 38.1 mm tungsten carbide sphere (calibration sphere) at a calibration barge. The theoretical target strength of the sphere for 200 kHz is -39.2 dB (Faran 1951). Measured target strengths of the calibration sphere varied from -38.6 to -40.9 dB between transducers. Calibrations were

verified in the field using the same type of calibration sphere. The effective near-surface, sampling capability was tested by suspending the calibration sphere from a boat driven slowly over the transducers.

The HTI system was set to operate continuously through the peak of smolt passage. We obtained target strength values for individual smolt from the split-beam transducers by manually selecting smolt tracks displayed on 40 Log R electronic echograms and outputting the target strength (TS) values using HTI's Echoscape software. Printed charts were examined to obtain qualitative information regarding the smolt cross-river and diel distributions.

## **BioSonics' and Video Systems**

Outmigrating smolt passage rates were estimated in 2001 with side-looking BioSonics' sonar and up-looking video data. We echo integrated data across a large portion of the river and calculated an acoustic scaler based on the mean TS of individual smolt. A combination of 2-D and 3-D video techniques were used to estimate smolt passage in a region overlapping the acoustic beam for the purpose of scaling the echo integration data and as an independent estimate to validate the acoustic estimates. The data used to determine the video depth distribution was collected in 2001.

### ***Acoustic Data Collection and Editing***

Acoustic data were collected using a BioSonics DE 6000 echosounder and a side-looking transducer (2° circular, 208 kHz). The transducer was bolted to a Model 661 HTI automated rotator and a Honeywell HMR 3000 attitude sensor (supplied by BioSonics) was attached. The transducer was positioned nearshore 0.27 m below the water surface and aimed cross-river perpendicular to the river's current approximately 0.5–1° down from horizontal to skim along the river's surface (Figure 7). Acoustic data were collected using the following parameters: 1–110 m range; 3 pings/s (changed to 1 ping/s on June 1 to reduce file size and analysis time); 0.2 ms transmitted pulse length; -55 dB threshold; and threshold type R<sup>2</sup>. The TS data were stored electronically and sample echograms, color-coded by TS, were printed.

Prior to collecting data, we field-calibrated the BioSonics' transducer using a 36.4 mm tungsten carbide sphere with a theoretical TS of -39.8 dB at 208 kHz. The 36.4 mm sphere was used because the 38.1 mm sphere's TS falls 12 dB in the frequency range surrounding 208 kHz. The average measured TS of the calibration sphere was -32.25 dB, so a calibration offset of 7.55 dB was used for the data analyses. The effective near-surface sampling depth was tested by suspending the same sphere at depths varying from 0–10 cm from a boat driven slowly across the river along the beam of the transducer. We were able to detect the sphere within a few cm of the surface from 40–100 m from the transducer.

Acoustic data compromised by rain, wind, boat-induced bubbles, and intermittent reductions in the echo voltage caused by a problem with the transducer were excluded by cutting out the entire time blocks containing these events. The field crew edited noise from the data inseason using the BioSonics' software. Postseason, Echoview software was used to process the data. Missing or edited data within an hour were compensated for in the Echoview software by the echo integration process which averaged the echo voltages based on the actual time sampled within each hour. A band of echoes, likely reflected from bubbles near the surface, clouded the echograms at ranges less than 55 m from the shore-based transducer. The echoes were removed by excluding the 0–55 m range from the echo integration. The relatively high side lobes (-13 dB) of the transducer were

likely the cause of this unwanted reverberation. Entire hours of missed data and missing or removed range strata were expanded based on methods described later in this section.

### ***Equivalent Beam Angle Adjustment***

Standard echo integration uses the equivalent beam angle (EBA) in the density calculation (Simmonds and MacLennan 2005; Clay and Medwin 1977). Mueller et al. (2006) modified the EBA equation to compensate for the bias related to the nonuniform depth distribution inherent in the side-looking system. An important component in the calculation of the adjusted EBA (EBA') is knowledge of the smolt depth distribution. We modeled this distribution from the small video sample of smolts and added 2 hypothetical distributions to test the sensitivity of the methodology to error. The first hypothetical distribution assumed that all smolts were uniformly distributed within the top 1.2 m of the water column (UTD); 1.2 m was the maximum depth of the smolts observed by video. The second distribution assumed that all smolts were within the top 0.4 m of the water column with a distribution skewed towards the surface (SkD). The UTD should underestimate abundance, while SkD overestimates abundance providing lower and upper boundaries for the estimate. The video-derived distribution (ViD) should fall between these 2 extreme values. A fourth depth distribution, derived from the acoustic split-beam data, was discarded because of the poor quality of the positional information. The 3 depth distributions (UTD, SkD, and ViD), illustrated in Figure 8, were used separately to calculate EBA' values and obtain estimates of smolt passage. We also estimated smolt passage without adjusting the EBA.

The standard echo integration EBA ( $\Psi$ ), is given by:

$$\Psi = \iint D_{(\theta,\phi)}^4 \sin \theta d\theta d\phi \quad (1)$$

where:

- $D$  is the transducer directivity (Clay and Medwin 1977);  $D^4$  is also referred to as the 2-way beam pattern; and
- $\theta, \phi$  are the spherical coordinates of a given point;  $\theta$  is the angle of the point from the acoustic axis, and  $\phi$  is the angle between the x axis and the point projected onto the xy plane at the transducer face.

Integration for  $\phi$  was from 0 to  $2\pi$  and for  $\theta$  from 0 to  $\pi$ . The double integral can be replaced by summation over the angles of the split-beam transducer ( $\alpha$  and  $\beta$ ):

$$\Psi = \sum \sum D_{(\alpha,\beta)}^4 \Delta\alpha \Delta\beta \quad (2)$$

where  $D_{(\alpha,\beta)}^4$  is the 2-way beam pattern for split-beam angles  $\alpha$  and  $\beta$ . The BioSonics' effective beam size for smolt detection was  $2.2^\circ$ , so  $\alpha$  and  $\beta$  were summed from  $-1.1^\circ$  to  $1.1^\circ$ .

Although we used a circular transducer, the transducer directivity  $D$  was calculated for a rectangular transducer using (Clay and Medwin 1977):

$$D = \frac{\sin[(ka \sin \alpha)/2]}{(ka \sin \alpha)/2} \times \frac{\sin[(ka \sin \beta)/2]}{(ka \sin \beta)/2} \quad (3)$$

where  $k$  is the wave number and  $a$  is the width of the rectangular transducer face. This was done to ease our calculations and tests show that results for both transducer types are essentially identical for our situation. We calculated an adjusted EBA ( $\Psi'$ ) for each of our 3 distributions by summing the 2-way beam pattern across  $0.2^\circ \times 0.2^\circ \Delta\alpha\Delta\beta$  incremental areas and weighted the sum by the relative number of targets seen in each incremental area:

$$\Psi' = \sum \sum D_{(\alpha,\beta)}^4 \left( \frac{n_{(\alpha,\beta)}}{\bar{n}} \right) \Delta\alpha \Delta\beta \quad (4)$$

where  $n_{(\alpha,\beta)}$  is the number of targets seen in the incremental area  $\Delta\alpha\Delta\beta$ , and  $\bar{n}$  is the average number of targets in the incremental area described by the rectangular region bounded by split-beam angles,  $\alpha = \pm 1.1^\circ$  and  $\beta = \pm 1.1^\circ$ ;  $\bar{n} = \frac{\Delta\alpha\Delta\beta}{\Delta\beta}$  is therefore the mean density of targets in

the bounding rectangle of the circular beam cross section covering  $1.1^\circ$  off axis.  $\frac{n_{(\alpha,\beta)}}{\bar{n}}$  was modeled by simulating the split-beam angles of 2,000 fish for each of the 3 depth distributions (UTD, SkD, and ViD). For each 0.1 m depth stratum, we calculated the vertical angles  $\beta$  corresponding to each upper and lower boundary using the equation below whose components are illustrated in Figure 9:

$$\beta_{(D,R)} = \arctan\left(\frac{O-D}{R}\right) - \delta \quad (5)$$

where:

- $\beta_{(D,R)}$  is the vertical split-beam angle for a target at depth  $D$  and range  $R$  (positive is up from the acoustic axis, negative is down from the acoustic axis);
- $O$  is the depth at the center of the transducer face;
- $D$  is depth of the target;
- $R$  is range of the target; and
- $\delta$  is the tilt angle of the transducer (positive is up from horizontal, negative is down from horizontal).

We used a transducer tilt angle  $\delta$  of  $-0.6^\circ$ , based on the split-beam angle at which the calibration sphere was seen when it was suspended 5 cm below the surface at 10 m range intervals from 50–90 m.

In our simulation of split-beam target angles, we created  $n_d$  random numbers for each 0.1 m depth stratum, ranging from the upper to the lower boundary of the acoustic beam as defined by the split-beam angle.  $n_d$  equals the percentage of the 2,000 simulated fish corresponding to the percent of smolt seen in a given depth stratum and depth distribution.

While the smolt depth distribution is assumed to be constant across the river, its pattern within the xy cross-section of the beam is range dependent. Figure 10 shows an example of these range-dependent effects using the UTD and the expected effect on the ratio between  $\psi/\psi'$  (also referred to as the EBA correction factor). We calculated an adjusted equivalent beam angle  $\psi'$  for a video reference range at 97.5 m and for 20 m range increments from 50–110 m. We estimated  $\psi'$  for additional ranges by fitting a 5<sup>th</sup>-order polynomial function through the modeled points and interpolating at 5 m range intervals.

The standard volume backscattering coefficient ( $sv$ ) was calculated as follows:

$$sv = \frac{\int V^2 dt}{Sl \times Rs \times \frac{c\tau}{2} \times \psi} \quad (6)$$

where:

- $V$  is the output voltage from the echo sounder; integration is over the time interval that covers the range of interest;
- $Sl$  is the source level of the echo sounder;
- $Rs$  is the receive sensitivity of the echo sounder;
- $c$  is the speed of sound; and
- $\tau$  is the pulse duration.

(Note: Equation 6 assumes that the echosounder uses a 20 log R time-varied gain and compensates for absorption loss.)

The  $\psi/\psi'$  ratio was used to adjust the  $sv$  values in the 5 m range intervals for each of the 3 depth distributions:

$$sv' = sv \times \frac{\psi}{\psi'} \quad (7)$$

where  $sv'$  is the volume backscattering coefficient adjusted for a given distribution. Note that  $sv$  is proportional to the target density in the cone described by the effective beam width, whereas  $sv'$  is proportional to the target density in the bounding polyhedron of the cone (Figure 11).

### ***Scaling the Volume Backscattering Coefficient***

The adjusted volume backscattering coefficient ( $sv'$ ) is directly proportional to the density of targets in the volume of the bounding polyhedron of the cone. A proportionality factor, or scaling constant, is used to convert the  $sv'$  values to the number of smolt per unit volume (smolt density). We scaled the  $sv'$  values using both a video and acoustic scaler. Because the computation of the video scaler uses the same density to flux conversion factor described in the next section, the methods for the video scaler are included later in the report.

The traditional approach to obtaining an acoustic scaler is to determine the acoustic size of an individual fish either by analyzing the mean backscattering cross section ( $\bar{\sigma}_{bs}$ ) of single echoes or using experimental acoustic size-length relationships and physically measuring the length of the fish (Simmonds and MacLennan 2005). We analyzed the  $\bar{\sigma}_{bs}$  values of single echoes using BioSonics' Visual Analyzer 4.0 software. To analyze potential time and range biases, we averaged and plotted  $\bar{\sigma}_{bs}$  values by day and hour across 10 m range bins. We selected periods when smolt passage rates were low by visually examining echograms and extracted single echoes using a threshold of -55 dB, a pulse duration (measured 6 dB from peak) of 0.8–1.2 times the length of the transmitted pulse, a minimum pulse shape correlation coefficient of 0.95, and a maximum off-axis angle of 3 dB. A single acoustic scaler  $\bar{\sigma}_{bs}$ , averaged from data obtained across the field season, was used to convert the  $sv'$  values in each range and time cell to densities by:

$$D_{aR} = \frac{sv'_R}{\bar{\sigma}_{bs}} \quad (8)$$

where  $D_{aR}$  is the mean smolt density in the bounding polyhedron of the conical 2.2° beam in range bin  $R$ .

### ***Converting Smolt Density to Flux***

To convert smolt density to flux, or smolt passage rate, we used a conversion factor ( $C_R$ ), which is a function of range, calculated for each 5 m range increment:

$$C_R = s_R v_R w_R \times 3600 \quad (9)$$

where:

$s_R$  is the estimated smolt velocity (m/s) in the range bin;

$v_R$  is the vertical height (m) of the bounding polyhedron of the conical beam;

and

$w_R$  is the cross-river width (m) within a range bin.

The constant, 3600, converts the time variable from seconds to hours. We calculated the hourly fish passage rate ( $F$ ) across the sampled 5 m range bins ( $R$ ) from 55–110 m by:

$$F = \sum_R (D_{aR} \times C_R) \quad (10)$$

### ***Expanding Smolt Estimates Across Unsampled Hours and Range***

Although the BioSonics' system was operated continuously during the field season, we expected to lose data when boats traveled through the sampling area, heavy rains clouded the images, or other events created acoustic noise on the echograms. In addition, our sampling did not encompass the entire river. To account for unsampled hours and cross-river range, we adopted the same strategies traditionally used to expand the Bendix counts (Crawford and West 2001). To expand for missed hours, we multiplied the daily smolt passage estimates by the ratio of total hours in a day over the actual number of hours sampled. For the range expansion, we first assumed that no smolt passed between 0–9 m or beyond 128 m (the opposite bank was 138 m distant), the same assumption used for the Bendix counter. To expand the estimates for unsampled range, we assigned zero values to the 0–9 m and beyond 128 m range bins and linearly interpolated to the closest range bin sampled, 55–60 m nearshore and 105–110 m for the far shore. The true flux in the unsampled range is probably not linear, but linear interpolation was chosen because of its historic use with the Bendix data, and because the true function is unknown.

### ***Video Scaler***

Because of the potential inaccuracies in an acoustic scaler from the side-looking system, we developed an alternative approach. To scale the  $sv'$  values, we used an independent smolt estimate from the video system, paired it with the acoustic data, and solved for the mean acoustic size of an individual smolt. From the video data, we counted smolts in a series of 30 s images if they crossed a 1 m  $\times$  1.2 m area (cross-river  $\times$  depth), and compared the count to acoustic  $sv'$  values averaged across the same time and a similar area. As we aligned the paired data, we included only good quality video and acoustic images.

Ideally, we would have liked to use the same 3-D video techniques used to determine the smolts' depth distribution, but the methodology was extremely time consuming and not practical for the larger samples needed for the comparison. Instead, we developed a method that allowed us to combine data from a single camera with the 3-D information from the smolts' depth distribution to estimate smolt flux. We first digitized the nose and tail coordinates of smolts as they passed across the middle of the field of view of a single camera. Next, we determined the probability that each smolt was actually within a range bin defined by 2 vertical planes parallel to the current and separated by either 0.25, 0.5, 0.75, or 1 m. By summing these probabilities for all the smolts in a given time period, we were able to estimate smolt flux within the range bin for each time period. This procedure is diagrammed and further explained in Figure 12. We checked the accuracy of this method by plotting how the estimate of fish passage rate changed with range bin width. If the 3-D geometry was working properly, the smolt were not avoiding the cameras, and all the smolt within the range bin were visible to both cameras (i.e., no smolts within the range

bin were traveling deep enough to pass above or below the camera's field of view), the plot should be linear with an intercept of zero and a slope of one. This test was passed for all five 1-h time periods examined, except May 22, 0500–0600 hours. Further analysis showed that during this time some smolt within the 1 m range bin were swimming deep enough to avoid the camera's field of view. To correct this, we recalculated the smolt depth distribution and flux using a narrower 0.75 m range bin that allowed the camera to see the deeper smolts. For the other 4 time periods, we used the 1 m range bin to estimate smolt flux.

Video estimates of smolt passage were expressed as flux (smolt/s) within a 1 m × 1.2 m cell (cross-river range × depth). The subset of acoustic data was echo integrated in 1 m × 30 s cells (cross-river range × time) to produce estimates of smolt density (smolt/m<sup>3</sup>). To bring the 2 datasets into a common frame of reference, we converted the video flux estimates to mean density in a volume equivalent to the volume sampled by acoustics. Figure 2 illustrates the relationship between cross-sections from an up-looking and side-looking beam. We used the conversion factor  $C_R$  (Equation 9) defined as the midpoint of the 1 m video range to convert video flux ( $F_v$ ) to density ( $D_v$ ) by:

$$D_v = \frac{F_v \times 5 \times 3600}{C_R} \quad (11)$$

We originally deployed the video mount directly under the acoustic beam assuming it would remain below the beam, but the mount created unwanted echoes on the echogram, and we were forced to move it further downstream. Without an exact overlap range, we were uncertain which 1 m range interval of the acoustic beam to compare with the video, so we ran a linear regression comparing the acoustic data from 2 range intervals with the video estimates using the average density ( $D_v$ ) from the video as the independent variable and the average  $sv'$  as the dependent variable after adjusting the 2 estimates to equivalent volumes. The  $sv'$  values were averaged across 96–99 m and 96–98 m to determine which range bin would correlate better with the video estimates. The midpoint of the selected range bin was then used in the calculation of  $C_R$ . To calculate the  $sv'$  values, we used the video depth distribution. A video scaler ( $\sigma_{video}$ ) was calculated using Thompson's (2002) ratio estimator method:

$$\sigma_{video} = \frac{\sum_{j=1}^n sv'_j}{\sum_{j=1}^n D_{v_j}} \quad (12)$$

where  $n$  is the number of paired video and acoustic samples. The video scaler was substituted for the acoustic scaler ( $\bar{\sigma}_{bs}$ ) in Equation 8 to obtain an alternate estimate of smolt passage.

## COMPARISON OF THE BENDIX AND NEW SYSTEMS

The Bendix estimates (Crawford 2001) were compared with the acoustic-video estimates (video scaler and video depth distribution). During data collection, the side-looking BioSonics' transducer was located approximately 40 m downstream of the Bendix arrays (Figure 13). The side-looking hourly smolt passage estimates,  $F$  (Equation 10), expanded for unsampled time and range were used for the comparison. The 2 datasets were subdivided into night (defined as 2200–0600 hours) and day passage. To compare the 2 systems, we examined the time series, the ratio between the day and night estimates from both systems, and calculated a linear regression.

## RESULTS

### EVALUATION OF THE BENDIX SMOLT COUNTER

A functional description of the Bendix smolt counter was collected from interviews with Al Menin, the designer and maintainer of the Bendix system, by Don Degan (Aquacoustics, Inc.), Ed Belcher (University of Washington Applied Physics Lab), and Suzanne Maxwell (ADF&G). Ed Belcher used the electronic schematics for the Bendix smolt counter, interview notes from Al Menin, and laboratory calibrations to put together a comprehensive description of the Bendix smolt counter (Appendix B). The smolt counter was calibrated and beam plots for each transducer were produced at the University of Washington Applied Physics Lab by Ed Belcher in February 2000 (Appendix C).

The Bendix smolt counter's mean near-surface detection limit for the 38.1 mm calibration sphere was 10 cm below the river's surface, varying from 5–20 cm. This limitation is close to the theoretical one-half pulse length limitation (68  $\mu$ s or 9.8 cm using a sound speed of 1,435 m/s). We found that the Bendix beams overlap when they reach a range of 1.9 m (9° beam and 0.3 m spacing). At the second deployment site (Figure 1), the maximum sampling depth at the Bendix arrays is 2.6 m, an overlap of 6% of the total sample volume of each array. We do not know how this overlap affects the count, or whether it was corrected for in the electronics.

### SMOLT BEHAVIOR

The behavior of smolt as they pass the sonar site was determined from both video and sonar analyses. The video analyses provided the depth distribution, velocity, body orientation, and school structure of smolts. Results from each analysis are separated into periods of the day that include early morning, day, late evening, and mid-night. The sonar analyses provided cross-river and diel distributions, and the target strength of smolt from up-looking and side-looking perspectives.

The smolt depth distributions varied by time of day, but overall, smolts swam in the top 100 cm of the water column (total water depth 3.5 m at the video site), and often the top 30 cm (Figure 14). Smolts swam closest to the surface in late evening and early morning, 20–25% within 10 cm of the surface and 95% within 30 cm. During the day, smolts swam deeper, 10% within the top 10 cm and 65% within the top 30 cm. In the mid-night period, fish swam 40–80 cm from the surface (one school analyzed). The mean smolt depth was more similar during late evening and early morning and more variable during the mid-night and day periods.

Smolt velocities centered around zero, after the current velocity was subtracted (Figure 15). The mean direction of travel was related to body orientation, which varied as a function of time of day. Smolt velocities averaged 0.05 m/s upstream during late evening, 0.10 m/s downstream during early morning, 0.02 m/s upstream during the day, and 0.40 m/s downstream during the middle of the night (this value is suspect because of the few data points obtained). The current velocity at the location of the cameras was 1.10 m/s. From these results, we determined that a reasonable approximation for smolt velocity was the current velocity. Current velocity was measured on June 6, 2001 in 10 m increments across the river and used as a surrogate for the smolt velocity in the density to flux conversions. Current velocity across the river averaged 1.17 m/s ranging from 0.75–1.37 m/s.

The body orientation of smolt was polarized, although not uniformly at any one time, and the pattern of polarization changed over the 24 h period (Figure 16). Smolt pointed mostly within 90° of a nose-upstream direction with a small number pointing downstream in late evening, downstream or sideways (one school analyzed) in the mid-night period, mostly sideways with some pointed upstream or downstream in early morning, and mostly sideways and upstream with a few pointed downstream during the day.

During late evening, early morning, and day, schools were thin and spread out, weakly polarized and diffuse (Figure 17). Nearest neighbor distances were typically well over a fish length with estimated fish length modes at 7–8 cm in late evening, 11–12 cm in the mid-night period, and 8–9 cm in early morning and day (Figure 18). During the mid-night period, school structure changed, with nearest neighbor distances falling to under a fish length. Boundaries between schools were less distinct during late evening compared to the other periods possibly due to larger numbers of outmigrating smolts, which may blur the boundaries between schools.

Diel patterns in smolt behavior observed from echograms were similar to the video observations. During late evening and early morning, the schools were less dense as the smolts spread out across the river's surface (Figure 19). Smolt passed by the sonar site predominately at night. Passage during the day was more similar to the mid-night period with the smolt congregated into dense schools and concentrated in the deepest and fastest portion of the river (Figure 20).

### **HTI Target Strength Comparisons**

The HTI sonar provided smolt target strengths and a qualitative look at the cross-river and diel distribution from data collected May 24 to June 7, 2000. In near-surface detection tests of the up-looking HTI transducers, echoes reflected from the 38.1 mm calibration sphere were first visible on electronic echograms along with surface noise at a depth of 20 cm and became distinct echoes at 30 cm deep. For the side-looking system, the calibration sphere was detectable as soon as the sphere dimpled the water's surface.

The average TS (40 Log R) of individual smolt are listed in Table 1. The mean TS and sigma (linear voltage measure) for the split-beam transducers are essentially the same; however, the modal TS from the up-looking transducer was 8 dB higher than the side-looking one (Figure 21, top). The TS from the side-looking system was relatively consistent across the ensonified range (Figure 21, bottom).

Table 1.—Average target strength and sigma values of individual sockeye smolt from up-looking and side-looking split-beam HTI transducers, Kvichak River, May 27–28, 2000.

	Up-looking	Side-looking
Number of Individual Smolts	498	9,783
Avg TS (dB)	-47.6	-47.5
StDev of TS (dB)	5.2	4.9
Avg Sigma (Volts)	3.16E-05	3.99E-05
TS of Sigma (dB)	-45.0	-44.0

Printed echograms from the HTI system showed that the vast majority of smolt outmigrated at night. Smolt passed predominantly between 40–110 m from the shore-based, side-looking transducer, with few observed closer than 40 m. During the highest smolt passage, the smolt amassed in the deepest part of the channel at 90–100 m. We initially suspected some kind of noise event, but later concluded the band contained a dense region of smolt. This range was offshore of the outermost Bendix array.

### SMOLT PASSAGE ESTIMATES

Acoustic data were collected with the BioSonics' sonar from May 18 to June 10, 2001. The paired video and acoustic datasets were narrowed to data collected between 0600 hours May 22 and 1800 hours May 24. We analyzed 230 30-s data samples that represented high quality video and acoustic data. The video depth distribution was obtained by subsampling 2 short time periods from each of 5 hours of data and pooling the results. Sample sizes averaged 82 smolt per 1 h sample, ranging from 57–114 smolt. The resulting distributions (Figure 22) were used to determine the percentage of smolt in 0.1 m depth bins. The video depth distribution and 2 modeled distributions are compared in Table 2.

Table 2.—The percentage of smolt in range increments for the 3 depth distributions used in the adjustment of the equivalent beam angle, Kvichak River, 2001.

<i>Depth</i>	Best estimate <i>% Smolt</i>	Uniform Top 1.2 m	Skewed Top 0.4 m
		Underestimate <i>% Smolt</i>	Overestimate <i>% Smolt</i>
0 – 0.1 m	11	8.3	32.5
0.1 – 0.2 m	14	8.3	27.5
0.2 – 0.3 m	12	8.3	22.5
0.3 – 0.4 m	13	8.3	17.5
0.4 – 0.5 m	12	8.3	0
0.5 – 0.6 m	10	8.3	0
0.6 – 0.7 m	9	8.3	0
0.7 – 0.8 m	8	8.3	0
0.8 – 0.9 m	5	8.3	0
0.9 – 1.0 m	4	8.3	0
1.0 – 1.1 m	2	8.3	0
1.1 – 1.2 m	0	8.3	0
>1.2 m	0	0	0

The EBA correction factor ( $\psi/\psi'$ ), a function of the target distribution and range, was fairly smooth across the ranges sampled, with variations of 0.88–0.93 (Video Distribution), 0.78–0.87 (Uniform Top Distribution), and 1.17–1.25 (Skewed Distribution). If the smolt were randomly distributed throughout the entire beam, the EBA correction factor becomes 1.00, i.e.  $sv = sv'$ . The EBA correction factor is therefore a direct indicator of the specific bias in each depth distribution and is the multiplier used to compensate for the bias.

### Acoustic and Video Scalers

We used a single acoustic scaler to scale the echo integrals for all range and time cells. The mean acoustic backscattering cross-section ( $\bar{\sigma}_{bs}$ ) of the single targets increased only slightly with range, and no trend was observed when plotted by time of day or by date (Figure 23). The overall average of the acoustic cross-section backscattering intensity was 2.30E-05 Volts (TS = -46.4 dB).

The video scaler, based on the 2-D video techniques aligned with the acoustic data, was derived from an estimate of 13,879 smolt. For this scaler, the range interval selected for the comparison with the acoustic estimates was the 96–99 m interval with a midpoint of 97.5 m. The resulting video scaler was 1.86E-05 Volts, or -47.3 dB, 1.24 times smaller than the acoustic scaler. This smaller scaler would result in larger passage estimates.

We used the paired acoustic and video samples to compare flux estimates from the 2 methods. During the aligned sampling periods, smolt passage came in pulses and at times was very dense. Peak passage periods in the smolt flux estimates coincided with peaks in the acoustic estimates (Figure 24). Using the video flux estimates as the independent variable with the assumption that most of the error is in the acoustics estimate, the 2 estimates were strongly correlated, although 95% confidence intervals for the slope did not include one ( $y = 0.74x \pm 0.04$ ; 95% confidence interval 0.68–0.80;  $R^2 = 0.71$ ). The regression was interpreted with caution because the standard deviation of the estimates increased as the density estimates increased. Logging the data did not resolve this issue, and instead resulted in the standard deviation decreasing as estimates increased.

### Estimates of Outmigrating Smolt Passage

Estimates of outmigrating smolt passage using the video scaler and video depth distribution resulted in a smolt abundance estimate of 15.31 M for the 2001 field season. The estimates from the 2 scalers and 3 depth distributions ranged from 11.28 M–20.43 M (Table 3). As predicted, the uniform top distribution produced the lower boundary for the estimates and the skewed distribution the high boundary. With no EBA correction factor, an assumption of uniform distribution throughout the beam, the resulting passage estimates fell within the range of the other estimates, but were most similar to the estimates using the video depth distribution.

Table 3.–Estimates of smolt passage using the 3 depth distributions and 2 scalers.

Depth Distribution	Acoustic Scaler (M)	Video Scaler (M)
Uniform Top 1.2 m	11.28	13.95
Video	12.38	15.31
Skewed in Top 0.4 m	16.53	20.43
True Uniform (no EBA correction)	13.59	16.80

## COMPARISON OF THE BENDIX AND NEW SYSTEMS

The Bendix smolt counter and BioSonics' sonar were both operated from May 18–June 10, 2001. Differences between the daily smolt passage estimates from the 2 systems were so large the 2 variables could not be plotted on the same axis. The 2001 Bendix estimate was 325.9 M. Nighttime Bendix estimates (defined as 2200–0600 hours) ranged from 1–26 times higher than the side-looking BioSonics' estimates. Daytime Bendix estimates showed dramatic increases on several days and ranged from 12 to 1500 times higher than the BioSonics' estimates. A 7-fold adjustment to the scale of the axis for the night estimates and an 80-fold adjustment for the day estimates allow the data from both systems to be plotted together (Figure 25). With this adjustment, the time series shows a sequence of generally coinciding peaks similar in height from the 2 systems. Regression analyses using the BioSonics' data as the independent variable resulted in a slope of 6 for the night estimates and 72 for the day estimates with  $R^2$  values of 0.65 and 0.74, respectively. The day/night ratio of smolt passage estimates from the BioSonics' sonar averaged 0.4 and remained below or close to 1 for most of the sampling period, while the same ratio for the Bendix system averaged 3.1 with one peak exceeding 12 (Figure 26).

Smolt passage estimates obtained from the BioSonics' sonar in 2001 were highest from 75–110 m (measured from the transducer) peaking at 2,380 smolt/h in the 80–85 m range bin (video scaler and distribution). Smolt passage estimates dropped off sharply nearshore of 75 m. The lowest passage rate sampled (929 smolt/h) was measured at the closest range sampled (50 m). Figure 27 shows the cross-river distribution of smolt passage estimates, the near-surface current velocity, and the location of the Bendix arrays with the percentage of Bendix counts at each array. The percentage of smolt traveling across the Bendix arrays in 2001 was 22% at the 55 m nearshore array, 27% at the 78 m center array, and 51% at the 85 m offshore array. Mean Bendix hourly estimates were not available so an arbitrary value was chosen for the nearshore array and the percentages used to determine the center and offshore array values. The large increase in passage rates shown by the BioSonics' sonar were observed in the offshore Bendix array, but the expected increase was not observed in the center Bendix array. Current velocity varied little, ranging from 1.16 to 1.38 m/s, much less than the variation seen in the cross-river distribution of smolts, and was poorly correlated with the cross-river distribution ( $R^2 = 0.18$ ).

## DISCUSSION

### EVALUATION OF THE BENDIX SMOLT COUNTER

The functional description of the Bendix smolt counter (Appendix C) and an analysis of the methodology revealed potential inconsistencies in both areas. Although the electronics of the counter were calibrated annually, a single validation experiment was performed, and was not repeated when significant changes were made to the counter or when the system was moved to a new site. We identified several sources of bias in the counter, first tackling the issue of how the daytime smolt passage estimates from the Bendix smolt counter could be 80 times higher than the estimates from the new system.

Historically Bendix estimates of smolt passage have been higher at night, except during 1996, 1999, 2000, and 2001, when the overall daytime estimates were higher. In 2001, the Bendix daytime estimates were 3 times higher than at night. The video data (Figures 14 and 22) showed

that at night smolts outmigrated close to the surface except during the dark of night, which only lasts 3–4 h this time of year. During the day, smolts ran deeper. According to target tests, the calibration sphere was not detectable by the Bendix counters in the upper 10 cm of the water column. This surface limitation may have reduced smolt detection during the time periods when they were close to the surface. If the counter's validation was performed during periods when the smolts were near the surface, counts made during deeper smolt periods (daytime) would be amplified. The 10 cm detection limit widened during wind and rain events, which required reducing the Bendix's vertical sampling range.

Passing boats may amplify the daytime count. Boat traffic occurred mostly during the day and has increased substantially in recent years. We examined the Bendix estimates, but found no relationship between documented boat passage and high daytime counts (personnel communications Drew Crawford, ADF&G's Kvichak River Sonar Project Leader). The voltage contribution from passing boats was difficult to quantify because the echo strength depended on the boat's direction of travel, size and location, and the Bendix operator's response. When the operators were away tending the fyke net, the built-in boat detector automatically disabled the counter in response to passing boats for a preset period of time. Later, operators reviewed the counts and edited out suspected false counts. If present, the Bendix operators switched off the counter when a boat passed, relying on the counter's blinking red lights to dictate when the boat was sufficiently out of the counting range. According to the functional description of the counter, the red light threshold is 1 dB lower than the count threshold, implemented at the level of an individual transducer. The count threshold receives the summed voltage from each half-array. This makes it possible for the red light threshold to be triggered without triggering counts and vice versa. For example, if one transducer returns voltage, the voltage may be high enough to trigger a red light, but remain below the count threshold, i.e., the red light will flash, but no counts are generated. In the reverse situation, counts may be generated without flashing the red lights if the transducers return signal below the red light threshold, but above the half-array count threshold. The potential bias created by the differences in the 2 thresholds is unknown.

In 1993, the 1976 Model Bendix smolt counter was replaced by a higher frequency, 1982 Model counter because an obsolete printer failed and could not be serviced (Crawford and Cross 1994b; Appendix A). The newly installed counter may have picked up more reverberation from entrained air near the surface caused by either wind or wave events, or passing boats. Reducing the threshold would offset these disturbances, but would not entirely filter the noise echoes from the data. The calculated threshold of the Bendix system was -66 dB, 11 dB below the BioSonics' threshold. A 10 dB threshold change is illustrated in BioSonics' echograms (Figure 28) for boat-induced reverberation. Although no definitive link could be established between higher boat traffic and increased daytime Bendix counts, data from June 3, 2001 showed that boat reverberation increased the Bendix counts 27% over non-edited counts for the same period (personal communication Drew Crawford, ADF&G, retired Commercial Fisheries Biologist). When few smolts were present, noise events of this magnitude were obvious, but when large numbers of dispersed smolts were passing the site, distinguishing noise events embedded in the Bendix counts would be more difficult. During periods of high smolt passage, it is likely that noise events elevated the counts.

The vertical placement of the Bendix transducers on the mounts and the beam sizes were coordinated to sample specific river depths. Our calculations of beam width and water depth at the existing site showed that the beams overlap by 6%. It appears that the system was sized for

the first sample site, and it is unclear whether this was taken into account when the sampling location was changed in 1989. Error in the estimates from this overlap is small relative to the observed difference between the Bendix and BioSonics' estimates, but the magnitude of the overcount depends on conditions. When smolts are close to the surface, overcounting will be greater, suggesting that the Bendix nighttime estimates should be amplified. The increased signal amplitude due to this overlap would also be more sensitive to boat noise or other sources of entrained air.

The difference in scale between the nighttime Bendix and BioSonics' estimates may be related to the equipment and site changes made after the initial validation took place. The functional description of the Bendix smolt counter provided a better understanding of how the counter operates, but the key operational component relates back to the initial validation. Because smolt counts from fyke net catches were used to tune the electronics, the sonar parameters are less important. There are 2 (or more) potential flaws in the initial validation process. First, smolt may exhibit net avoidance. Second, the validation does not address the issue of the cross-river distribution and where to place the arrays. There were no further validation tests performed following the change in frequency and beam size or the move to a new site. Annual calibrations with the smolt simulator only test the machine's electronics, not potential effects created by changes to the equipment and environment. After all the changes took place, more testing should have ensued to re-calibrate the equipment.

The video data showed the average smolt velocity to be similar to the current velocity. The Bendix counter uses a smolt velocity 0.34 m/s faster than current speed to determine smolt estimates, potentially inflating the estimates by a factor of 3. During the validation of the Bendix smolt counts, the smolt velocity may have been one of the parameters used to correct the count. After the site and equipment were changed, all of the parameter settings and assumptions became suspect.

## **EVALUATING SONAR ASSUMPTIONS**

New information regarding how smolts behave as they outmigrate past the sonar site did not agree with many of the assumptions inherent in the Bendix estimate. The smolt velocity was not greater than current speed, the depth of outmigrating smolts was not wholly within the sampling range of the Bendix transducers, and the assumed cross-river distribution, i.e., the linear transition between transducers and a linear drop to zero from the end arrays to shore, was incorrect. The video data and echograms provided the behavioral information to test the Bendix assumptions, and determine whether a side-looking acoustic system would be feasible. The side-looking sonar has its own assumptions including: a uniform depth distribution, consistent up-down smolt aspect, a deep enough river segment to fit the side-looking beam across the region of smolt passage, and reliable target strength information for scaling the echo integrals.

The video data showed that the depth distribution of smolt was not uniform, but skewed toward the surface. This skewness increased as the acoustic beam spread. All smolts were observed within the top 100 cm of the water column and most were in the top 30 cm. This created problems for the up-looking HTI array of transducers. Target testing showed that the transducers were unable to sample the top 30 cm. This surface 'dead' zone was greater than predicted considering the beam curvature and short 0.1 ms pulse length. The system's power level may have been the culprit. We ordered a 2000 Watt system because of the long sampling range

required by the side-looking transducer. A low-powered, up-looking system with a narrower beam and short pulse length should eliminate the near-surface sampling problem. This was not a problem for either the HTI or BioSonics' side-looking transducers. Both transducers were able to detect a target dimpling the surface across most of the transducer's range. We got around the nonuniform depth distribution by adjusting the equivalent beam angle using the video depth distribution.

The TS information from the HTI system was unexpected. Because smolts are not consistently oriented in the nose-upstream direction, we expected smaller TS values from the side-looking system when compared with the up-looking system. Although the model TS from the side-looking sonar was 8 dB less, mean TS values from the side-looking and up-looking sonars were essentially the same. The smolt behavior data showed that the orientation of smolt was predominately in the nose-upstream direction during the highest density periods (Figure 16), but there were enough side-aspect orientations to expect an observable reduction in the side-looking TS values.

Fitting an acoustic beam into the narrow water column at the site proved to be difficult. We found that the maximum range of the HTI's 3° circular beam ended within a region of high smolt passage. When the BioSonics' system was ordered, we requested a 2° circular beam. Narrow acoustic beams are difficult to engineer, and the developers were unable to keep the side lobes low. Two-way beam pattern plots showed side lobes less than 10 dB. Because of the high side-lobes, echoes reflected from the water's surface reached well above the threshold creating noisy echograms from 20–50 m. The reverberation from the surface movement was dynamic enough that we were unable to subtract it from the remaining echoes, so we started the integration process at 55 m and extrapolated the estimates from 55 m to within 9 m of shore. This problem was resolved the following field season by adding on a second transducer with a larger beam and lower side lobes to ensonify the nearshore region.

The acoustic-video system has several advantages over the Bendix smolt counter. The side-looking sonar sampled 40% of the river cross-section compared to the 7.5% sampled by the Bendix counter, which makes the system more robust to changes in the cross-river smolt distribution. The BioSonics' sonar displays and stores echograms used to identify noise or other potential problems in the data and provides information on individual echoes such as angular position and amplitude. But most important, the BioSonics' sonar is serviceable. We are no longer able to maintain and repair the Bendix counter.

### **Problems Encountered**

We encountered several problems in addition to those already discussed. Upriver winds and moderate to heavy rains resulted in lost sampling time for the up-looking and side-looking sonars. The bubbles in the near-surface layer of the river created by these events overshadowed all other echoes, making echo integration of the side-looking data during these events impossible. For the up-looking Bendix counter, the range was reduced during these events to prevent false counts. If the depth distribution during these events was known, estimates from an up-looking system could be expanded accordingly. However, neither acoustic nor video methods were capable of assessing smolt near the river's surface during severe wind and rain events, and the affects of these disturbances on smolt behavior is unknown. Regardless of whether a side-looking or up-looking system is used, reverberation echoes from wind and rain events will occasionally prevent the collection of usable data.

Another equipment-related problem experienced during sampling was a reduction of 10 dB in signal intensity of the BioSonics' system. The lower intensity data was deleted from the dataset and the missing data interpolated from surrounding data. The problem was fixed by the vendor following the field season.

Video data analyses proved to be very time-intensive. Although this process has the potential to be automated, a fair amount of development time would be required. As an alternative to video data, information on smolt velocity, depth distribution, and an independent flux estimate could be collected with an up-looking sonar provided the system was equipped with a narrow beam, short pulse width, and low power output. The sample size could be increased dramatically with an up-looking sonar, and the system could be used throughout the night providing more complete information on the diel patterns of smolt.

We did not account for time-dependent changes in the depth or cross-river smolt distributions. The video data indicated a diel pattern in the smolt depth distribution, skewed towards the surface during dusk and dawn, and more uniform during the day and mid-night. Using a mean smolt depth distribution will underestimate flux during dusk and dawn and overestimate flux during the day and mid-night. Differences in the smolt depth distribution across the sampling range will have a similar effect. Sampling smolt behavior using video or acoustic techniques for longer time periods and at multiple ranges would allow us to better understand and potentially correct this type of error.

## **ACOUSTIC-VIDEO COMPARISON**

We examined the effects of 2 parameters on the smolt passage rates, the selected depth distribution and the type of scaler used. The differences in parameter selection resulted in the estimate range from 11.28–30.43 M. Although we looked at the depth distribution obtained from the side-looking acoustic system, the positional information from the split-beam system was poor, and the distribution was discarded. In a ranked order of the remaining depth distributions, the lowest passage estimates came from the uniform top distribution, followed by the video, true uniform, and skewed distributions. As we expected, the estimate from the video distribution fell between the uniform top and skewed distributions. Because the sample size from the video data was small and range-limited, we were unable to rule out the possibility that the true estimate may be closer to either modeled distribution. Our results placed the estimate derived from the video depth distribution closer to the uniform top distribution than the skewed distribution.

Although the side-looking BioSonics' depth distribution was poor, target strength values from this system appeared to be adequate. The acoustic and video scalers were less than 1 dB apart, well within the noise of the system. The BioSonics' single target data showed similar target strengths by range and hour of the day enabling a single TS value to be used to scale all the echo integrals. This agrees with the HTI information suggesting there is little difference between up-looking and side-looking systems for obtaining target strength. The acoustic and video scalers were more similar than expected because the 2 estimates were taken across different sampling periods, and the 2 sampling systems were not perfectly aligned. The acoustic scaler was taken from the entire sampling period, while the video scaler came from a very small subset of the same period. Error from the acoustic and video biases, and the uneven alignment of the 2 systems was not quantified.

Our comparison of the small sample of overlapping video and acoustic counts was encouraging. Although 95% confidence intervals around the regression slope did not include one, there was a strong relationship between the datasets. There were several potential reasons for the differences between the video and acoustic estimates. The first, and perhaps most important, was the potential for error in the transducer tilt angle. According to the tilt sensor, which has a stated accuracy of  $0.4^\circ$ , the transducer was pitched at an angle of  $-0.6^\circ$ . If the true tilt angle was  $0^\circ$ , the smolt passage estimates would be 0.8 times smaller, if  $-1^\circ$  the estimates would double (Mueller et al. 2006). The uncertainty associated with the transducer's tilt angle increases if the smolt distribution is more skewed towards the surface and when the transducer is tilted at angles steeper than  $-1^\circ$ . This source of error can be reduced by using a more accurate tilt sensor.

Surprisingly, the true uniform distribution with no EBA correction was close to the video distribution. The difference between this estimate and what we considered to be the 'true' video estimate were so small that it may be reasonable to assume no EBA correction is needed at this site, i.e., across the range of the acoustic beam, the skewed distribution may become smooth. The EBA correction factors were close to one with relatively small changes across the sampled range interval.

Inaccurate smolt velocity estimates will also bias the passage estimates. An increase in smolt velocity translates to higher estimates. Accurate information on smolt behavior, provided by the video data, was needed to determine the velocity factor used in the density to flux conversions.

## **FUTURE STUDIES**

To address the problems with upriver winds, the wide and relatively flat river bottom, and other site-specific issues, we relocated in 2002 to a new site (Figure 1). Site selection was based on aerial photographs, a bathymetry survey, land use issues, and our knowledge of the river. The channel at the new site is straighter, narrower, and deeper, and the river bottom is more uniform, making the site more suitable for the side-looking sonar. At the prior site, the strongest current and subsequently, larger portion of smolt passage occurred along the far bank, outside the range of the Bendix arrays. A single side-looking acoustic beam can encompass close to 100% of the river at the new site compared to the existing 40% coverage. The river flows in a west-southwest direction, which may help reduce wind-induced noise. At the prior site, the river flows in a northwesterly direction where periodic southeasterly winds blow upriver creating larger disturbances in the surface layer.

We deployed the side-looking BioSonics' system in 2002 and 2003 at the new site. A second transducer ( $4^\circ$  single beam) was added to compensate for the high side-lobes of the  $2.3^\circ$  beam. We did not collect video data in 2002 and only obtained a few days of acoustic data because a late break-up and river-wide ice flows prevented the collection of data during the traditional sampling period. In 2003, we deployed the video cameras, but were unable to obtain detectable smolt images even during the clearest water conditions because of the stronger current and increased water depth. Although the analyses of the 2003 data are not complete, preliminary results indicated the tilt angle may be a much larger source of error than previously supposed. Acoustic results from the 2003 data will be summarized in a later report.

At the new site, a validation method for the side-looking sonar is needed, along with an independent method of determining the smolt depth distribution. A low wattage, up-looking, narrow beam sonar could be used to obtain this information at the deeper site. However, an

alternate technique that could measure the smolt depth distribution during surface disturbances would help reduce the uncertainty in the estimates during these periods. Neither the up-looking sonar nor video would provide usable information during these environmental events.

Our studies have not provided a methodology to correct the historical Bendix estimates. We do know that the Bendix estimate from 2001 was greatly amplified, with the daytime and nighttime comparisons vastly different from each other. More studies need to be done if the historical Bendix estimates are to be salvaged. We offer the following suggestions:

1. Compare the old and new Bendix smolt counters in a controlled environment (initial tests were performed, but the data has not yet been analyzed).
2. Group the historical Bendix estimates by site, counter model, and day versus night. For each grouping, analyze the consistencies and anomalies within the hourly estimates.
3. Repeat the initial validation tests performed by Al Menin at the 2001 site. (Note: the water depth at this site and the 2002 site may be too deep to fish a fyke net.)
4. Run a boat over the Bendix arrays at multiple ranges when no smolt are present and record the length of time the counter counts echoes, and analyze the counts obtained.
5. Collect paired data from the Bendix smolt counter at the 2001 site and the side-looking sonar at the new site. A longer comparison series might provide additional answers on how to correct the historical dataset.

The results of this study suggest that sampling smolt with a side-looking acoustic setup is feasible. Because environmental differences can affect both smolt behavior and the effectiveness of the acoustics, site-specific validation tests, accurate tilt angle information, and an independent means of acquiring the depth distribution information need to be part of sampling programs at a new site. At the Kvichak site, more data is needed to demonstrate the repeatability of this approach. Longer sampling periods with an alternative method (video or up-looking sonar) will better capture diel patterns. Multiple sample locations across the river for this alternate method will help understand and address range-related issues.

## **ACKNOWLEDGMENTS**

Fred Tilly provided logistical support, collected and edited the sonar data, trained the crew on how to operate the sonar, and assisted in the collection of the video data. Tim Mulligan and Robert Kieser devised the methodology for applying echo integration to a distribution that is not randomly distributed. Ed Belcher examined the Bendix counter, interviewed Al Menin on its operation, provided beam plots for the individual transducers, and wrote a functional description of the Bendix counter. Peter Dahl calculated theoretical target strength values for both calibration spheres. The Kvichak River crew, Susan McNeil, Brian Holder, Andrew Johnson, Susan Klock, and Corrie Whitmore assisted with the data collection. Lowell Fair, Robert Kieser, Nancy Gove, Debby Burwen, and April Faulkner provided editorial comment.

## REFERENCES CITED

- Bue, B. G., D. L. Bill, W. A. Bucher, S. M. Fried, H. J. Yuen, and R. E. Minard. 1988. Bristol Bay sockeye salmon smolt studies for 1986. Alaska Department of Fish and Game, Division of Commercial Fisheries, Technical Fishery Report 88-15, Juneau.
- Clay, C. S., and H. Medwin. 1977. *Acoustical Oceanography: Principles and Applications*. John Wiley & Sons, New York.
- Crawford, D. L., J. D. Woolington, and B. A. Cross. 1992. Bristol Bay sockeye salmon smolt studies for 1990. Alaska Department of Fish and Game, Commercial Fisheries Division, Technical Fisheries Report 91-2013, Juneau.
- Crawford, D. L., and B.A. Cross. 1994a. Bristol Bay sockeye salmon smolt studies for 1992. Alaska Department of Fish and Game, Commercial Fisheries Division, Technical Fisheries Report 94-19, Juneau.
- Crawford, D. L., and B. A. Cross. 1994b. Bristol Bay sockeye salmon smolt studies for 1993. Alaska Department of Fish and Game, Commercial Fisheries Division, Regional Information Report 2A94-14, Anchorage.
- Crawford, D. L., and B. A. Cross. 1997. Bristol Bay sockeye salmon smolt studies for 1996. Alaska Department of Fish and Game, Commercial Fisheries Division. Regional Information Report 2A97-10, Anchorage.
- Crawford, D. L., and F. C. Tilly. 1995. Bristol Bay up-ward looking sonar sockeye salmon smolt enumeration project instruction manual. Alaska Department of Fish and Game, Commercial Fisheries Division, Regional Information Report 2A95-14, Anchorage.
- Crawford, D. L., and F. W. West. 2001. Bristol Bay sockeye salmon smolt studies for 2000. Alaska Department of Fish and Game, Division of Commercial Fisheries, Regional Information Report 2A01-12, Anchorage. <http://www.sf.adfg.state.ak.us/FedAidPDFs/RIR.2A.2001.12.pdf>
- Crawford, D. L. 2001. Bristol Bay sockeye salmon smolt studies for 2001. Alaska Department of Fish and Game, Division of Commercial Fisheries, Regional Information Report 2A01-27, Anchorage. <http://www.sf.adfg.state.ak.us/FedAidPDFs/RIR.2A.2001.27.pdf>
- Crawford, D. L., and L.F. Fair. 2003. Bristol Bay salmon smolt studies using upward-looking sonar, 2002. Alaska Department of Fish and Game, Division of Commercial Fisheries, Regional Information Report 2A03-17, Anchorage.
- Faran, J. J., Jr. 1951. Sound scattering by solid cylinders and spheres. *Journal of the Acoustical Society of America* 23:405-418.
- Hughes, N. F., and L. H. Kelly. 1996. New techniques for 3-D video tracking of smolt swimming movements in still or flowing water. *Canadian Journal of Fisheries and Aquatic Sciences* 53: 2473-2483.
- Huttunen, D. C., and P. A. Skvorc II. 1991. Kvichak River side-looking sonar smolt investigations, 1990. Alaska Department of Fish and Game, Division of Commercial Fisheries, Regional Information Report 5J91-04, Anchorage.
- Huttunen, D. C., and P. A. Skvorc II. 1992. Kvichak River side-looking sonar abundance estimation. Alaska Department of Fish and Game, Division of Commercial Fisheries, Regional Information Report 5J92-07, Anchorage.
- McCurdy, M. L., and R. D. Paulus. 1972. 1969 Kvichak River sockeye salmon smolt studies. Alaska Department of Fish and Game, Division of Commercial Fisheries, Technical Data Report 3:1-34, Juneau.
- Mueller, A. M., D. J. Degan, R. Kieser, and T. Mulligan. 2006. Estimating sockeye salmon smolt flux and abundance with side-looking sonar. *North American Journal of Fisheries Management* 26:523-524.
- Paulus, R. D., and K. Parker. 1974. Kvichak River sockeye salmon smolt studies. Alaska Department of Fish and Game, Division of Commercial Fisheries, Information Leaflet 166, Juneau.
- Simmonds, J., and D. MacLennan. 2005. *Fisheries acoustics theory and practice*, second edition. Blackwell Publishing, Oxford, UK. p. 32 and 243-245.
- Thompson, S. K. 2002. *Sampling*. Wiley series in probability and statistics. John Wiley & Sons, New York.
- Woolington, J. D., B. A. Cross, B. L. Stratton, and B. G. Bue. 1990. Bristol Bay sockeye salmon smolt studies for 1988. Alaska Department of Fish and Game, Commercial Fisheries Division, Technical Fisheries Report 90-16, Juneau.
- Woolington, J. D., B. A. Cross, and B. L. Stratton. 1991. Bristol Bay sockeye salmon smolt studies for 1989. Alaska Department of Fish and Game, Commercial Fisheries Division, Technical Fisheries Report 91-19, Juneau.

## **FIGURES**

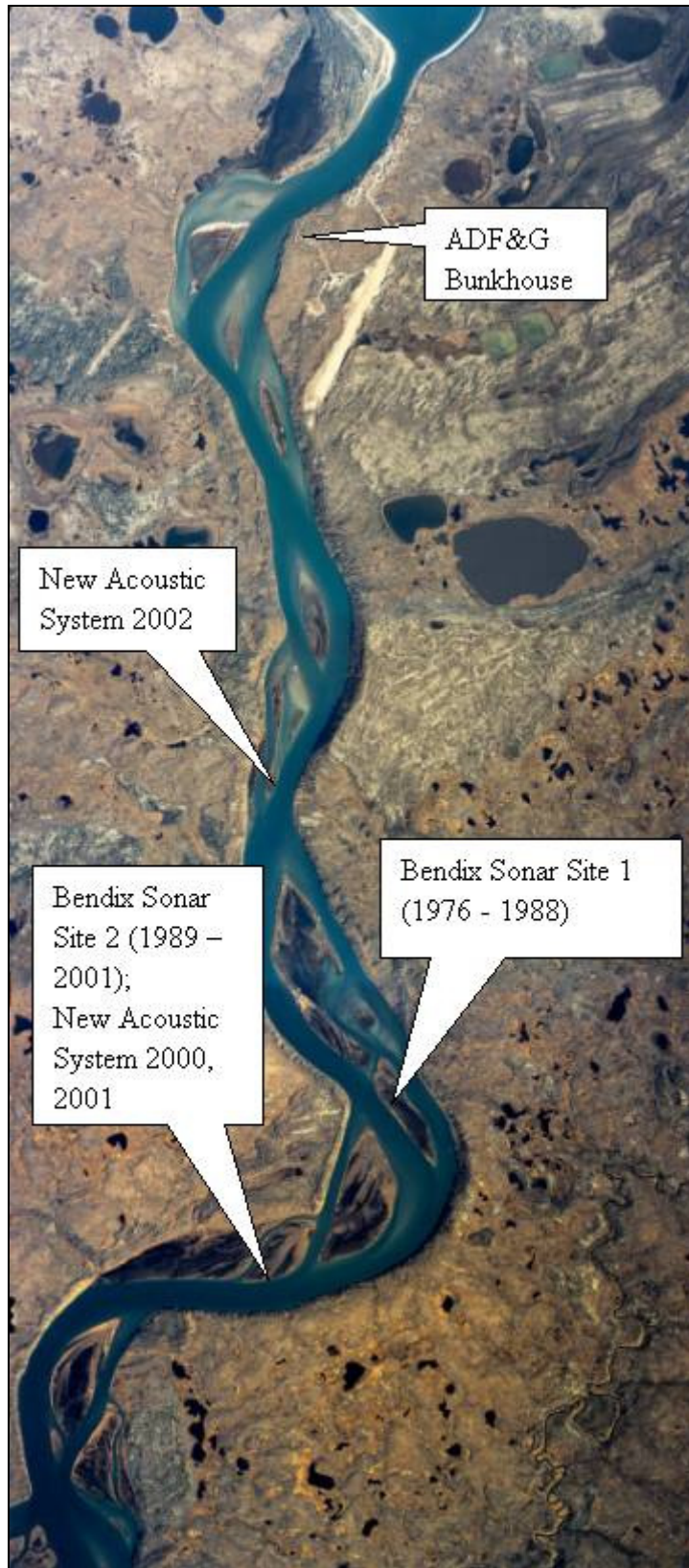


Figure 1.—Aerial photo of the Kvichak River showing the outlet of Lake Illiamna and the locations of each sonar site.

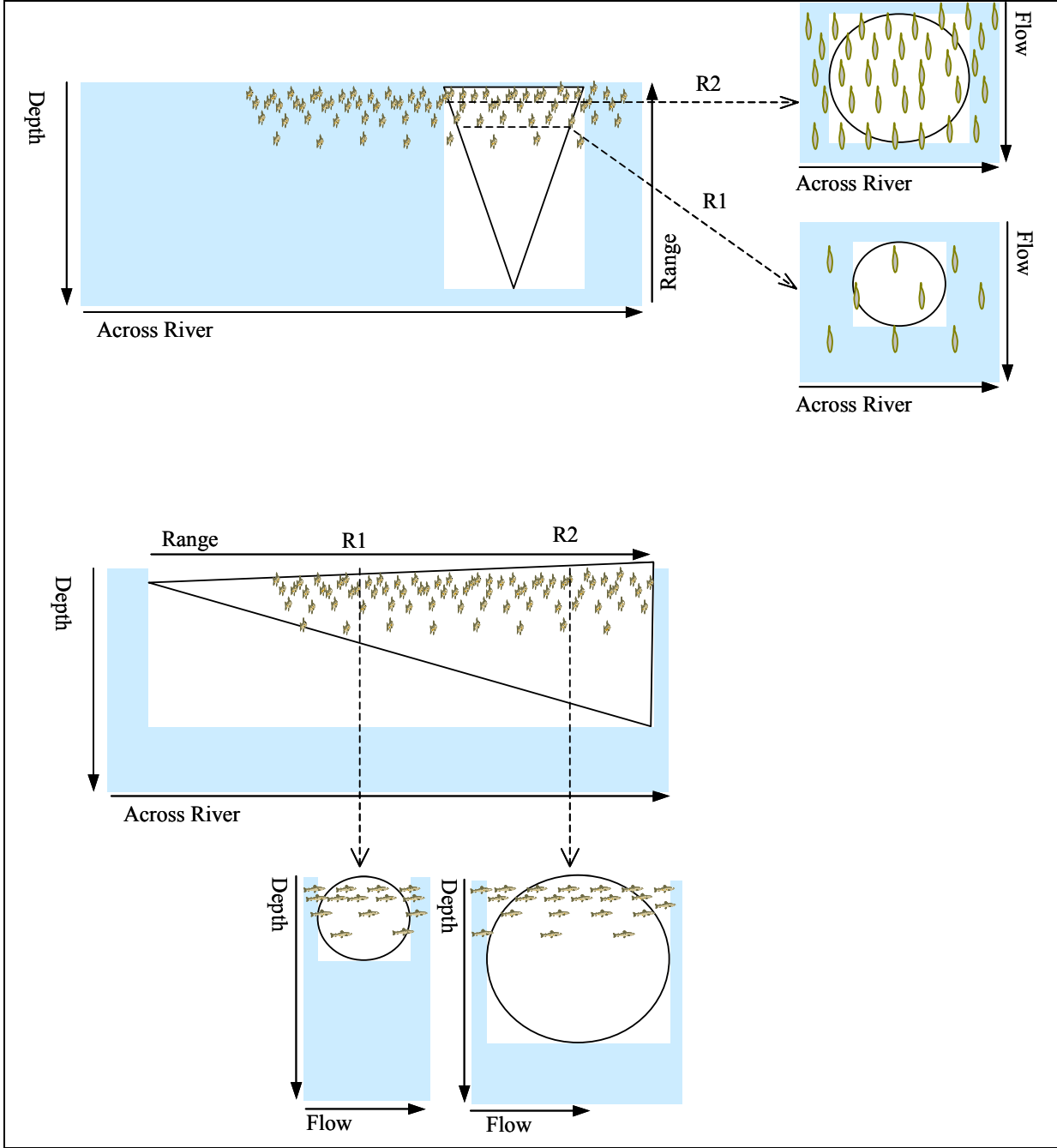
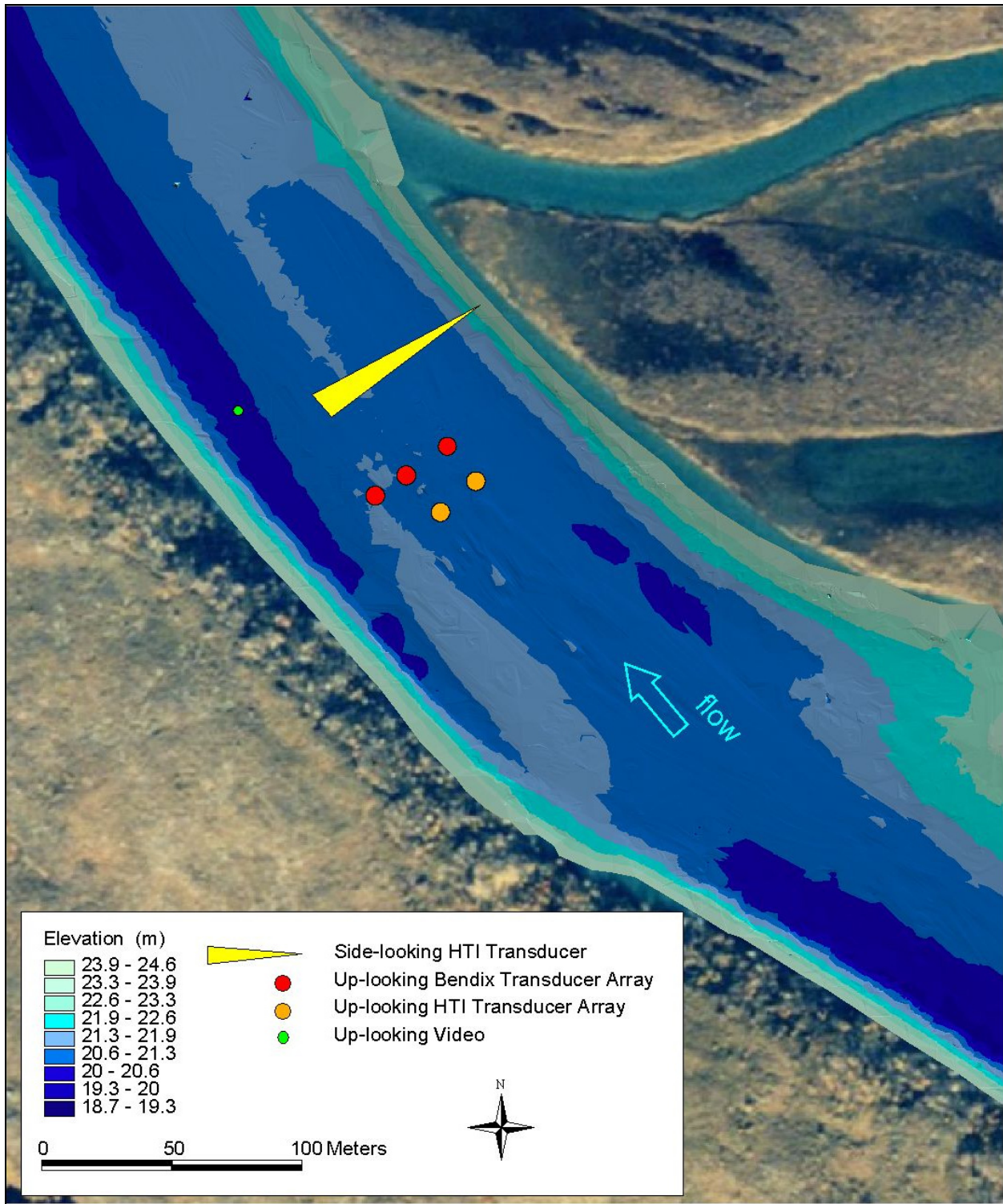
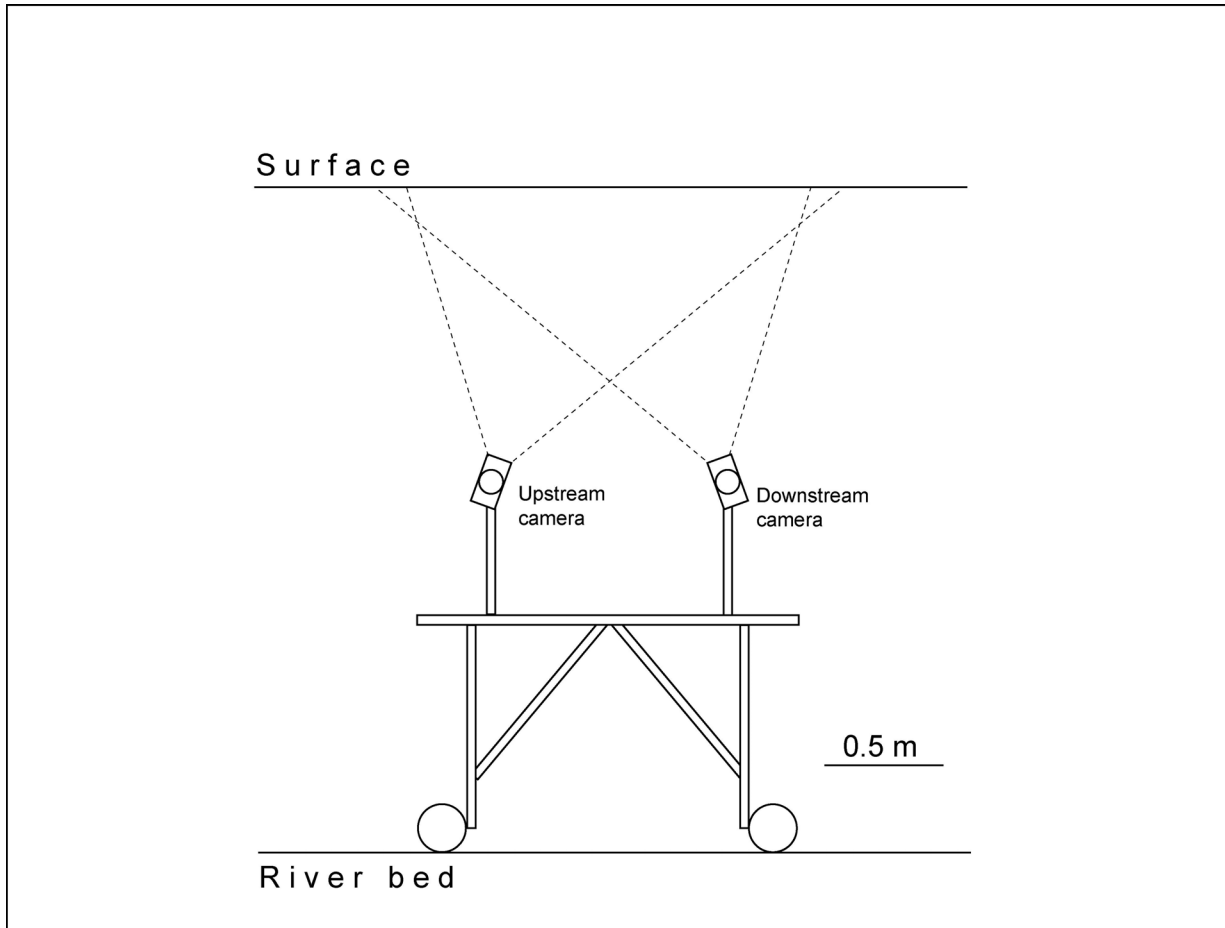


Figure 2.—An up-looking sonar (top) showing cross sections of the upstream-downstream plane of the sonar beam (top left) and the cross-river plane of the beam (top right) at 2 ranges (R1 and R2), and a side-looking sonar showing cross sections of the upstream-downstream plane of the beam (center) and the cross-river plane of the beam (bottom) at 2 ranges (R1 and R2).



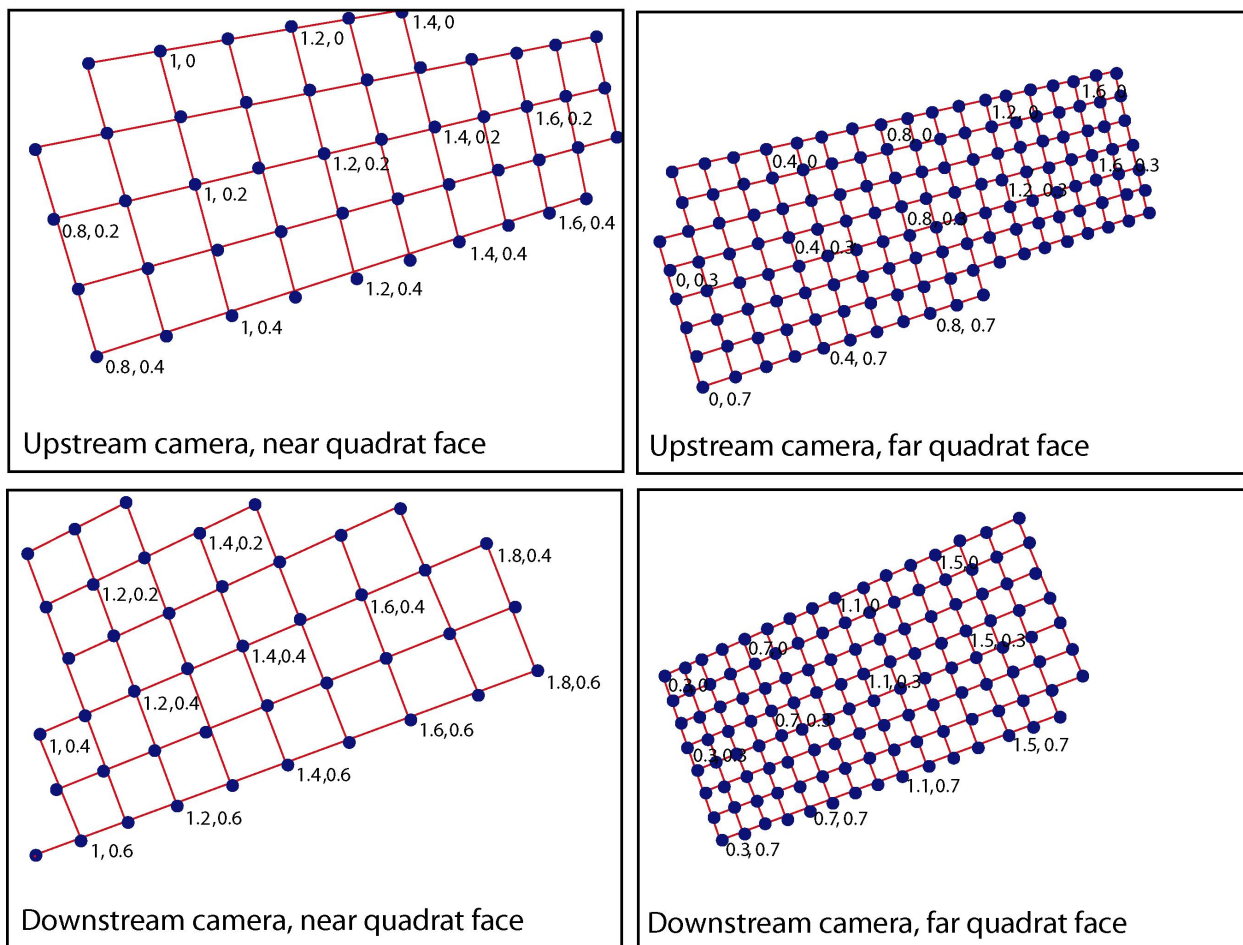
Note: The aerial photograph was taken in October 1989.

Figure 3.—The sampling locations used in 2000 based on bathymetry data collected in June 2000.



*Note:* The dotted lines show the field of view of the cameras. The river flows from left to right.

Figure 4.—Diagram of the video sled and cameras used in the Kvichak River, 2000.



*Note:* The upper panels show the location of visible nodes in the near and far faces of the quadrat as imaged by the upstream camera. The lower panels show the node locations imaged by the downstream camera. Selected nodes are labeled with quadrat x- and y-coordinates (in m), where x is the upstream/downstream axis, y is the cross-river axis, and the z-coordinates (depth axis) of the near plane and far planes of the quadrat are  $-1$  and  $0$ , respectively.

Figure 5.—Synchronous images of quadrat nodes in 2 camera views from the Kvichak River in 2000.

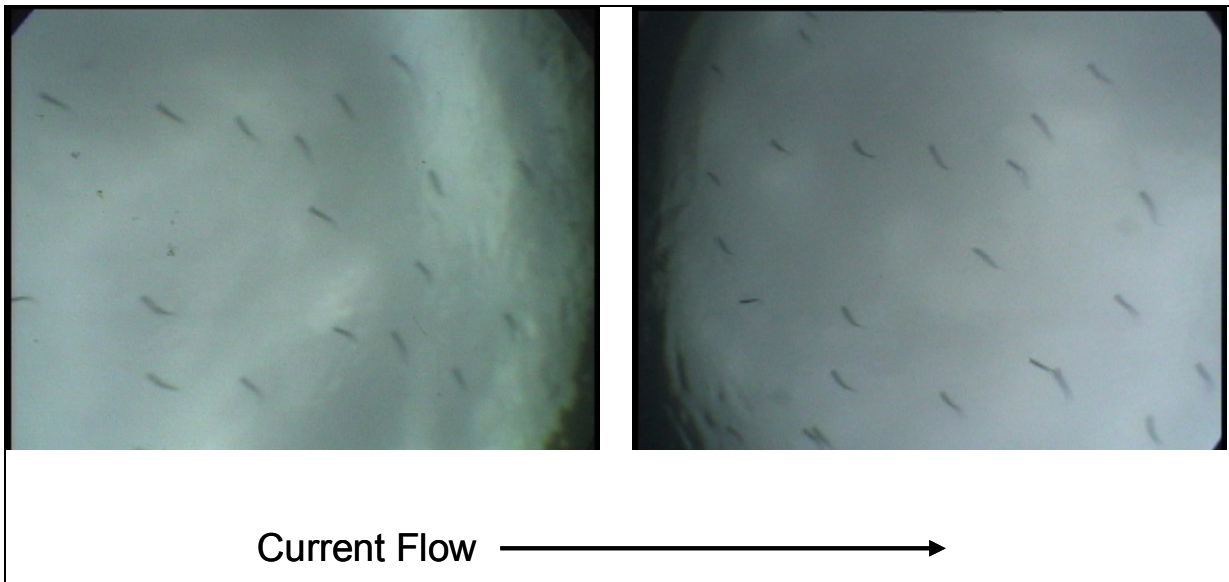


Figure 6.–Synchronous images of a smolt school passing over the upstream camera (left) and downstream camera (right) with clouds visible through the water’s surface and Snell’s window appearing on the inside of both images, Kvichak River, 2000.

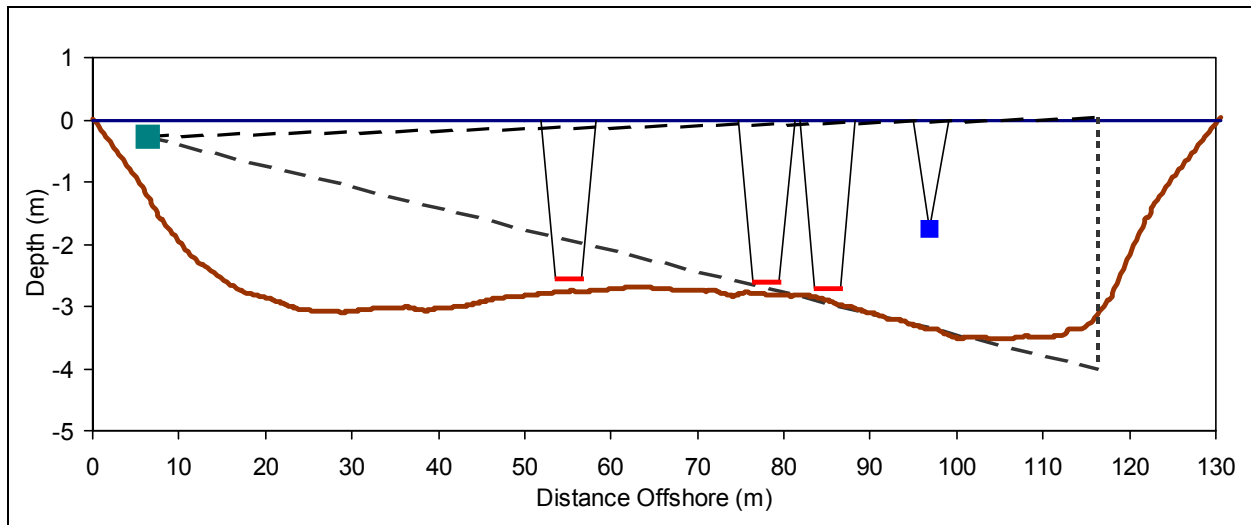
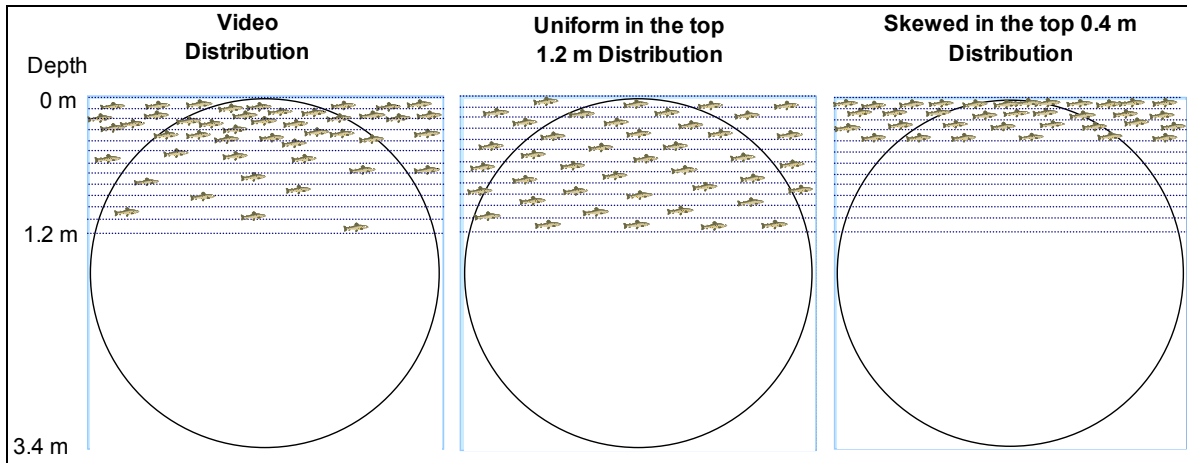
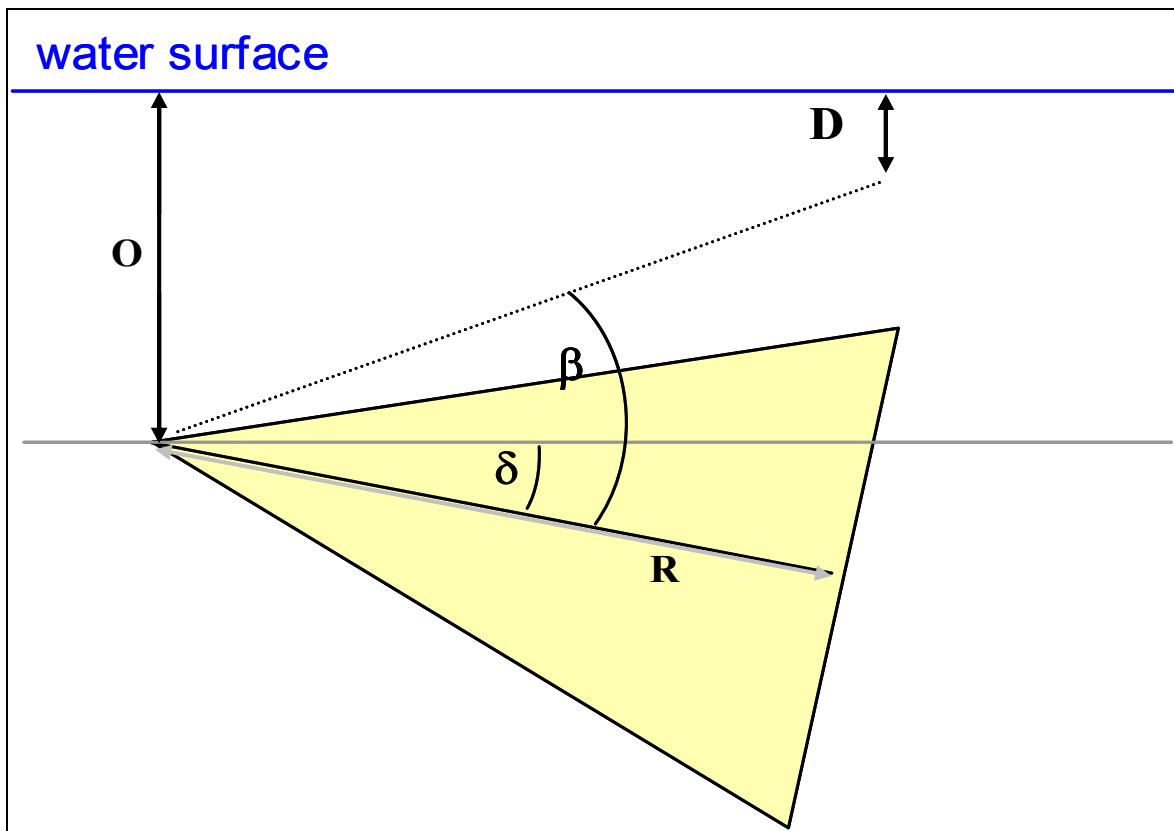


Figure 7.–Kvichak River bottom profile (thick line) from 2000 bathymetry data and the 2001 setup including the BioSonics’ side-looking transducer (large rectangle at 5 m), up-looking transducer arrays (short horizontal lines), video cameras (small square at 100 m) and approximate sampling areas of the cameras and transducers.



Note: The circles represent the side-looking acoustic beam with the upstream-downstream dimension running left to right and depth extending vertically. The horizontal dashed lines are 0.1 m divisions.

Figure 8.—Simulated smolt depth distributions at a range of 97.5 m from the transducer based on video observations and two modeled distributions.



Note: To convert the depth  $D$  of a boundary layer to the vertical split-beam angle  $b$  of Equation 5, we needed range  $R$  and the tilt angle  $d$  and depth  $O$  of the transducer.

Figure 9.—A cross-river slice of the side-looking acoustic beam diagramming parameters needed to calculate the vertical split-beam angles of the upper and lower boundaries of the 0.1 m depth strata shown in Figure 8.

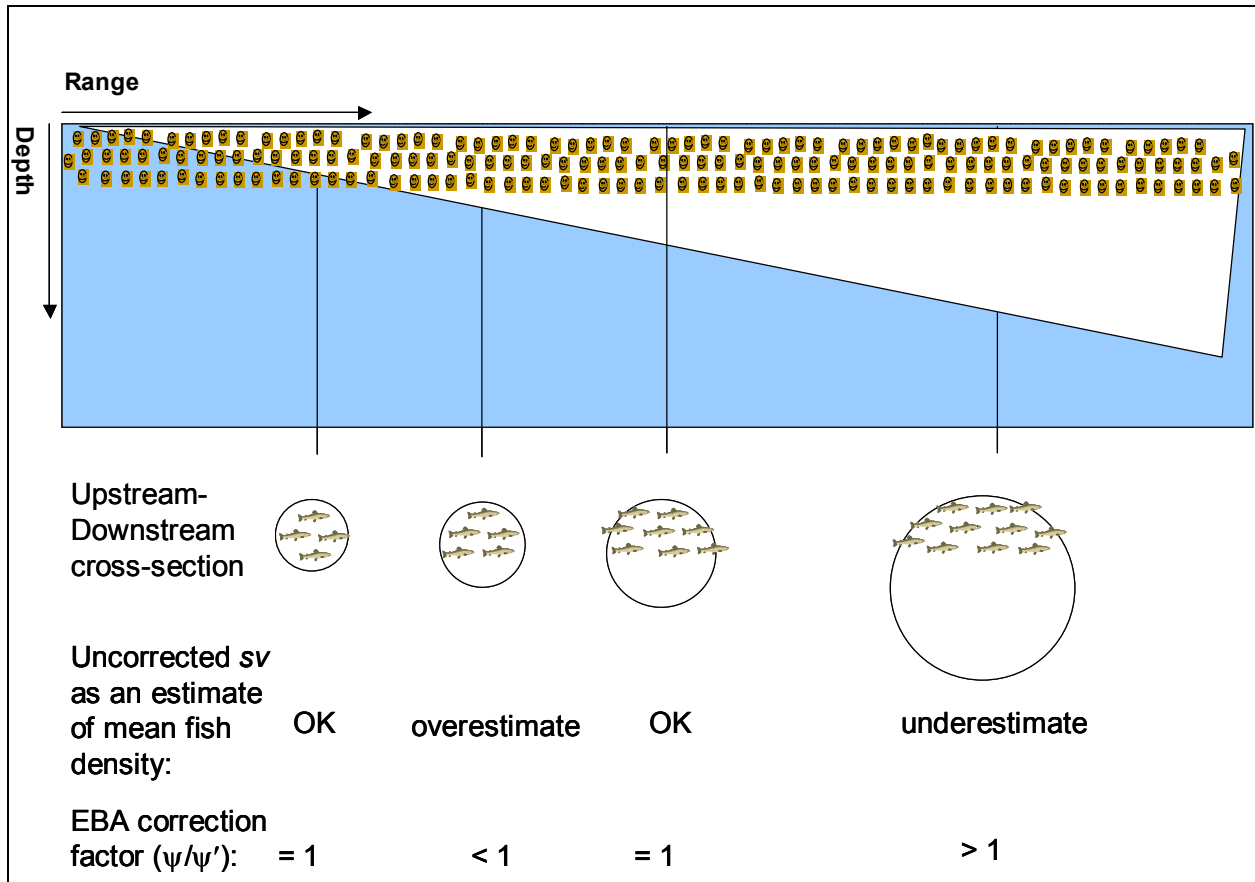
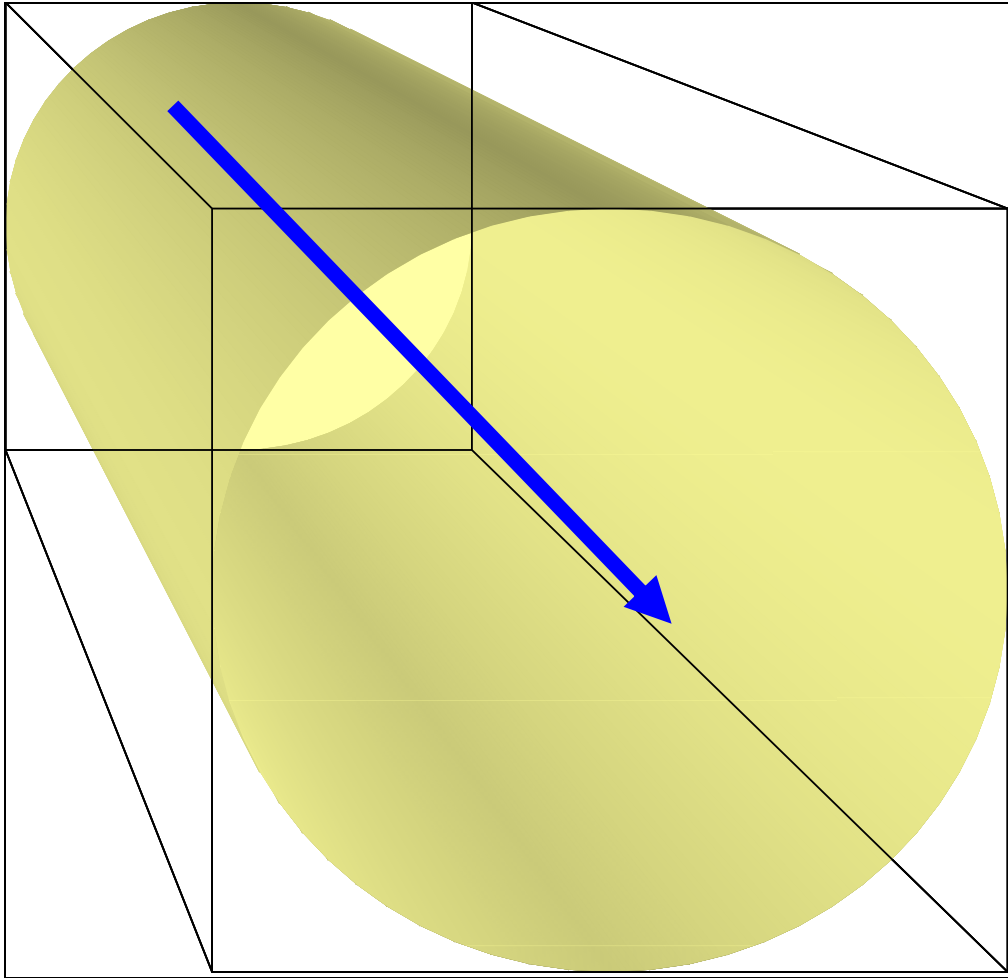
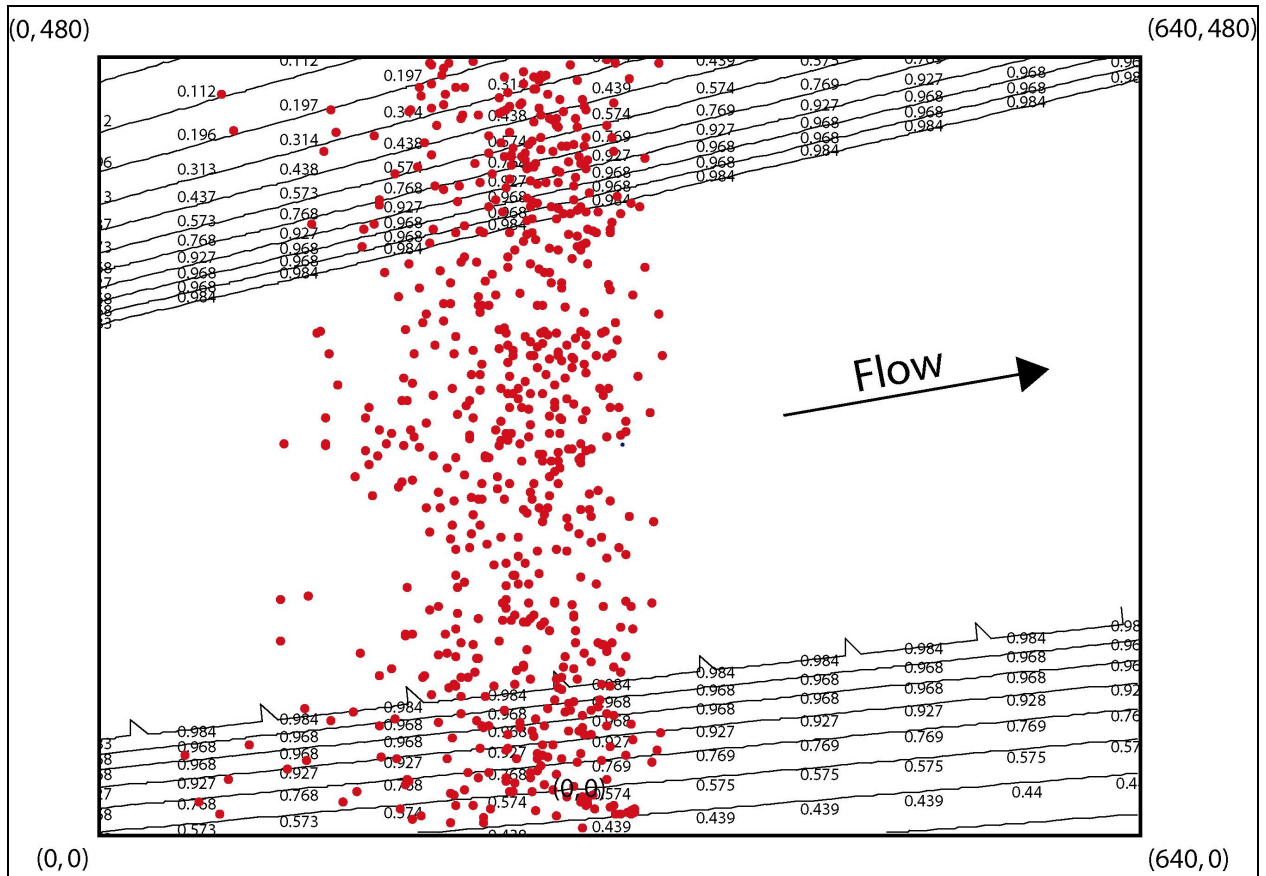


Figure 10.—A hypothetical smolt distribution uniformly distributed in the top 1.2 m of the water column shown against the acoustic beam, and the expected behavior of the equivalent beam angle (EBA) correction factor across the sampled range.



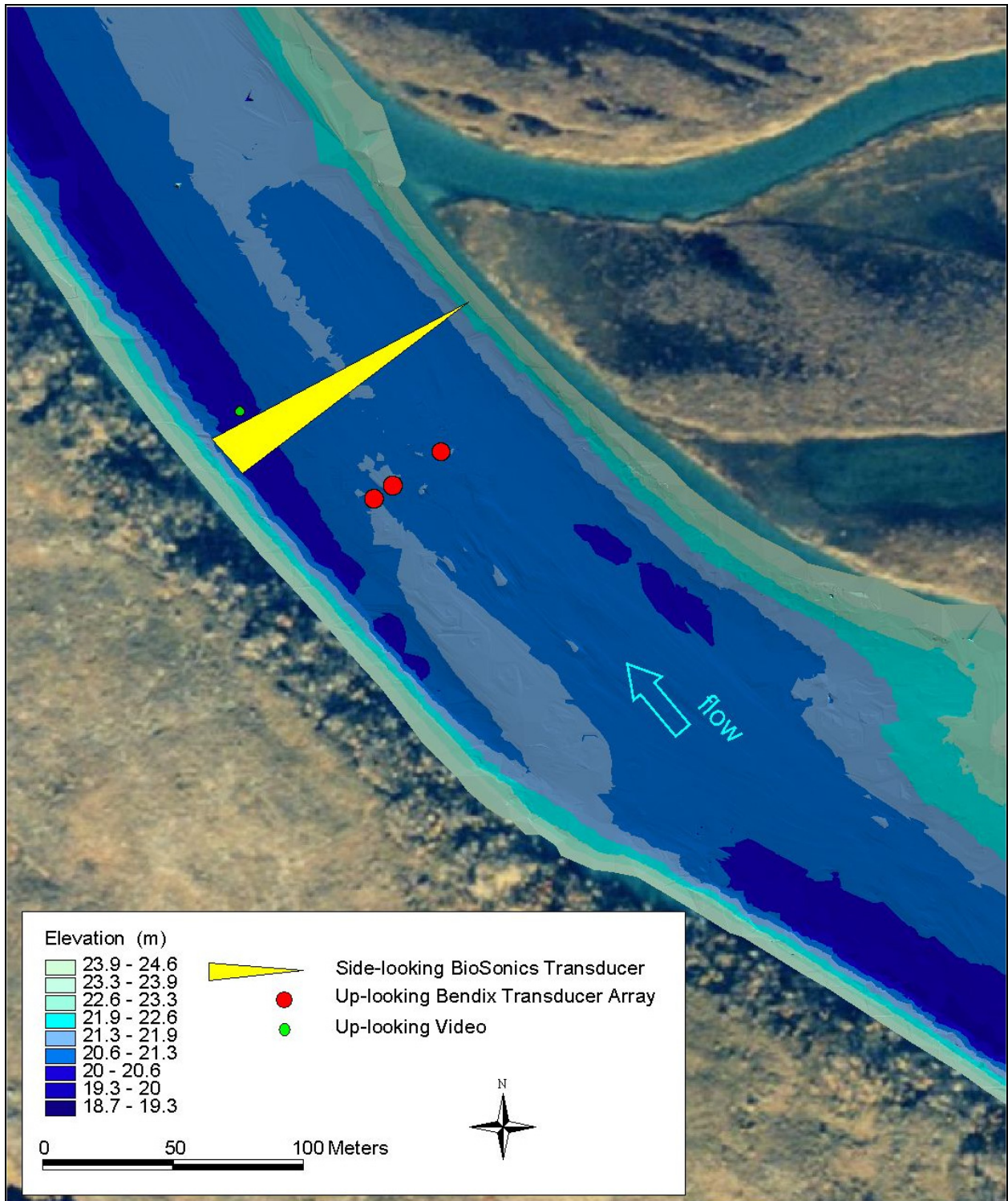
*Note:* At any given range, the cross section of the bounding polyhedron is perpendicular to the acoustic axis of the beam (shown as an arrow) and consists of a square encasing the circular beam.

Figure 11.—A conical beam shown with its bounding polyhedron.



*Note:* We defined a range bin using 2 vertical planes, parallel to the current and separated by 1 meter. The range bin is centered on the middle of the 640 x 480 pixel camera view. The uppermost line in the lower group of lines, and the lowermost line in the upper group show where the 2 planes defining the range bin intersect the surface of the water. Any smolts seen in the broad lane between these 2 lines must be within the range bin. The sloping lines successively nearer the bottom of the view or the top of the view show where the 2 planes defining the range bin intersect the horizontal plane at successively greater depths. In this case the depth interval is 0.1 m. The numbers between the lines show the probability that a smolt seen between 2 lines is actually within the range bin. We calculated these probabilities using information on the depth distribution of the smolts from the 3-D analysis and information on the 3-D geometry of the camera's field of view provided by the calibration quadrat. The red dots show nose and tail coordinates of smolts as they passed over the centerline of the field of view while the videotape was played in reverse (to give clearer images). Data are from May 22, 0603–0614. We estimated smolt passage rates by summing the probability that each of these points is in the range bin and dividing by 2. In this case 388 smolts passed across the field of view, and we estimated that 299 of these were within the range bin.

Figure 12.—A diagram of the procedure used to obtain smolt estimates from a single camera (2-D techniques) rather than 2 cameras in stereo.



Note: The aerial photograph was taken in October 1989.

Figure 13.—The 2001 sampling locations of the side-looking BioSonics’ system and the up-looking Bendix arrays overlaid on river bathymetry from June, 2000.

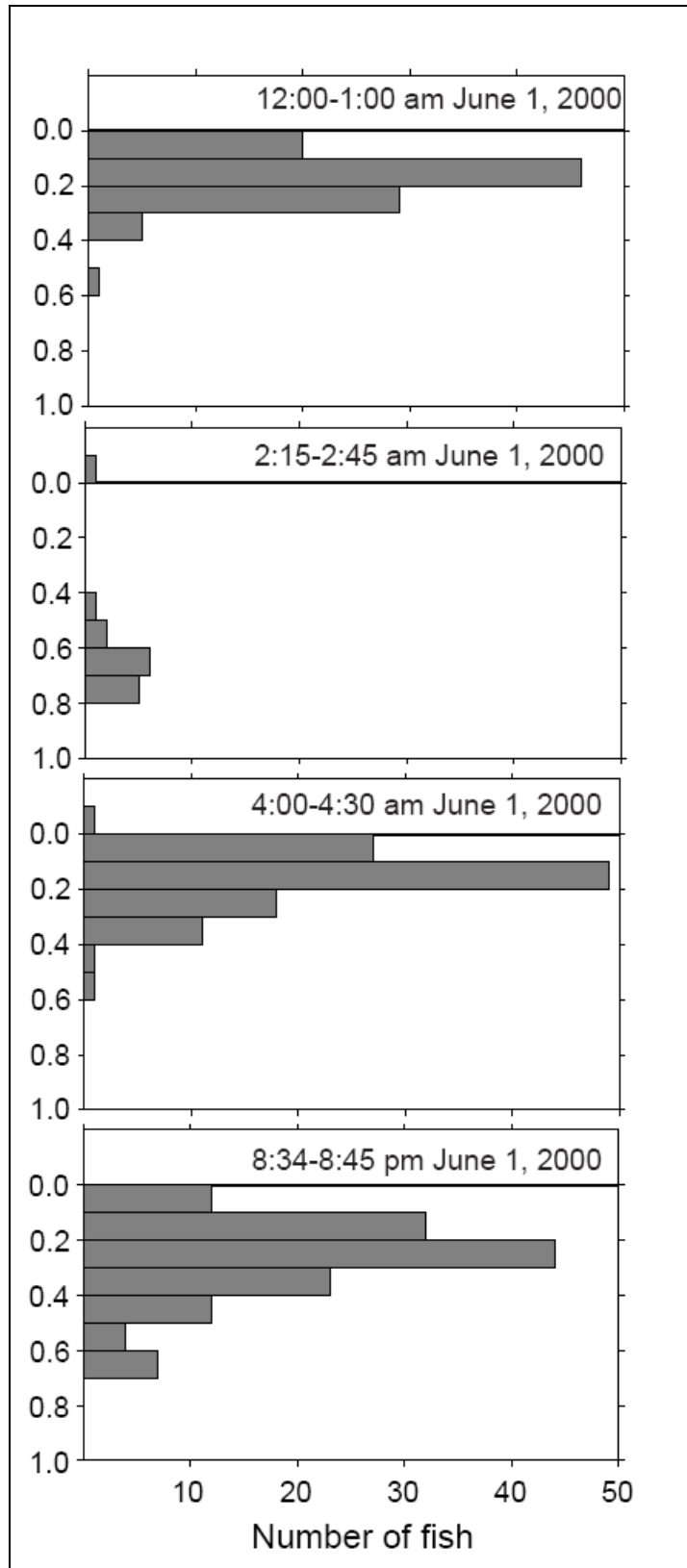


Figure 14.—Diel depth distribution of outmigrating smolt, Kvichak River, 2000.

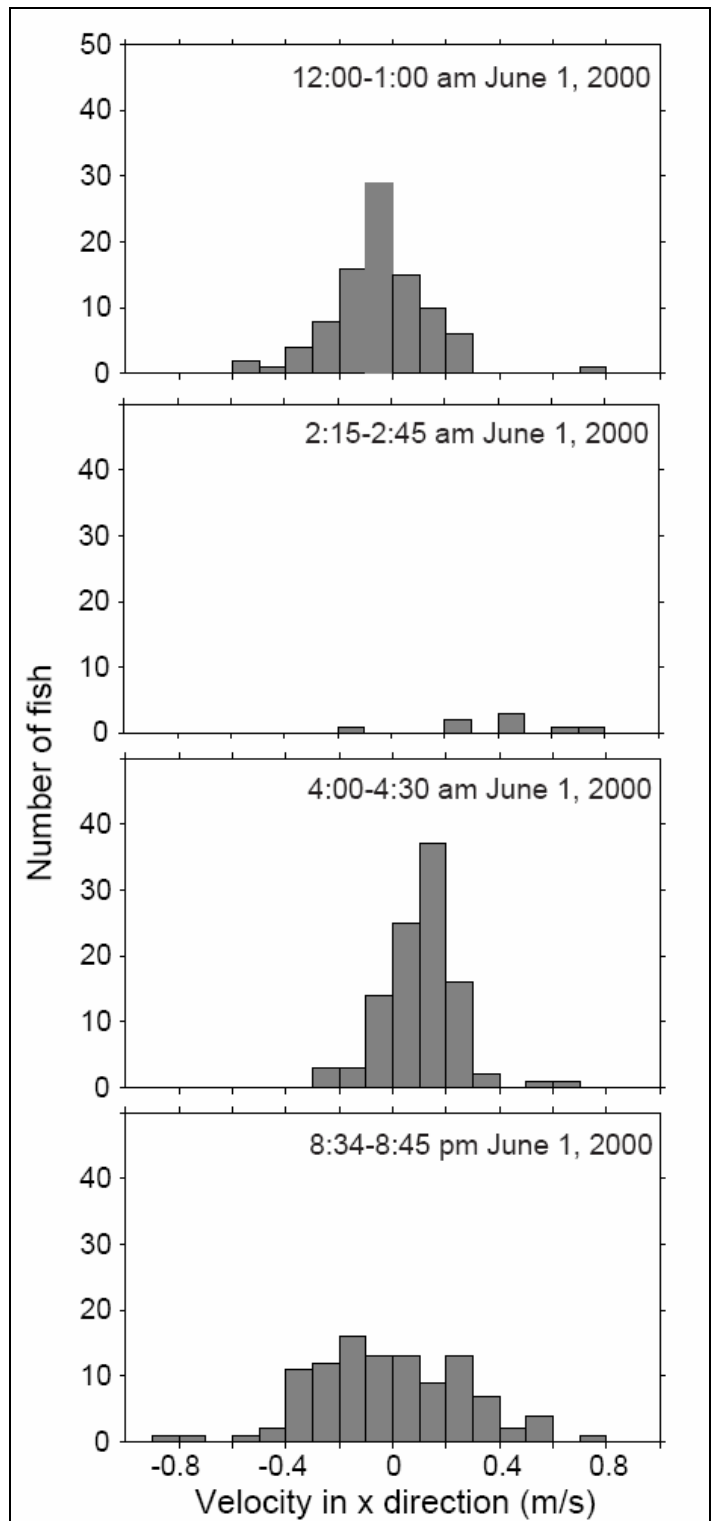


Figure 15.—Diel velocity of outmigrating smolt relative to current flow, Kvichak River, 2000.

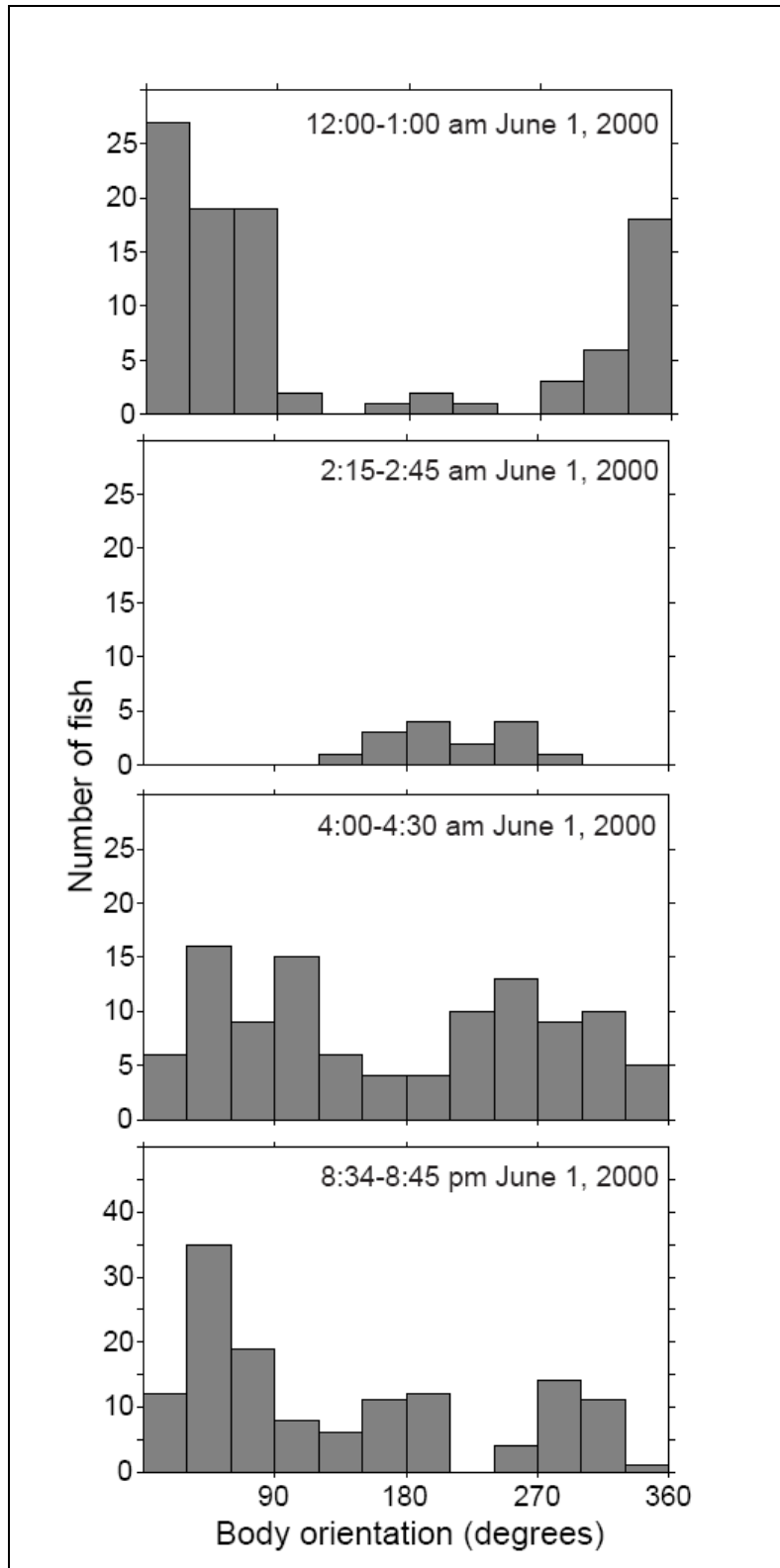
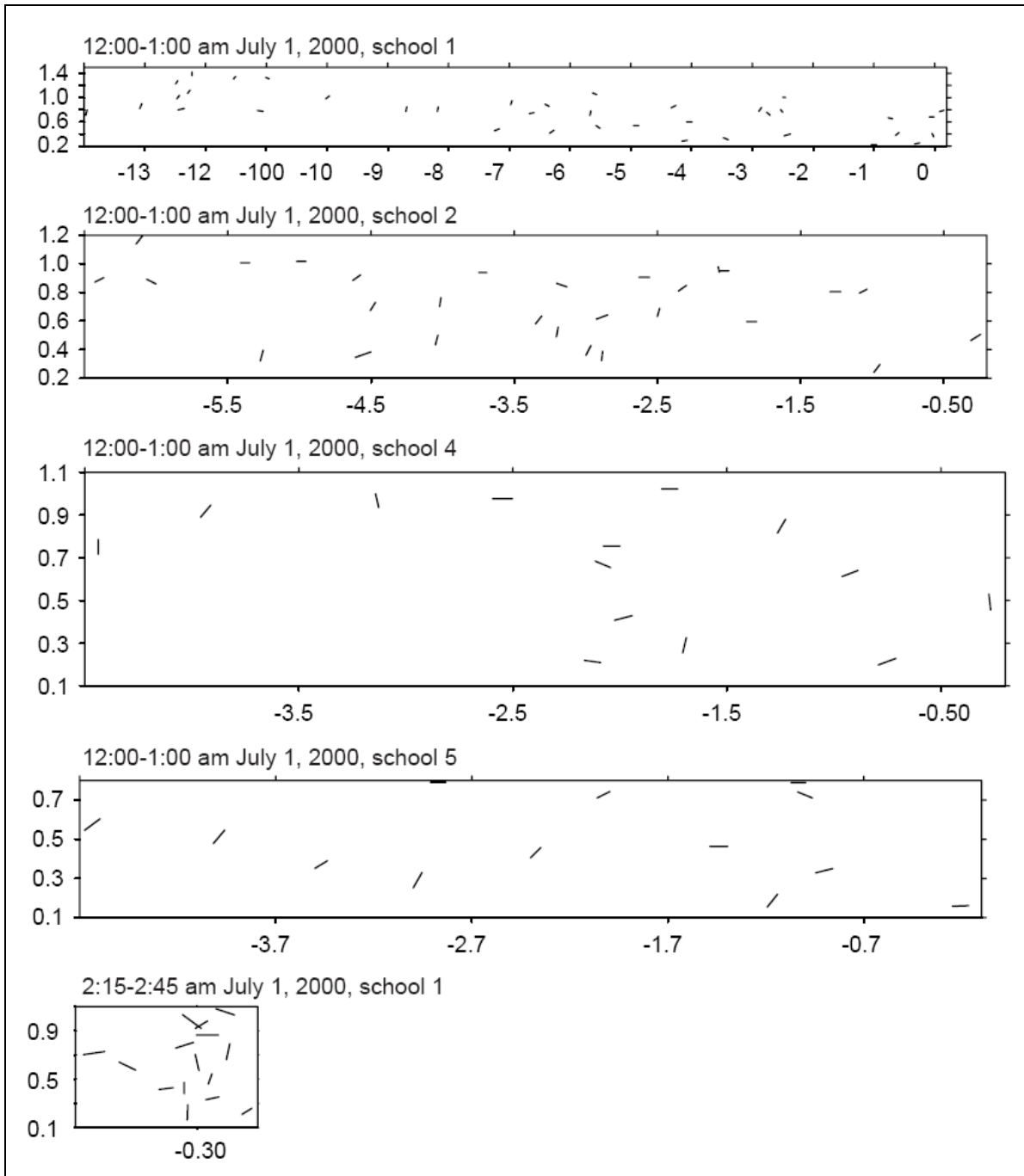


Figure 16.—Diel body orientation of outmigrating smolt, with 0° as the nose-upstream direction, Kvichak River, 2000.



Note: The x-axis represents the distance (m) between individual fish.

Figure 17.—School structure of outmigrating smolt, Kvichak River, 2000.

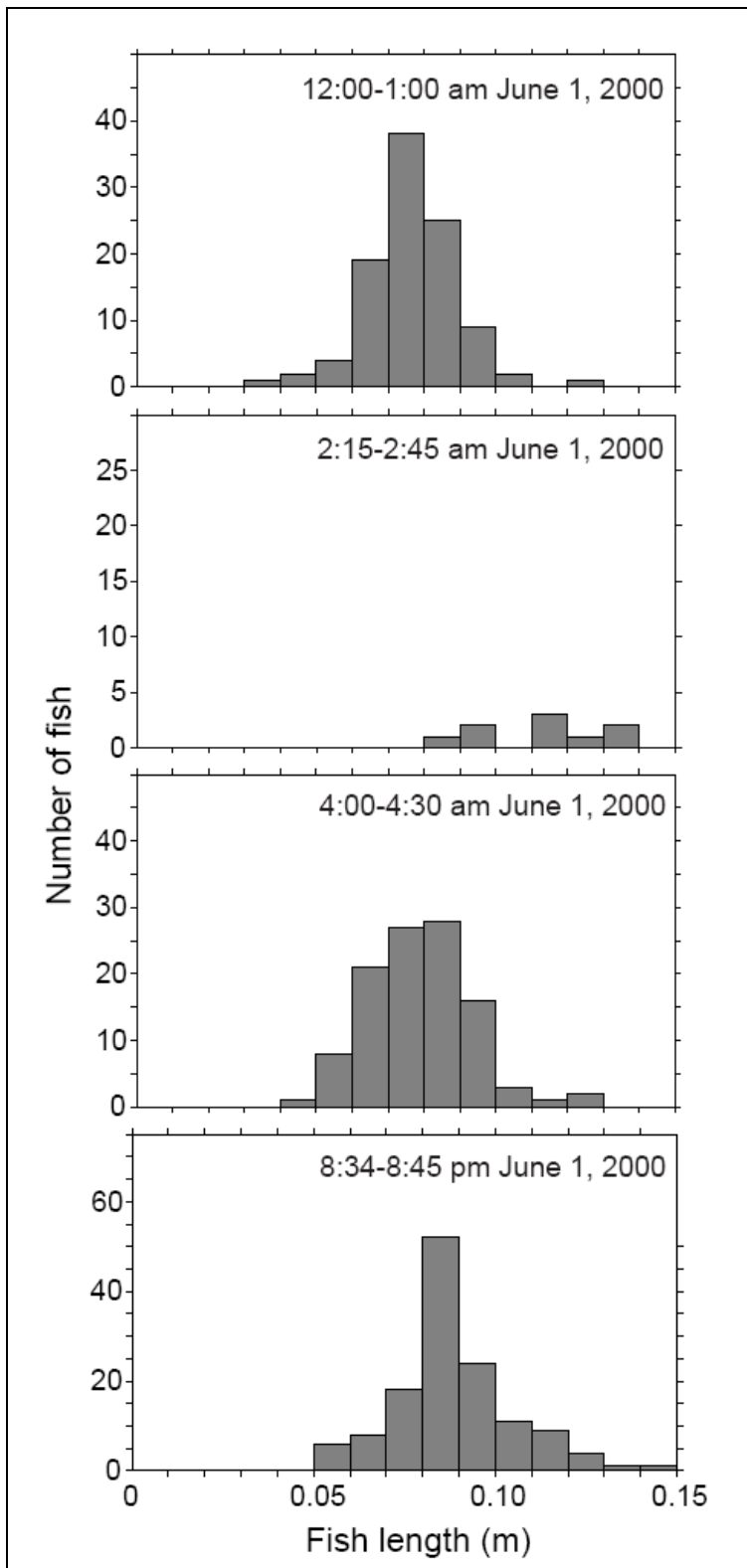
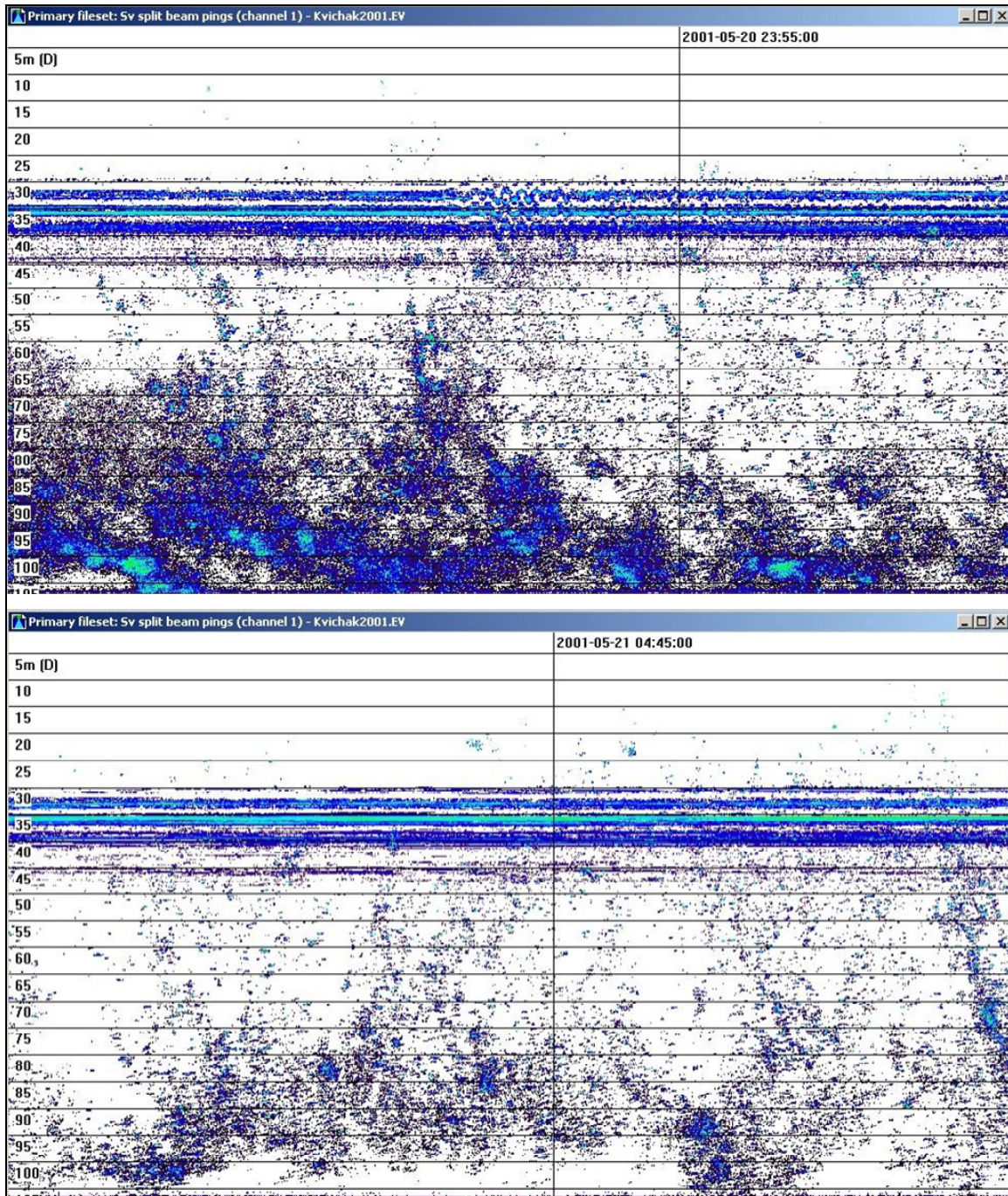
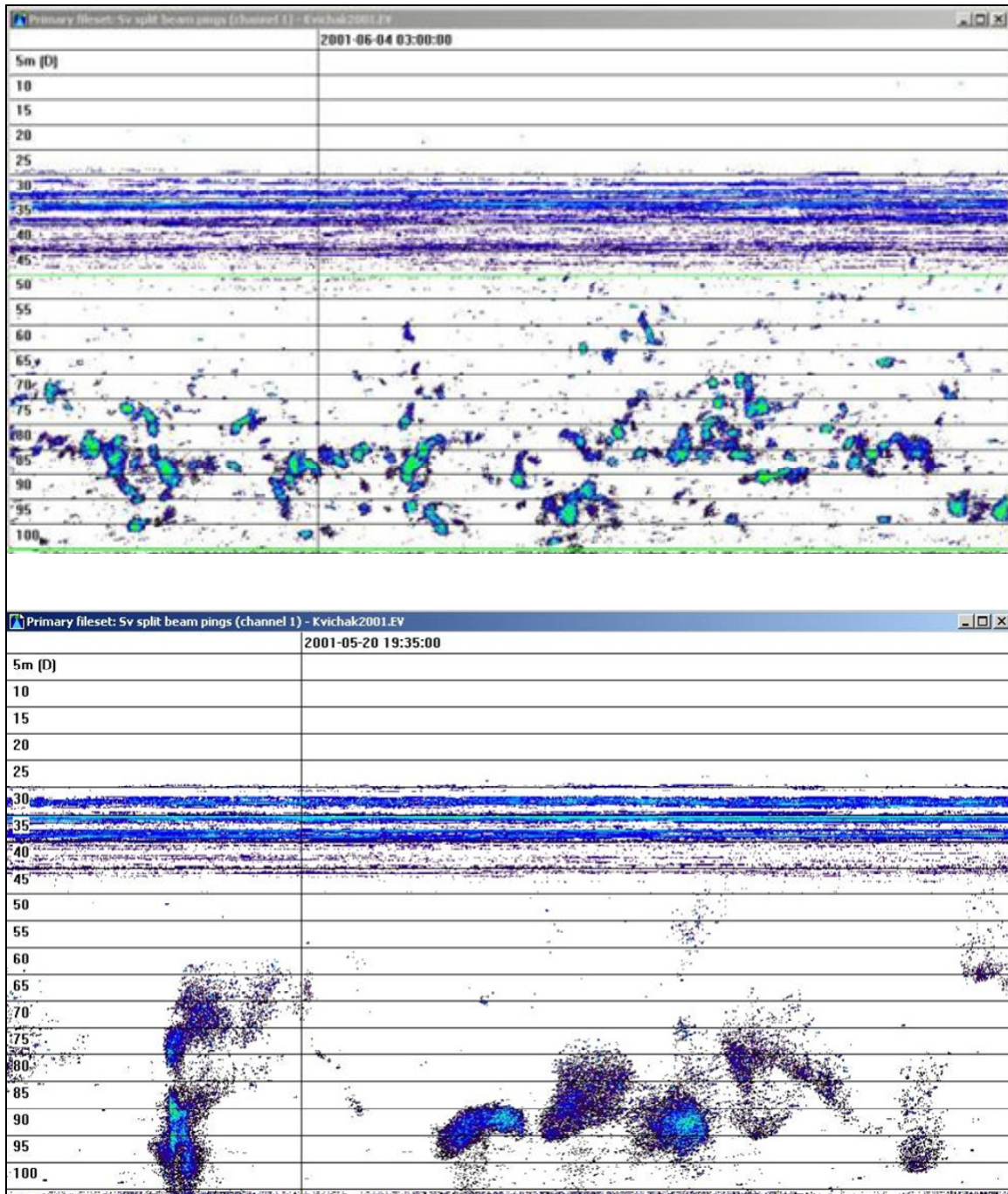


Figure 18.—Video length measures of outmigrating smolt, Kvichak River, 2000.



Note: The x-axis represents the ping interval (or time).

Figure 19.—Side-looking sonar echograms of outmigrating smolt during the late evening (top) and early morning (bottom), Kvichak River, 2001.



Note: Smolt are concentrated in range and congregated into dense schools. The x-axis represents the ping interval (or time).  
 Figure 20.—Side-looking sonar echograms of outmigrating smolt during the night (top) and day (bottom), Kvichak River, 2001.

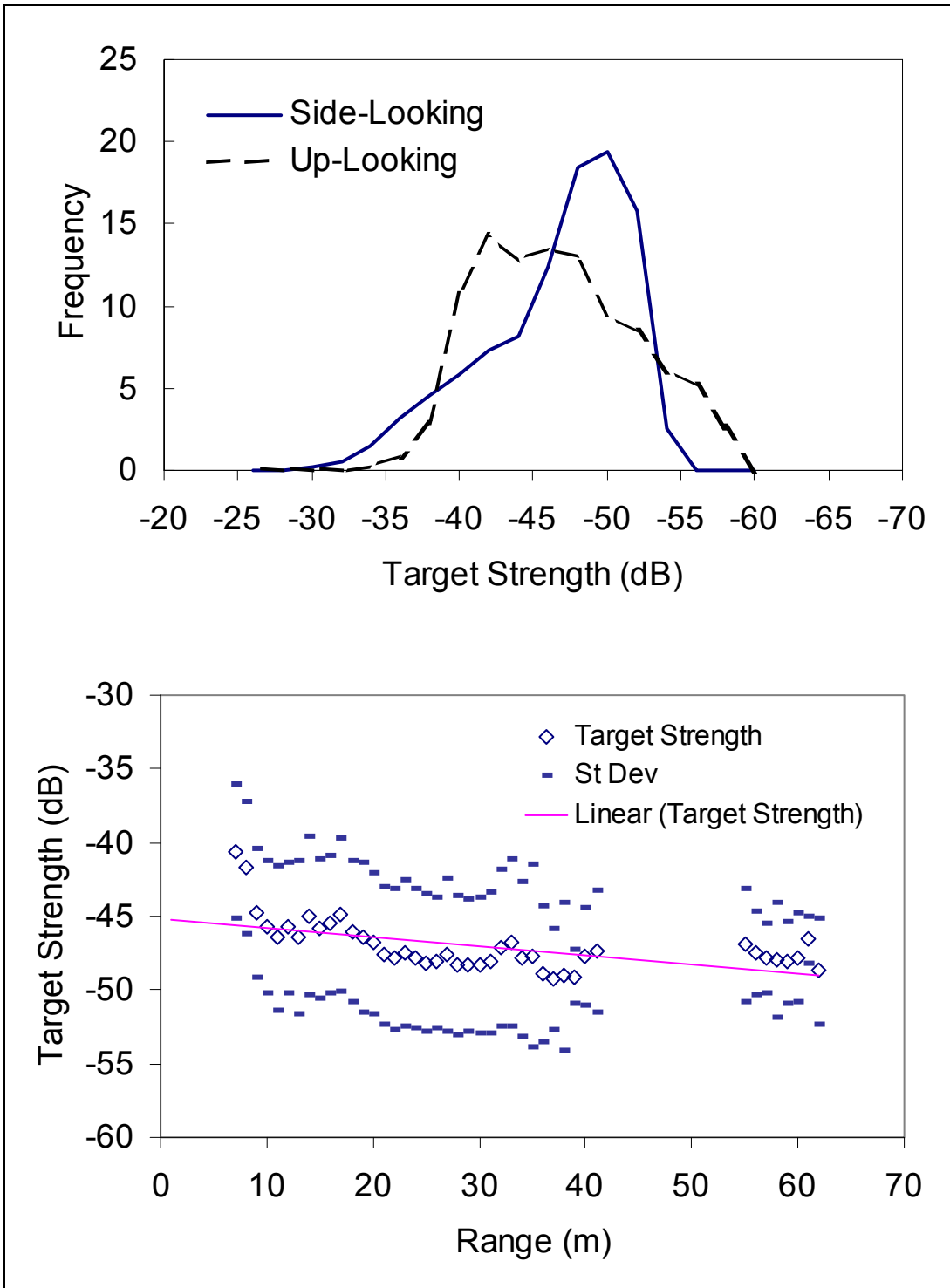
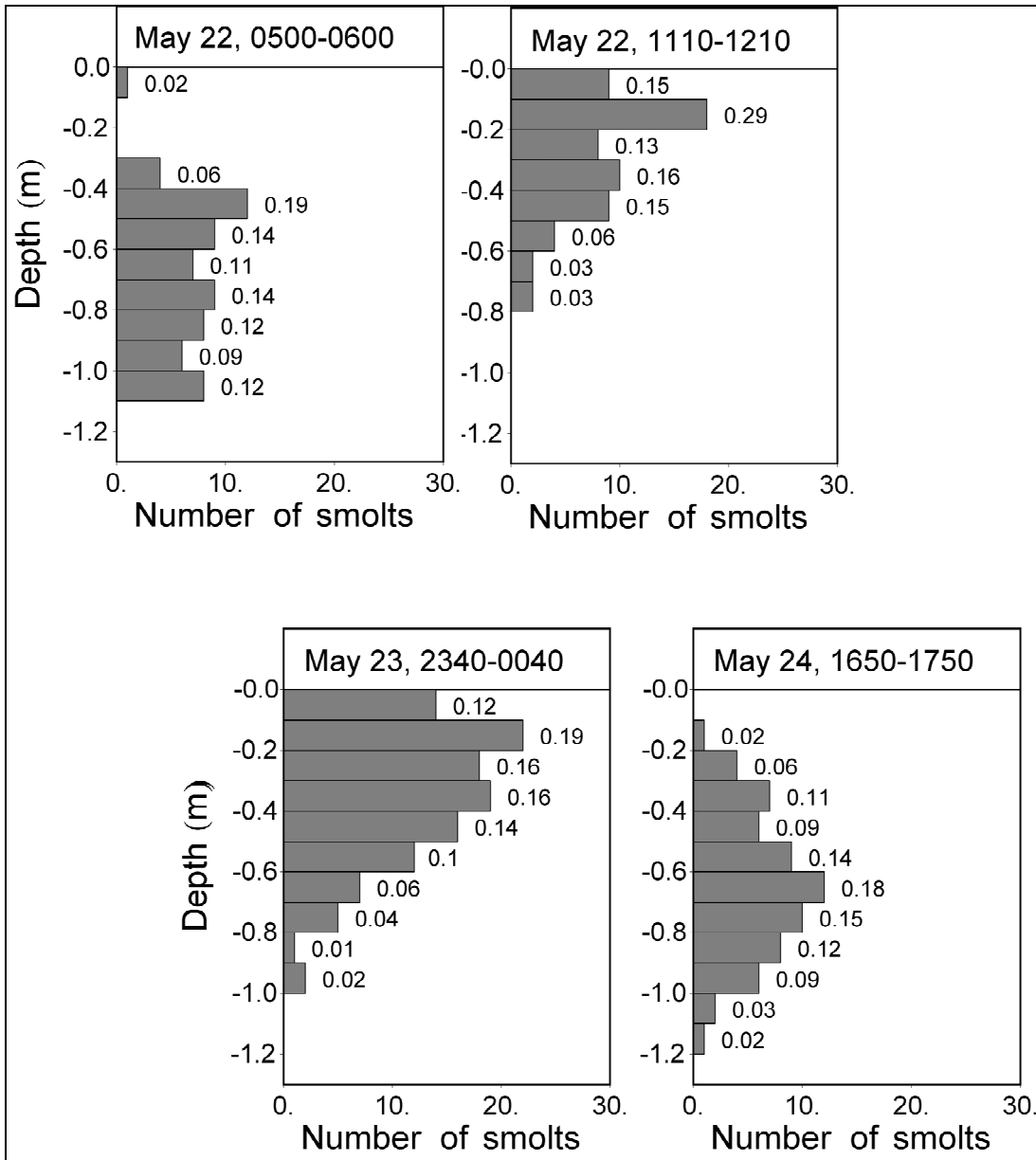


Figure 21.—Target strength frequency distribution for the side-looking and up-looking split-beam transducers (top) and side-looking target strength values by range (bottom) with a linear regression (line) and standard deviation (short bars), Kvichak River, May 27–28, 2000.



Note: The number after each bar is the proportion of smolts within that depth range.

Figure 22.—Estimated depth distributions of migrating smolts, Kvichak River 2001.

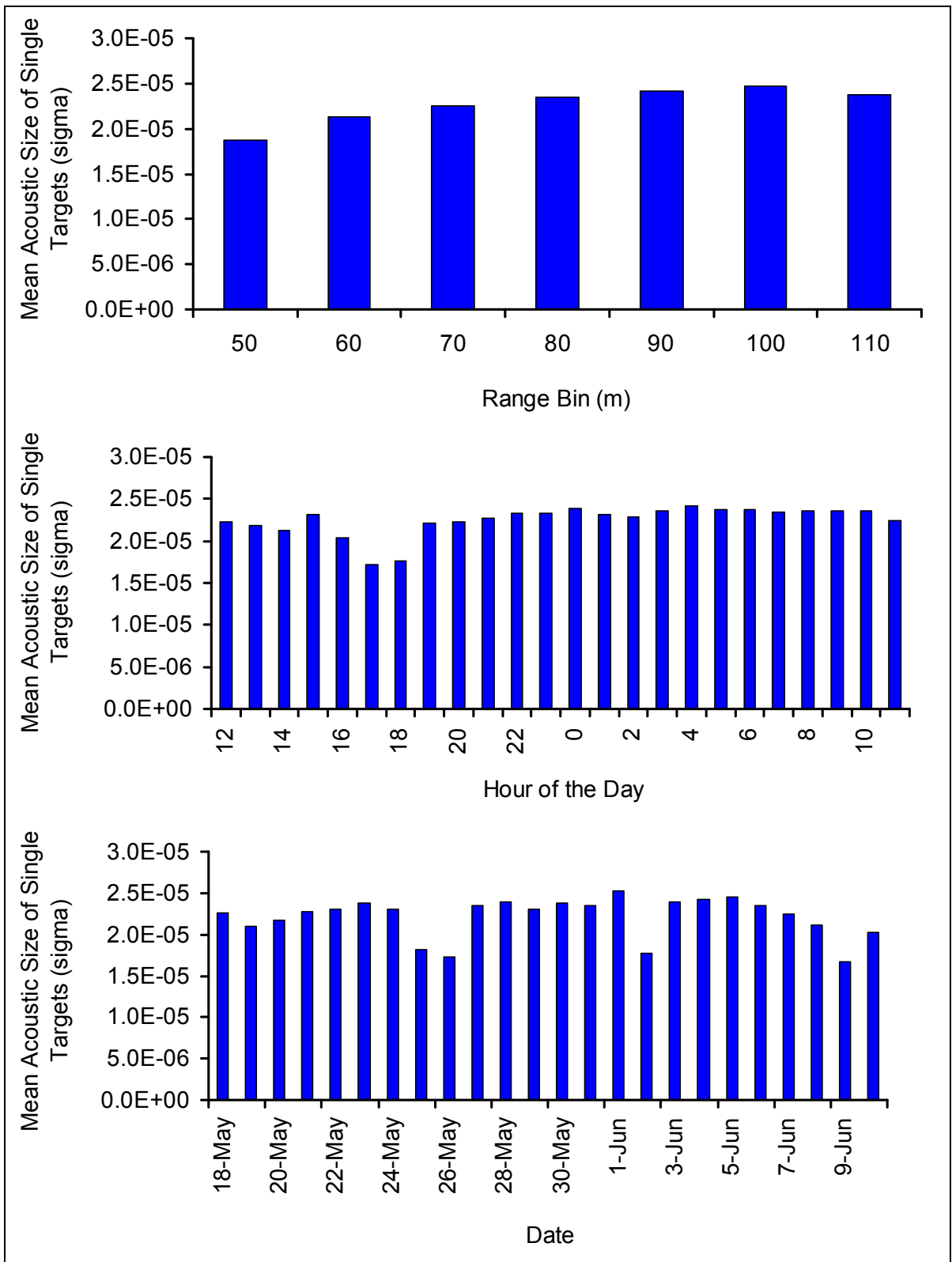


Figure 23.—Mean acoustic size of single targets by range (top), hour of the day (center), and date (bottom) from the side-looking Biosonics’ system, Kvichak River sonar, 2001.

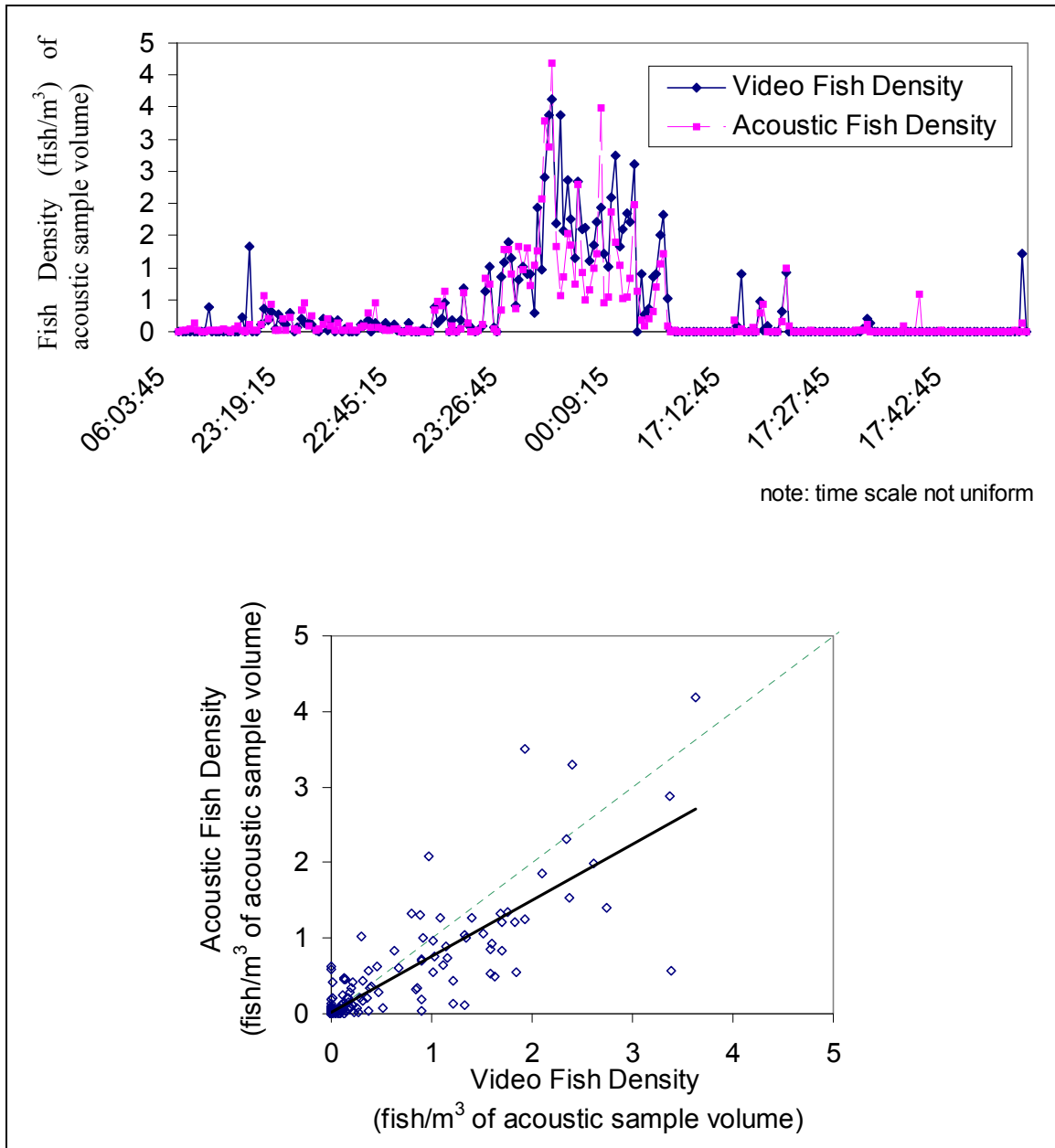


Figure 24.—Acoustic and video estimates of smolt density by time showing the similarity in peaks between the two assessment methods (top), and the linear regression (bottom) with the regression line (solid black line) compared against a slope of 1 (dotted line), 0600 May 22–1800 May 24, 2001.

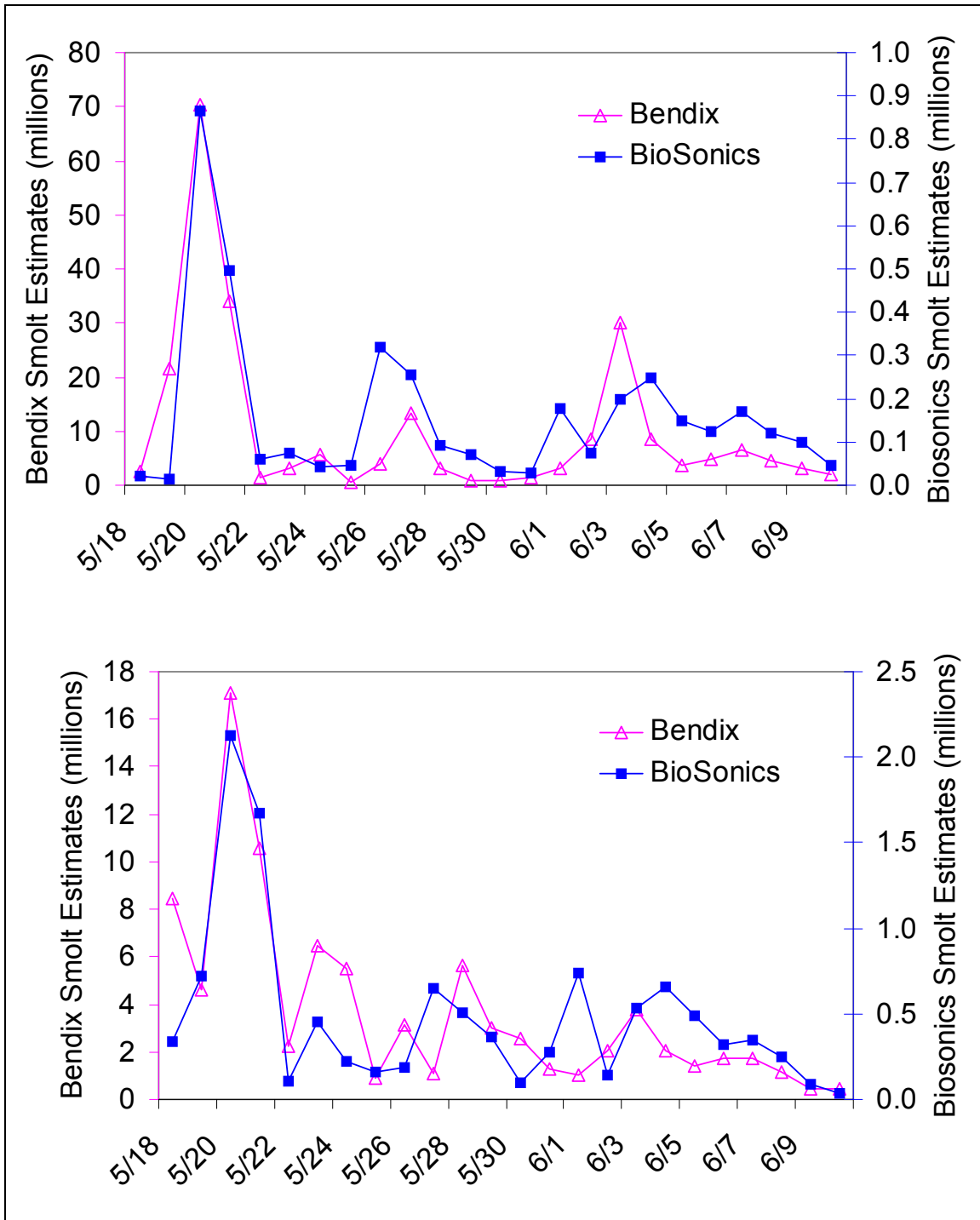


Figure 25.—Bendix and BioSonics’ acoustic smolt passage estimates during the day (top) and night (bottom), defined as 2200–0600, plotted on separate axes because of the wide spread between the two estimates, Kvichak River, 2001.

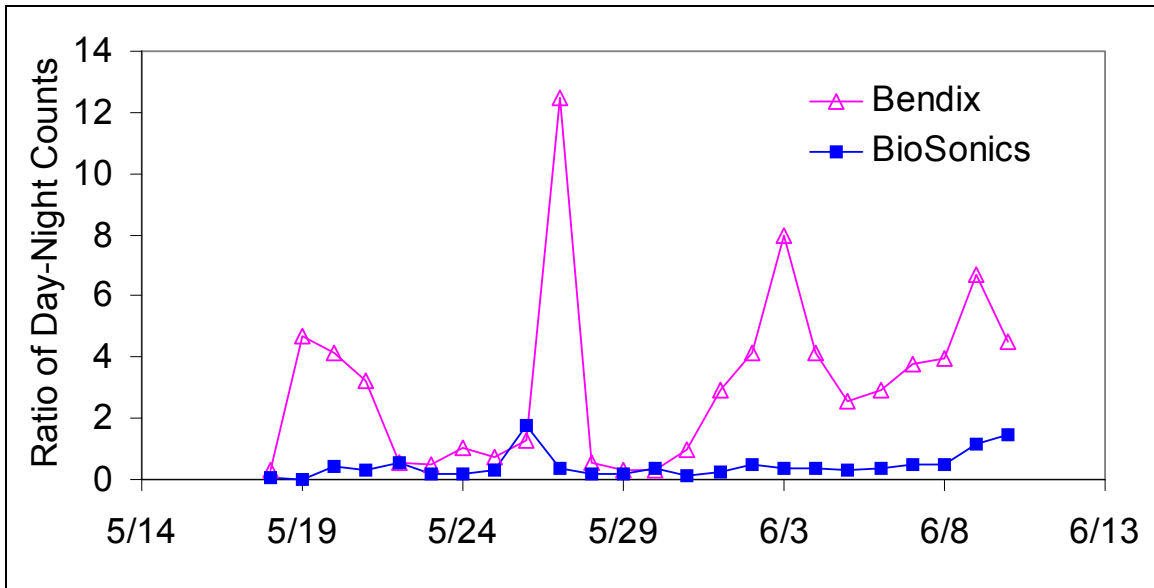


Figure 26.—The ratio of day/night smolt passage estimates using the Bendix and BioSonics' sonars, Kvichak River, 2001.

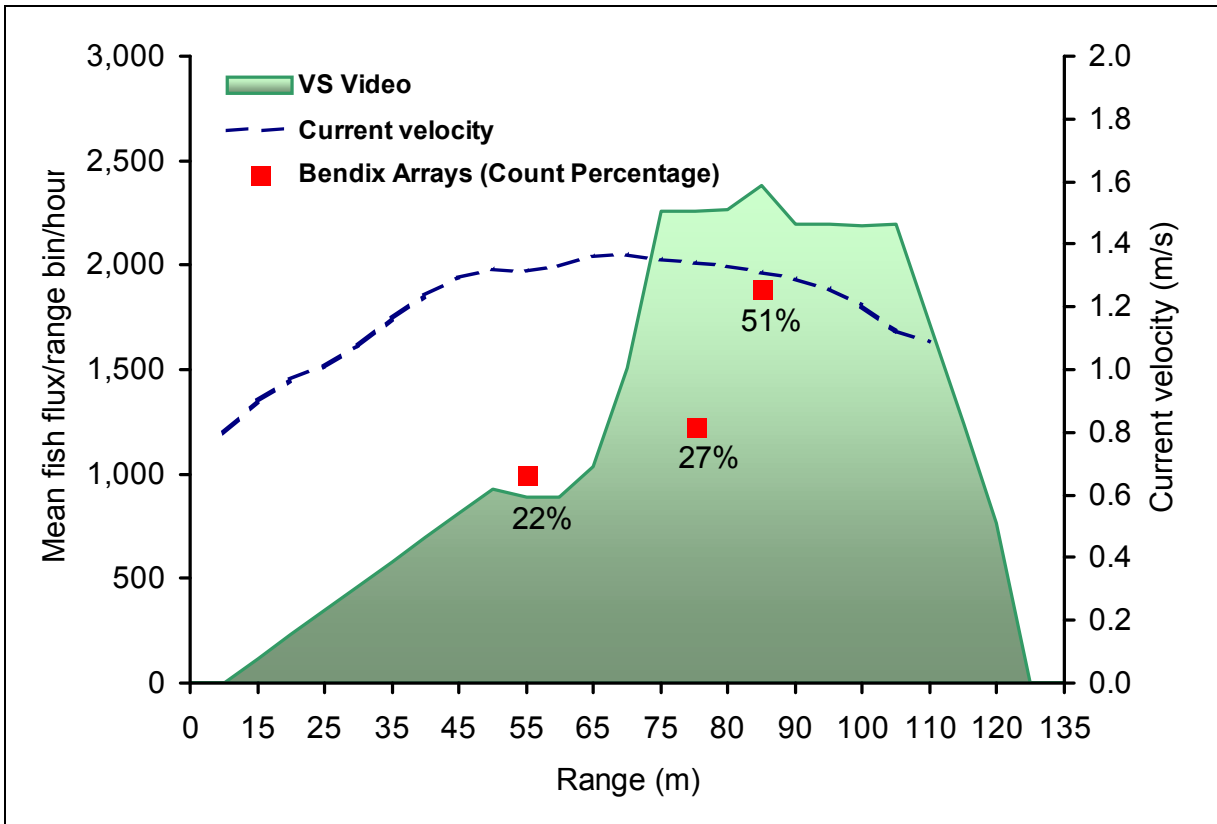
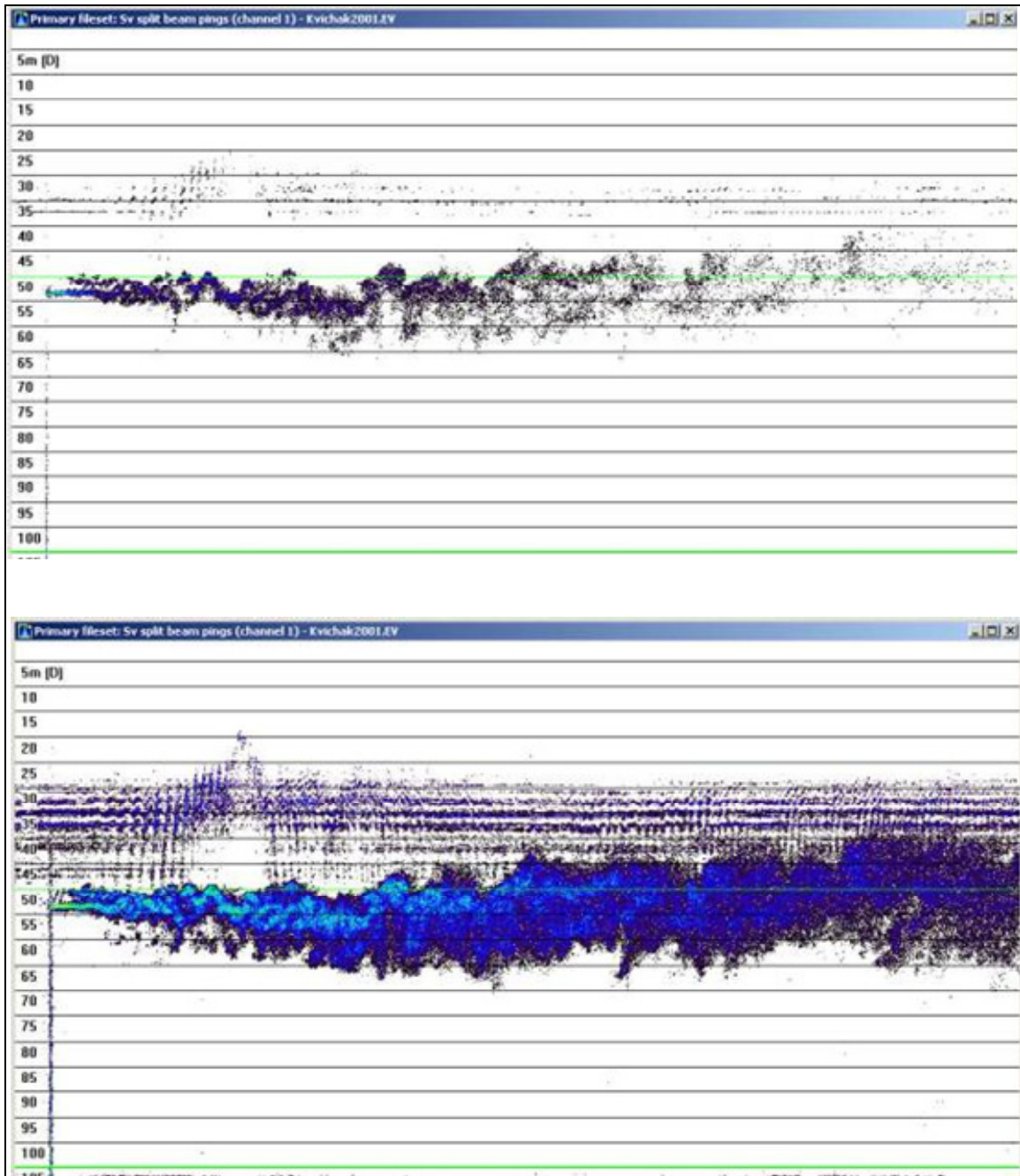


Figure 27.—The cross-river smolt distribution from the BioSonics' sonar estimates using the video scaler and video distribution (VS Video), the current velocity, and the percentage of the Bendix count for each of the three arrays (note: the first value is arbitrary), Kvichak River 2001.



*Note:* The x-axis represents the ping interval (time).

Figure 28.—Reverberation caused by a boat passing through the side-looking BioSonics' beam with a threshold of -65 dB (top) and -55 dB (bottom), Kvichak River, 2001.



## **APPENDIX A**

## **1976–1988**

The Bendix smolt counter was deployed 5 km below the outlet of Lake Iliamna on the Kvichak River (Figure 1; Site 1). A Model 1976 Bendix smolt counter was used with 3 arrays, each containing 7 up-looking and 7 downstream-facing 118 kHz, 18° transducers with 330' cables. To expand the counts, 1 count per 83.0 g of biomass was used (Woolington et al. 1990).

## **1989 Location and Equipment Changes**

The Kvichak River Bendix smolt counter was relocated to 6 km below the outlet of Lake Iliamna (Figure 1; Site 2). The prior site was located on an island and increased flows in side channels on both sides of the island raised concerns that smolt might be passing the sonar site undetected. The depth of the river at the new site was deeper than the 1976–1988 site, therefore the following equipment changes were implemented (Woolington et al. 1991):

1. A Model 1982 Bendix smolt counter was set up and operated from the right bank of the river. This system used 3 arrays each containing 10 up-looking, 235 kHz, 9° transducers with 330' cables. To expand the counts, 1 count per 41.5 g of biomass was used.
2. A Model 1976 Bendix smolt counter was modified in 1989 by Al Menin to operate in deeper water, and then set up and operated from the river's left bank. This system used 1 array with 7 up-looking and 7 downstream-facing 118 kHz, 18° transducers with 330' cables. For both the 1976 and 1989 counters, the count was expanded using 1 count per 83.0 g of biomass.

Because the left bank smolt counter (Model 1976) was not monitored continuously for false counts and the smolt outmigration estimate was not changed significantly by including the counts from this system, only counts from the Model 1982 counter on the right bank were used in the final 1989 Kvichak River smolt estimate.

## **1990 Modified Counter and Extended Cables**

The Model 1976 Bendix smolt counter was again modified. Al Menin implemented the following changes to the counter (Crawford et al. 1992):

1. Discontinued use of the 7 downstream-facing transducers.
2. Extended the offshore array cable to 415'.

The Model 1976 Bendix smolt counter was used with 3 arrays, each containing 7 up-looking 118 kHz, 18° transducers with 415' cables on the offshore array and 330' cables on the inshore and center arrays. To compensate for the additional 85' of cable on the offshore arrays, 10 -150 UH inductors were installed in the counters' electronic circuitry.

## **1991–1992**

No Changes.

### **1993 Switched Counter and Extended Cables**

Because of an unsolvable problem with the Model 1976 smolt counter's printer, we switched from to a Model 1982 smolt counter (Crawford and Cross 1994a). Al Menin extended the offshore array cables on a Model 1982 counter (e.g., previously used at Nuyakuk River 1983–1989) from 330' to 415' and installed 10–150 U<sub>h</sub> inductors in the counters' offshore array board. The Model 1982 Bendix smolt counter was used with 3 arrays, each containing 10 up-looking 235 kHz, 9° transducers with 415' offshore cables and 330' inshore and center cables. To expand the counts, 1 count per 41.5 g of biomass was used.

### **1994–1995**

No Changes.

### **1996 Cable Lengths Extended**

After the 1995 field season, Al Menin extended the center array cables on the Model 1982 Bendix counter from 330' to 415' and installed the 10–150 U<sub>h</sub> inductors. The 1982 Bendix smolt counter was used with 3 arrays, each containing 10 up-looking 235 kHz, 9° transducers with 415' offshore and center array cables and 330' inshore cables. To expand the counts, 1 count per 41.5 g of biomass was used (Crawford and Cross 1997).

### **1997**

No Changes.

### **1998 Boat Detector Inhibitor Installed**

Al Menin installed a boat detector/inhibitor system that would disable the smolt counter for ~2 min each time the system detected the outboard motor noise from a passing boat.

### **1999**

No Changes.

### **2000 Computer Interface Installed**

To provide a more complete inseason comparison of Bendix smolt counter data with counts from another hydroacoustic system, the department contracted the University of Washington Applied Physics Laboratory during the winter of 1999/2000 to design and insert computer interfaces into 3 smolt counters and write software to accept and store the electronic data. This system generated hourly files with counts from each array in 1 s intervals concurrent with the counter's printer output, which printed the hourly count. This system was tested and used at the Kvichak and Ugashik Rivers in 2000 (Crawford and West 2001).

### **2001**

No Changes. This was the last year the Bendix Smolt Counter was operated on the Kvichak River. Comparative studies were performed against a side-looking acoustic and up-looking video system.



## **APPENDIX B**

Precision Acoustic Systems  
7557 Sunnyside Ave N.  
Seattle, WA 98103-4942  
(206) 524-4218 (phone & fax)

May 21, 1996

Drew Crawford  
ADF&G Commercial Fisheries P.O. Box 37  
Main Street  
King Salmon, AK 99613-0037

Dear Mr. Crawford;

It was a pleasure performing hydroacoustics test services for your ITC Mode 5095 transducers. Please examine the patterns and calculations that I have provided and contact me if you have any questions.

I have included a spreadsheet with your calibration data that provides receiving sensitivity calculations. I won't go into detail as to how the calculations were done unless you request. The most useful sensitivity calculation is the last column labeled "Pwr Into 50 Ohms dEm". This calculation is the power that would be delivered into a 50 Ohm load relative to 1 milliwatt into 50 Ohms for the acoustic sound pressure level at the transducer of 154.73 dBuPa. This receiving power sensitivity results in a direct comparison between transducers because it properly takes into account the transducer/cable impedance to show relative efficiency between transducers -- assuming the same directivity for each transducer. Please note that I have assumed no cable losses.

I have looked at all the patterns and power sensitivities and can conclude that transducer # 3R does not reasonably match the others. It is much less directive and has a lower power sensitivity. All others seem to match OK with some noticeable variations in pattern and sensitivity.

Again, it has been a pleasure doing calibration work for you and I hope I will have a chance to serve you in the future.

Sincerely,  
Alan R. Wirtz, Chief Engineer

---

-continued-

ADF&G Calibrations, King Salmon

5/20/96 & 5/21/96

ITC Model 5095 Transducers, Receiving Sensitivity

Frequency: 235 kHz  
 Standard: PAS # 2633 →Ts=  
 Separation: 3.416 Meters

150.4 dBuPa/V @ 1 Meter  
 Drive Level to Standard =

Ss = -200 dBV/uPa  
 15.00 dBV

	Xducer	Vout	Rec.In	Vout	Rec Sens	Vrms Into	Pwr Into
Xducer SIN	IZI Ohms	dBV	IZI Ohms	Open Cir.	Sv	50 Ohms	50 Ohms dBm
187	232	-41.24	75	-29.00	-183.73	0.006292	-31.01
5R	53.4	-42.55	75	-37.88	-192.61	0.006172	-31.18
19R	187.5	-40.29	75	-29.41	-184.14	0.007126	-29.93
2R	59.53	-41.92	75	-36.84	-191.57	0.006564	-30.65
12R	197.5	-41.00	75	-29.79	-184.52	0.006542	-30.68
15R	268.5	-41.05	75	-27.83	-182.56	0.006371	-30.91
179	216.5	-42.55	75	-30.76	-185.49	0.005437	-32.28
7R	216.9	-40.93	75	-29.13	-183.86	0.006551	-30.66
2001	188.5	-40.50	75	-29.59	-184.32	0.006953	-30.15
6R	257.7	-39.84	75	-26.90	-181.63	0.007342	-29.67
11R	243	-39.69	75	-27.14	-181.87	0.007498	-29.49
11R	243	-27.43	43200	-27.38	-182.11	0.007295	-29.73
3R	138	-36.52	43200	-36.49	-191.22	0.003983	-34.99
182	257.5	-27.87	43200	-27.82	-182.55	0.00661	-30.59
200	160.9	-32.77	43200	-32.74	-187.47	0.00547	-32.23
6000	186.4	-31.18	43200	-31.14	-185.87	0.005864	-31.63
18R	242.4	-27.49	43200	-27.44	-182.17	0.00726	-29.77
171	191.6	-31.26	43200	-31.22	-185.95	0.005686	-31.89
164	255.8	-27.87	43200	-27.82	-182.55	0.006647	-30.54

-continued-

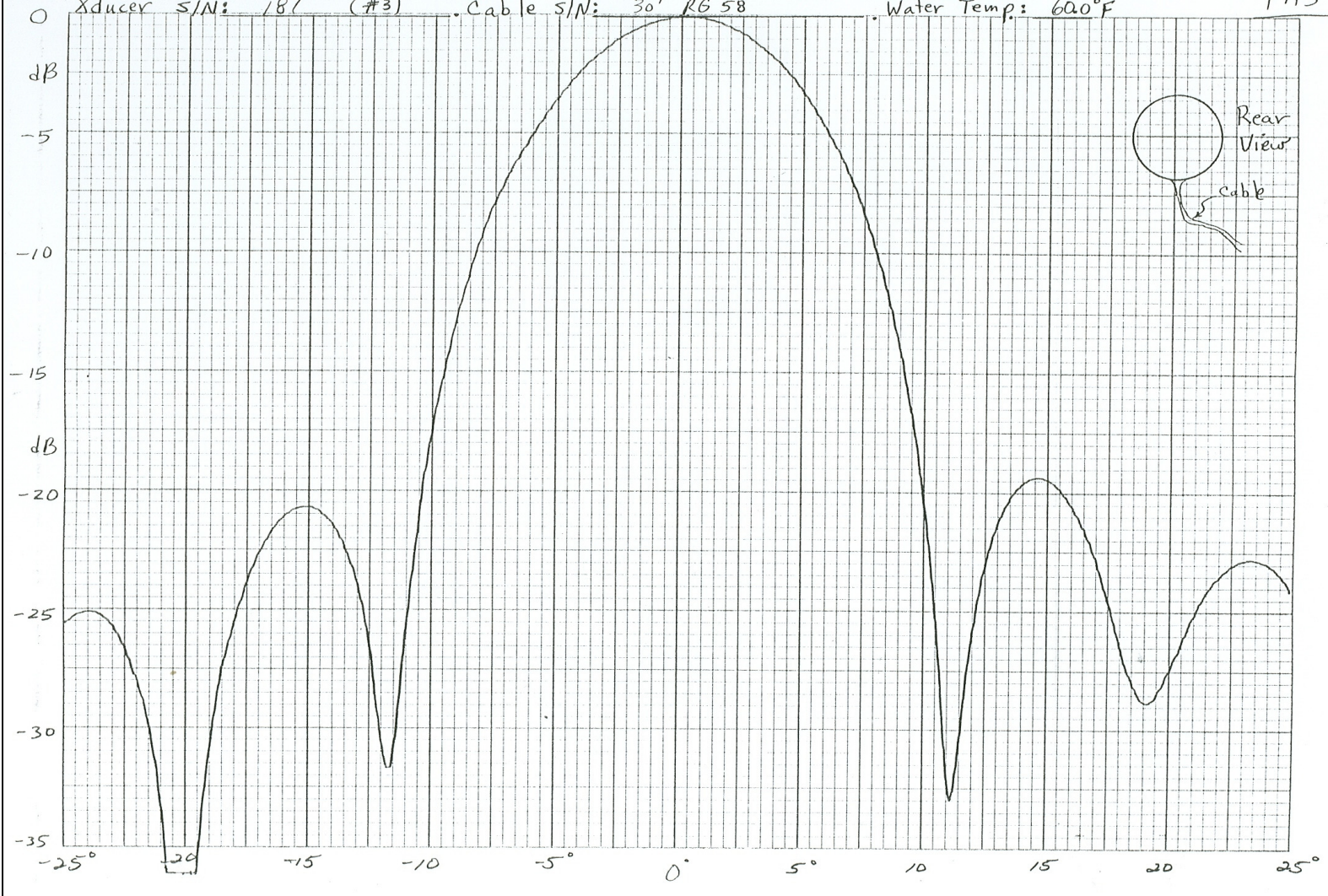
GRAPHIC CONTROLS CORPORATION  
BUFFALO, NEW YORK  
PRINTED IN U.S.A.

No. XY-1001-SP 3

Freq.: 235 kHz. Separation: 3.416 m. Rec. Sen. \_\_\_\_\_ dBV/μPa. Xmit Sen. \_\_\_\_\_ dBμPa/V @ 1 meter  
Transducer S/N: 187 (#3). Cable S/N: 30' RG 58. Water Temp: 62.0°F

5/20/96

PAS



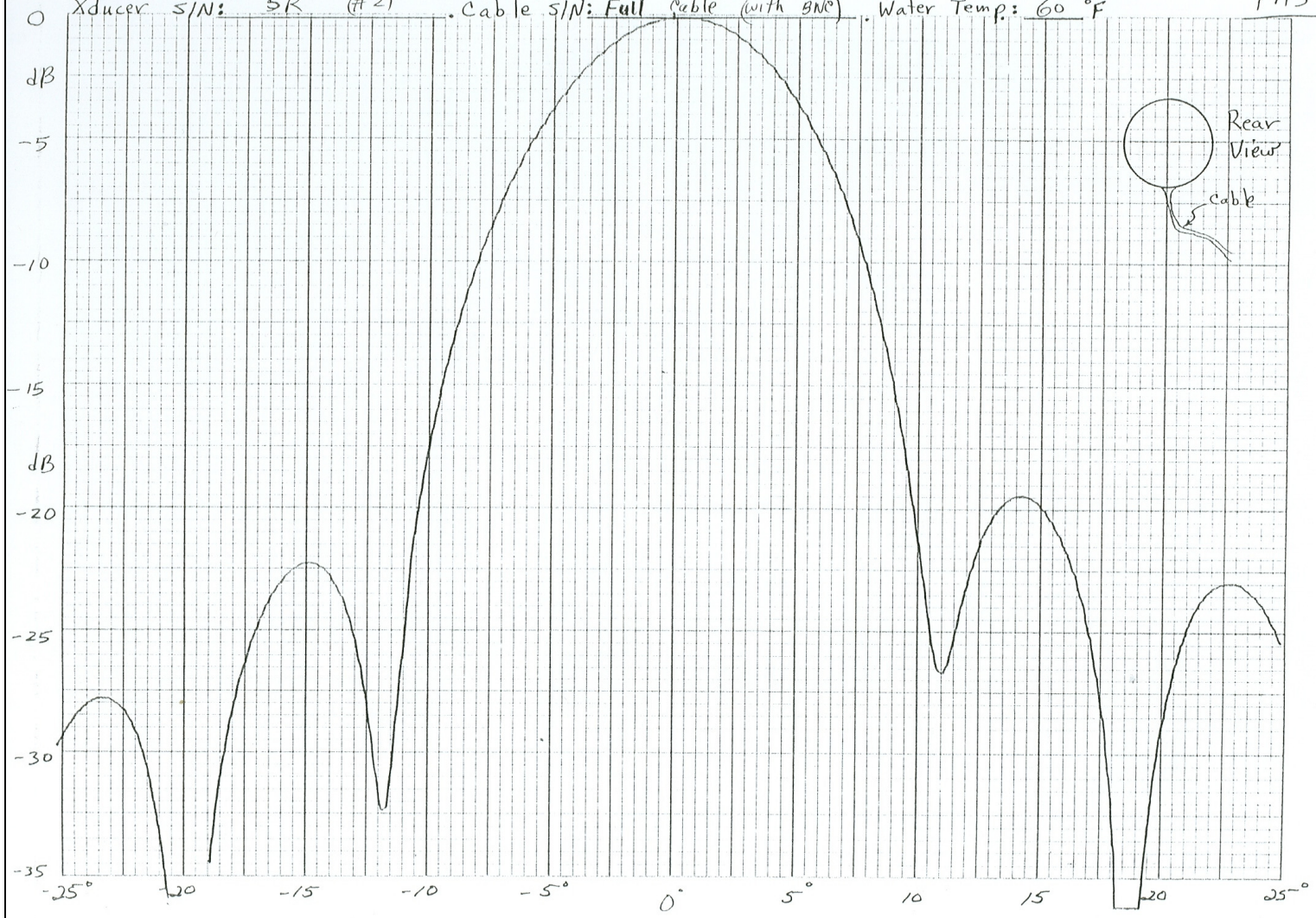
Appendix B2.-Calibrations and beam pattern plots for the Bendix smolt counter transducers.

GENERAL ELECTRIC CORPORATION  
DEFENSE RESEARCH AND  
TECHNOLOGY CENTER

NO. XY 1001 SP 3

Freq.: 235 kHz. Separation: 3.416 m. Rec. Sen. \_\_\_\_\_ dBV/uPa. Xmit Sen. \_\_\_\_\_ dB.uPa/V @ 1 meter  
Xducer S/N: 5R (#2) . Cable S/N: Full cable (with gne) . Water Temp: 60 °F

5/20/96  
PAS



63

Appendix B1.-Page 2 of 18.

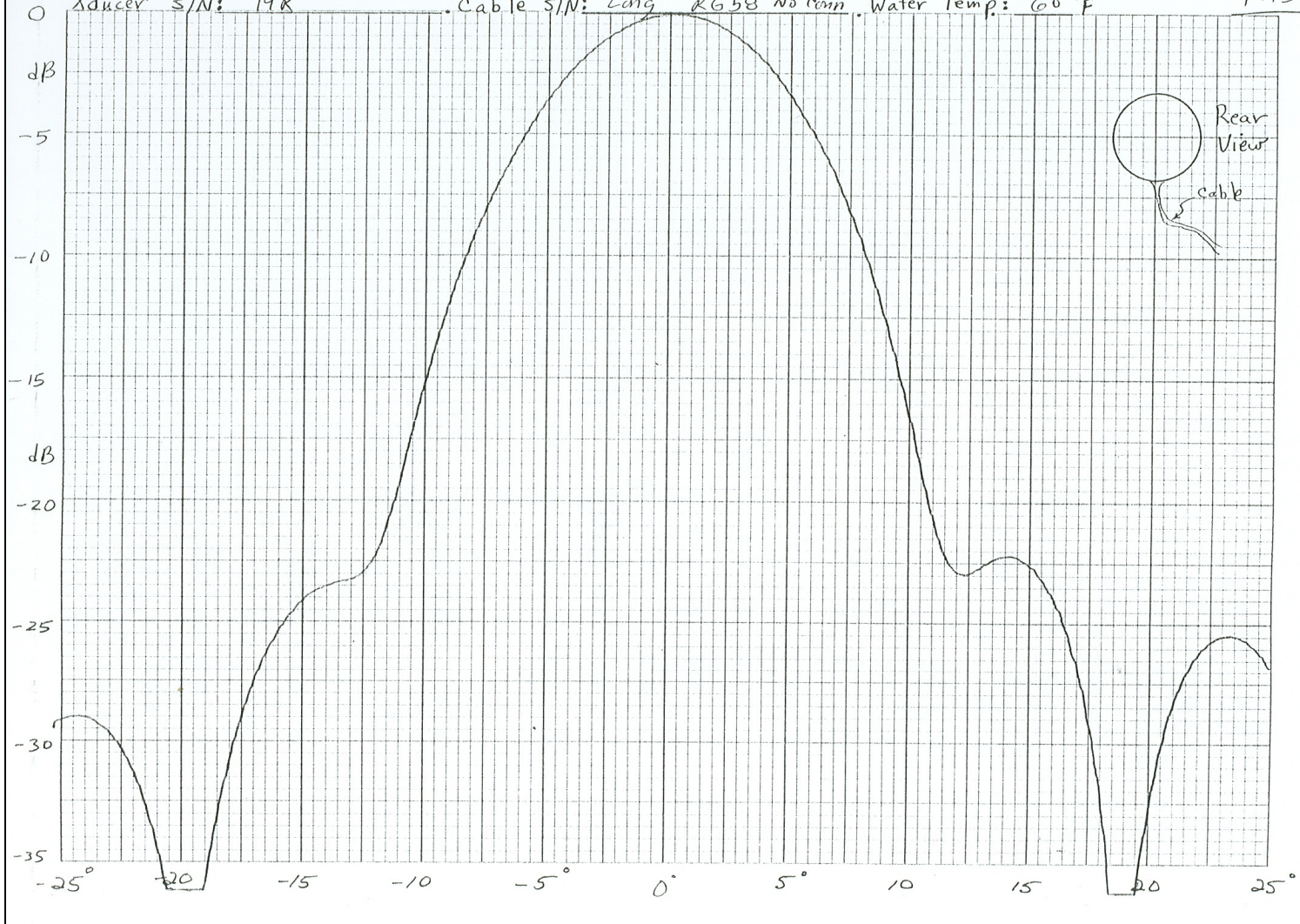
GRAPHIC CONTROLS CORPORATION  
BUFFALO, NEW YORK  
FACILITY NO. 1100

NO. XY 1001 - SP 3

Freq.: 235 kHz. Separation: 3.416 m. Rec. Sen. \_\_\_\_\_ dBV/μPa. Xmit Sen. \_\_\_\_\_ dBμPa/V @ 1 meter

Xducer S/N: 19R Cable S/N: Long RG 58 No Conn. Water Temp: 60 °F

PAS

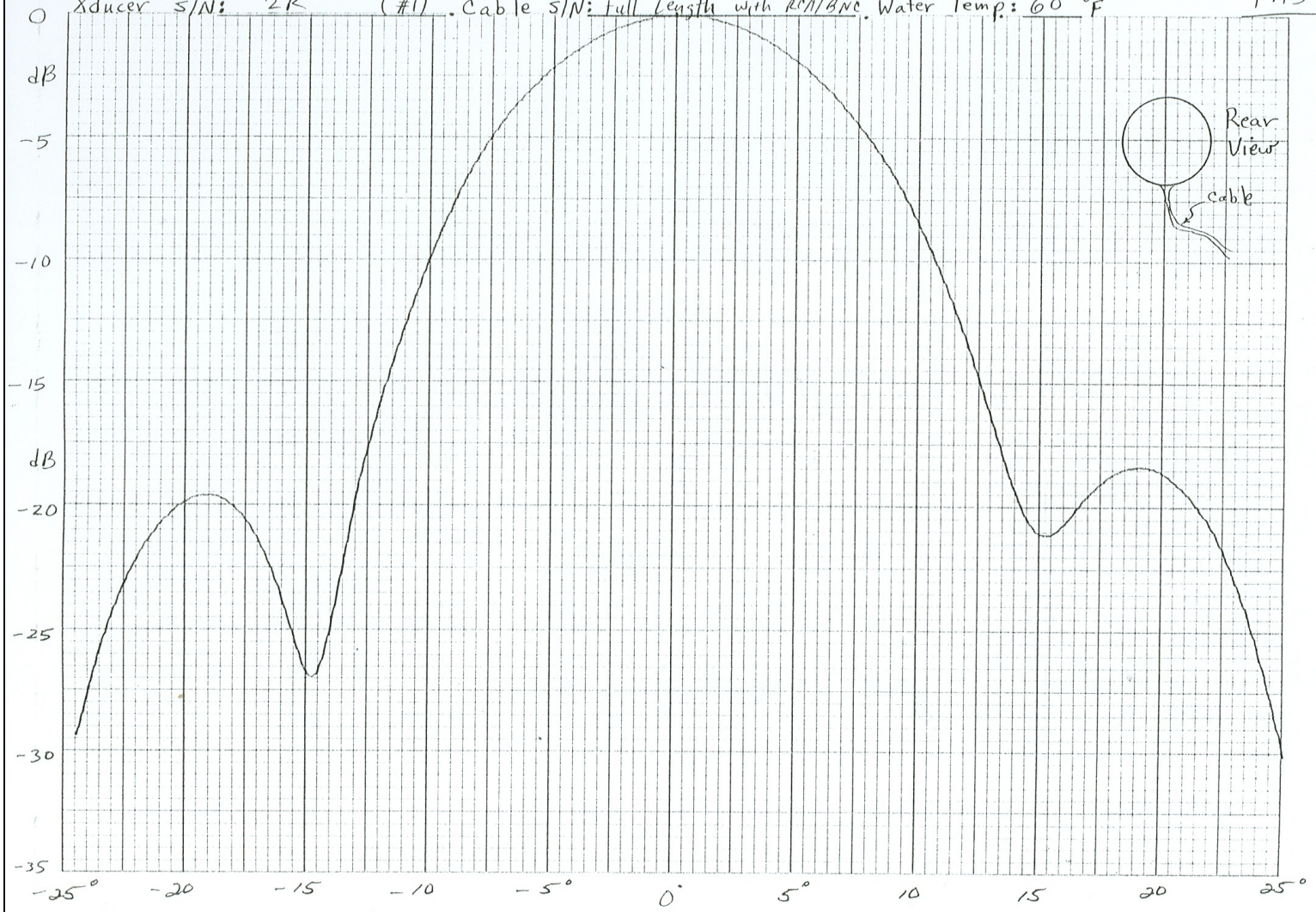


GEOMETRIC MEASUREMENTS LABORATORY  
DEPARTMENT OF ELECTRO-SCIENCE  
UNIVERSITY OF CALIFORNIA, BERKELEY

NO. BY 1001 SP 3

Freq.: 235 kHz. Separation: 3.416 m. Rec. Sen. \_\_\_\_\_ dBV/uPa. Xmit Sen. \_\_\_\_\_ dBuPa/V @ 1 meter  
Xducer S/N: 2R (#1) Cable S/N: Full length with RCA/BNC. Water Temp: 60 °F

5/20/96  
PAS



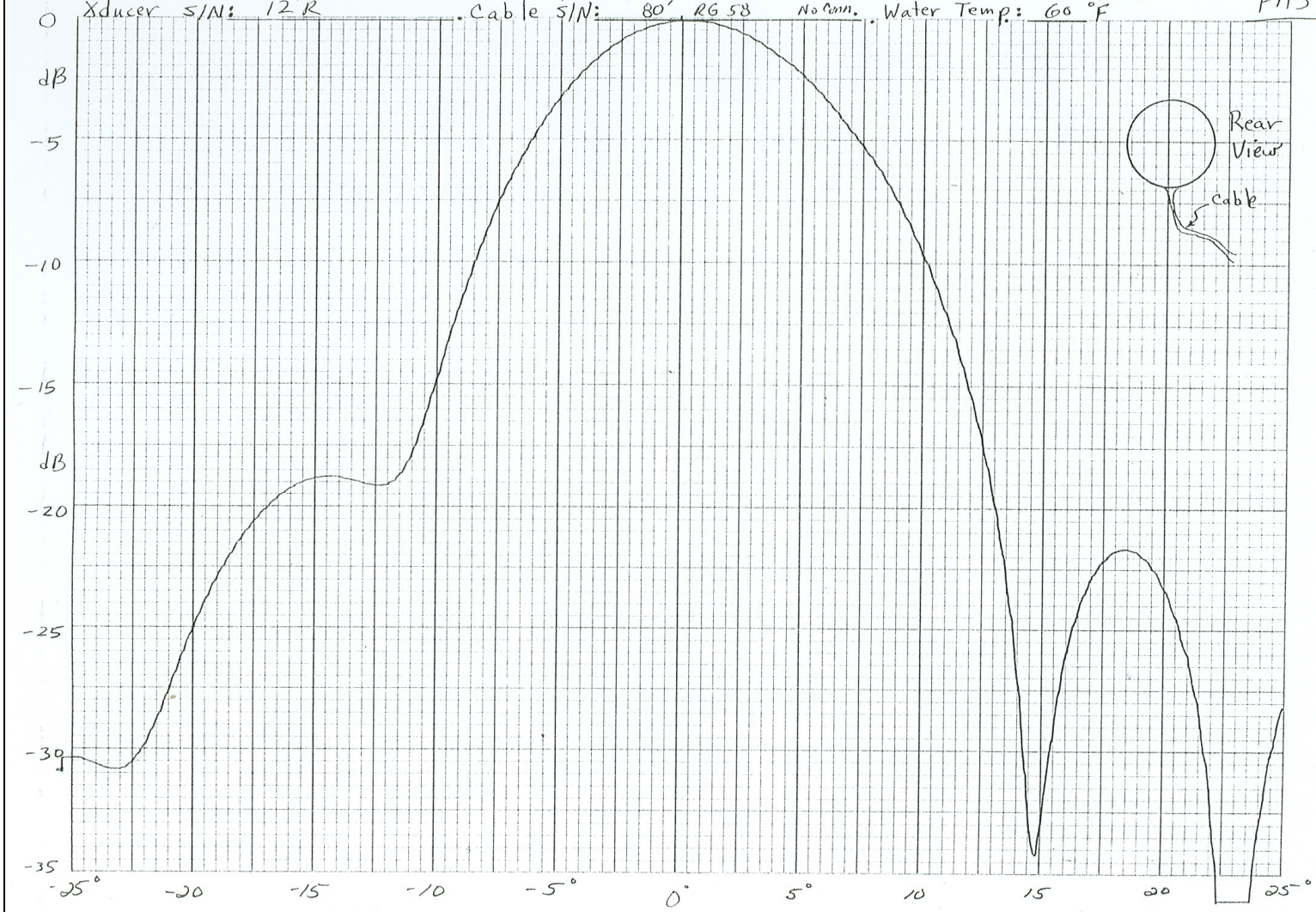
65

GRAPHIC CONTROLS CORPORATION  
BUFFALO, NEW YORK  
MADE IN U.S.A.

No. XY-1001-SP 3

Freq.: 235 kHz. Separation: 3.416 m. Rec. Sen. \_\_\_\_\_ dBV/uPa. Xmit Sen. \_\_\_\_\_ dBuPa/V @ 1 meter  
Xducer S/N: 12R Cable S/N: 80' RG 58 No. mm. Water Temp: 60 °F

5/20/96  
PAS

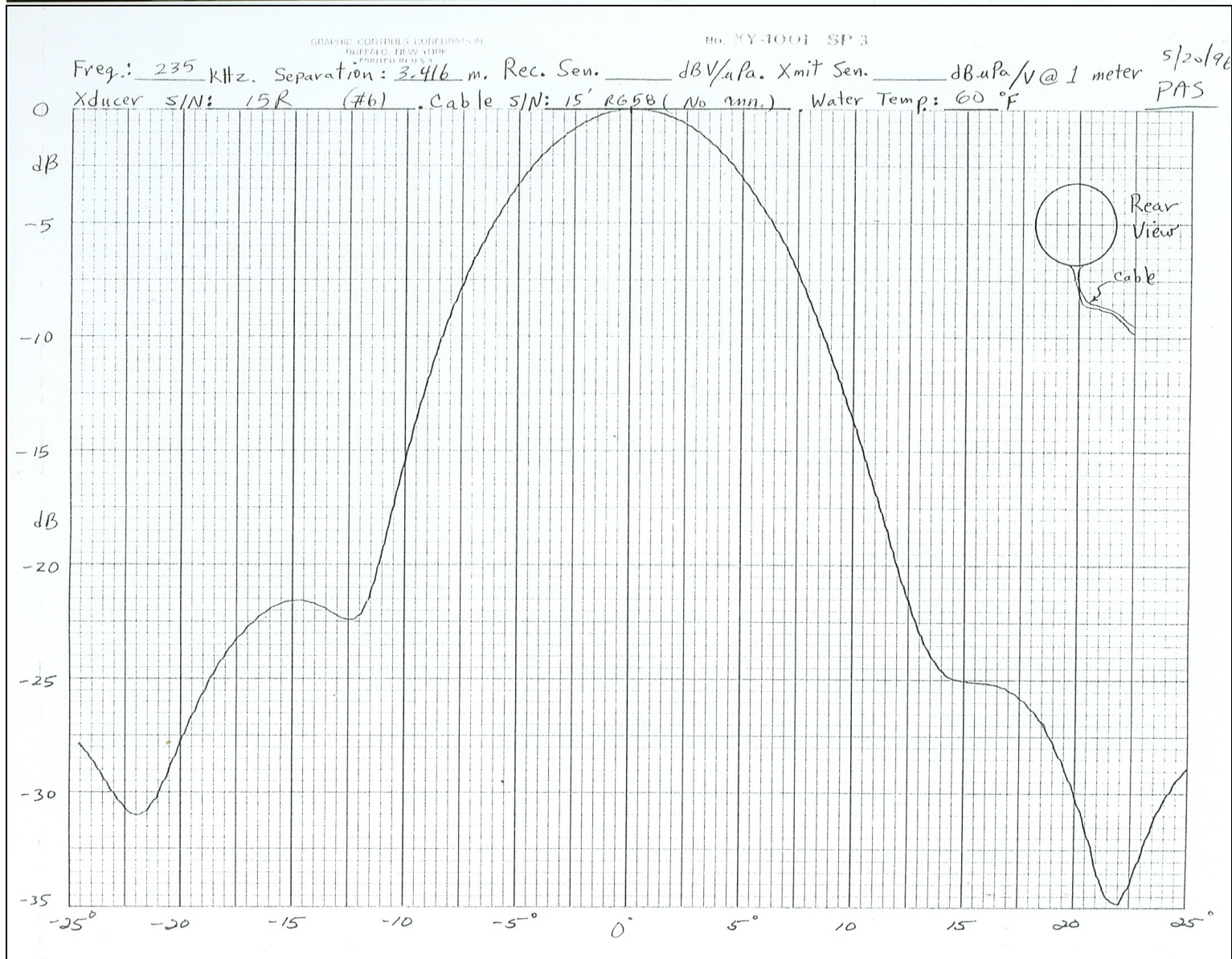


GRAPHIC CONTROLS CORPORATION  
BUFFALO, NEW YORK  
PRINTED IN U.S.A.

NO. XY-1001-SP 3

Freq.: 235 kHz. Separation: 3.416 m. Rec. Sen. \_\_\_\_\_ dBV/aPa. Xmit Sen. \_\_\_\_\_ dB.uPa/V@1 meter  
Xducer S/N: 15R (#6). Cable S/N: 15' RG58 (No. 2mm.) Water Temp: 60 °F

5/20/96  
PAS



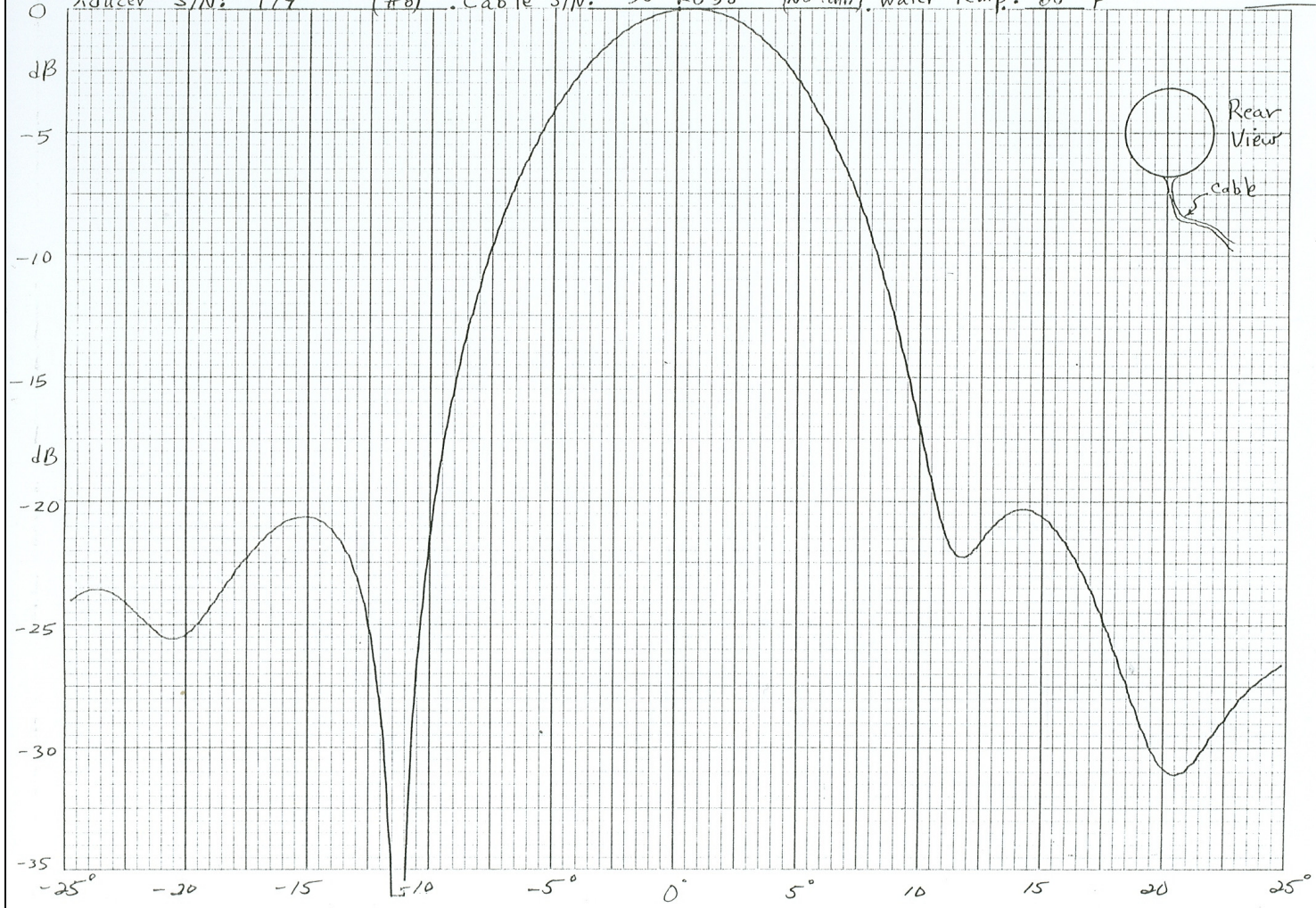
67

GRAPHIC CONTROLS CORPORATION  
BUFFALO, NEW YORK  
MADE IN U.S.A.

No. XY-1001 - SF 3

Freq.: 235 kHz. Separation: 3.416 m. Rec. Sen. \_\_\_\_\_ dBV/uPa. Xmit Sen. \_\_\_\_\_ dB.uPa/V @ 1 meter  
Xducer S/N: 179 (#8) . Cable S/N: 30' #658 (no run). Water Temp: 60 °F

S/20/96  
PAS



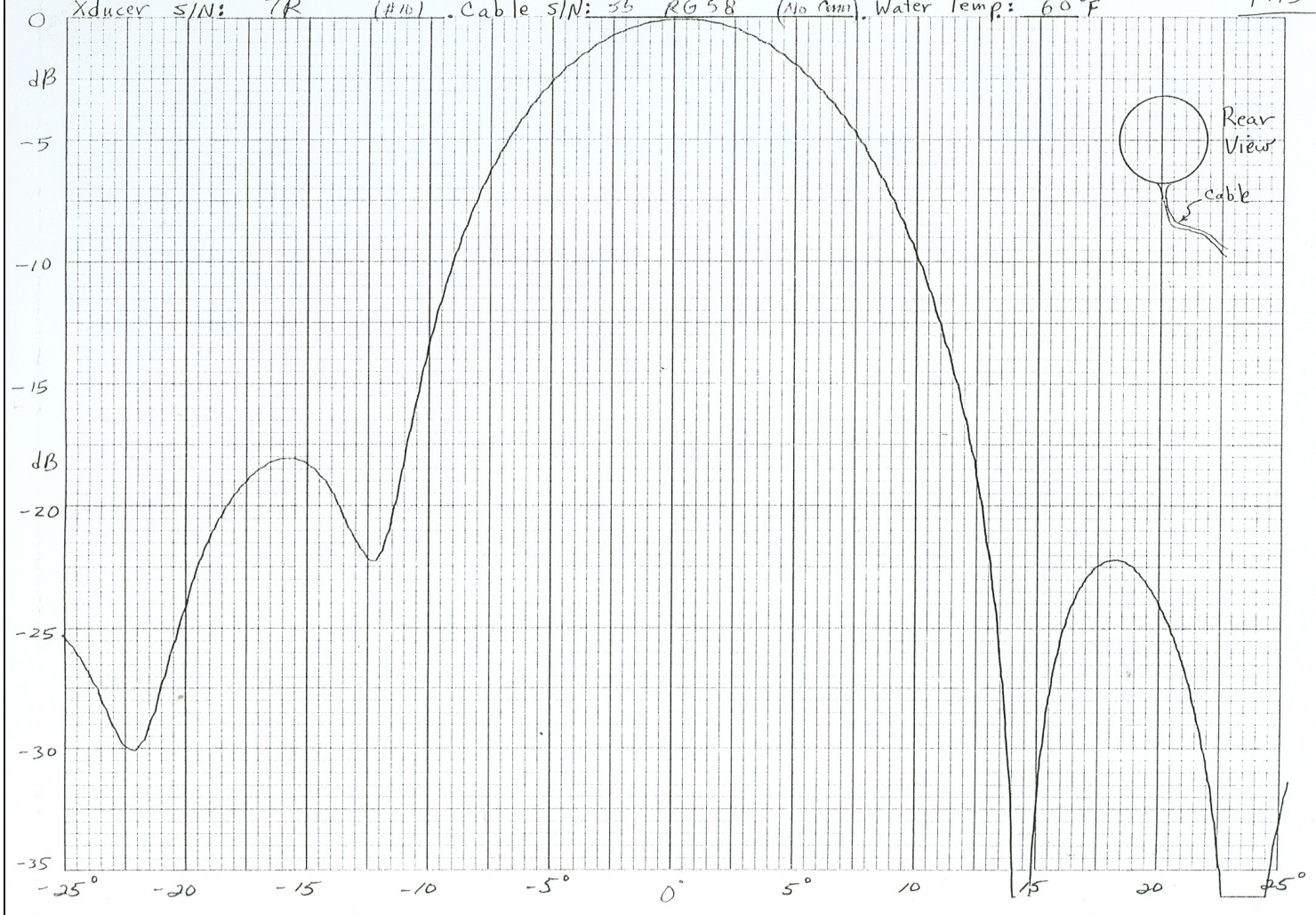
89

GRAPHIC CONTROL CORPORATION  
BOSTON, MASSACHUSETTS  
UNITED STATES OF AMERICA

Bo. XY-1001 SP 3

Freq.: 235 kHz. Separation: 3.146 m. Rec. Sen. \_\_\_\_\_ dBV/uPa. Xmit Sen. \_\_\_\_\_ dB-uPa/V @ 1 meter  
Xducer S/N: 7R (#10). Cable S/N: 35' RG 58 (No Am). Water Temp: 60°F

5/20/68  
PAS



69

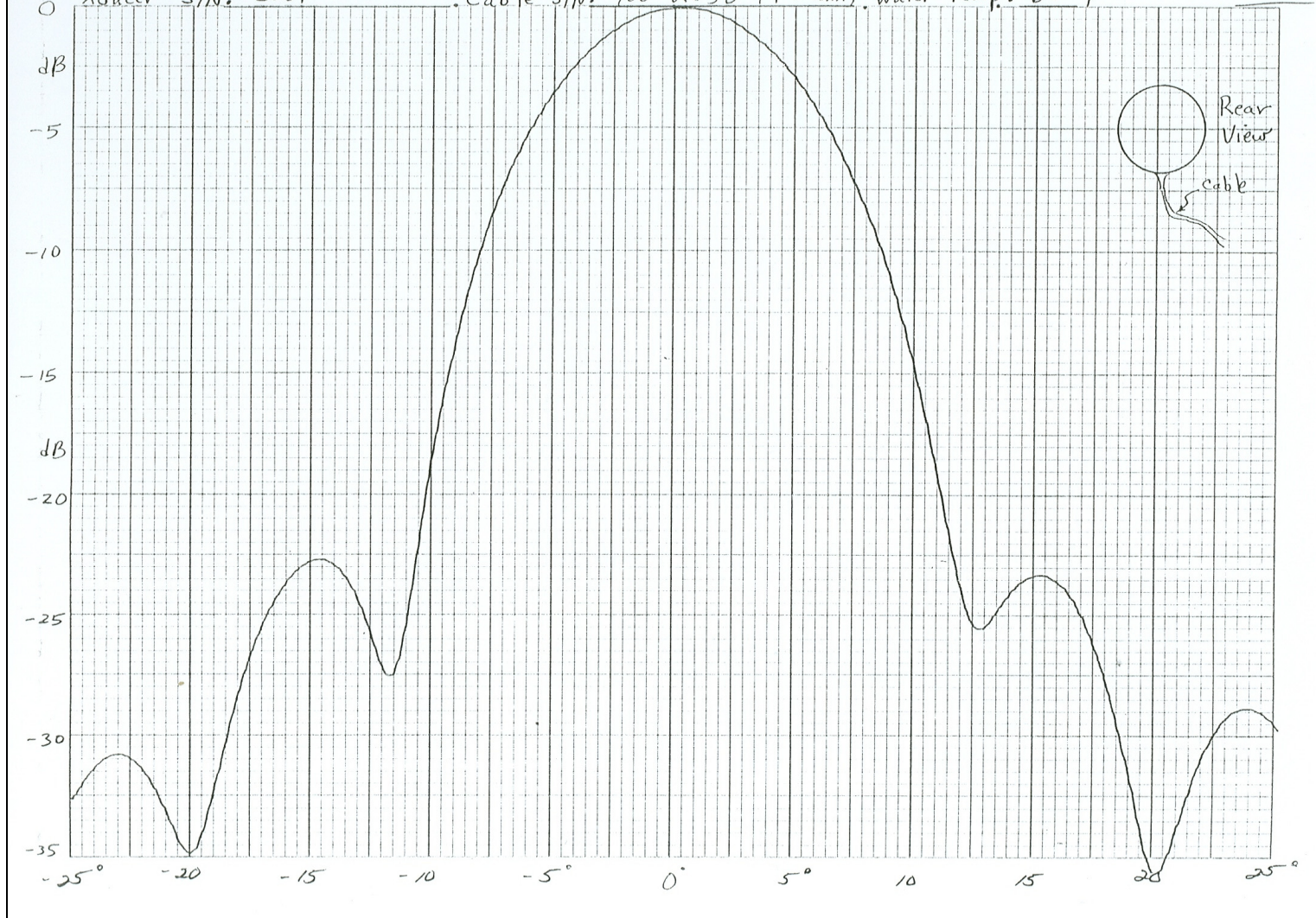
GRAPHIC CONTROLS CORPORATION  
BUFFALO, NEW YORK  
MADE IN U.S.A.

No. XY-1001 - SP 3

Freq.: 235 kHz. Separation: 3.416 m. Rec. Sen. \_\_\_\_\_ dBV/μPa. Xmit Sen. \_\_\_\_\_ dBμPa/V @ 1 meter

Xducer S/N: 2001. Cable S/N: 120' RG58 (No run). Water Temp: 60 °F

5/20/94  
PAS



70

JOSEPH GREEN'S CONSULTING  
BRIEFING FILE 508

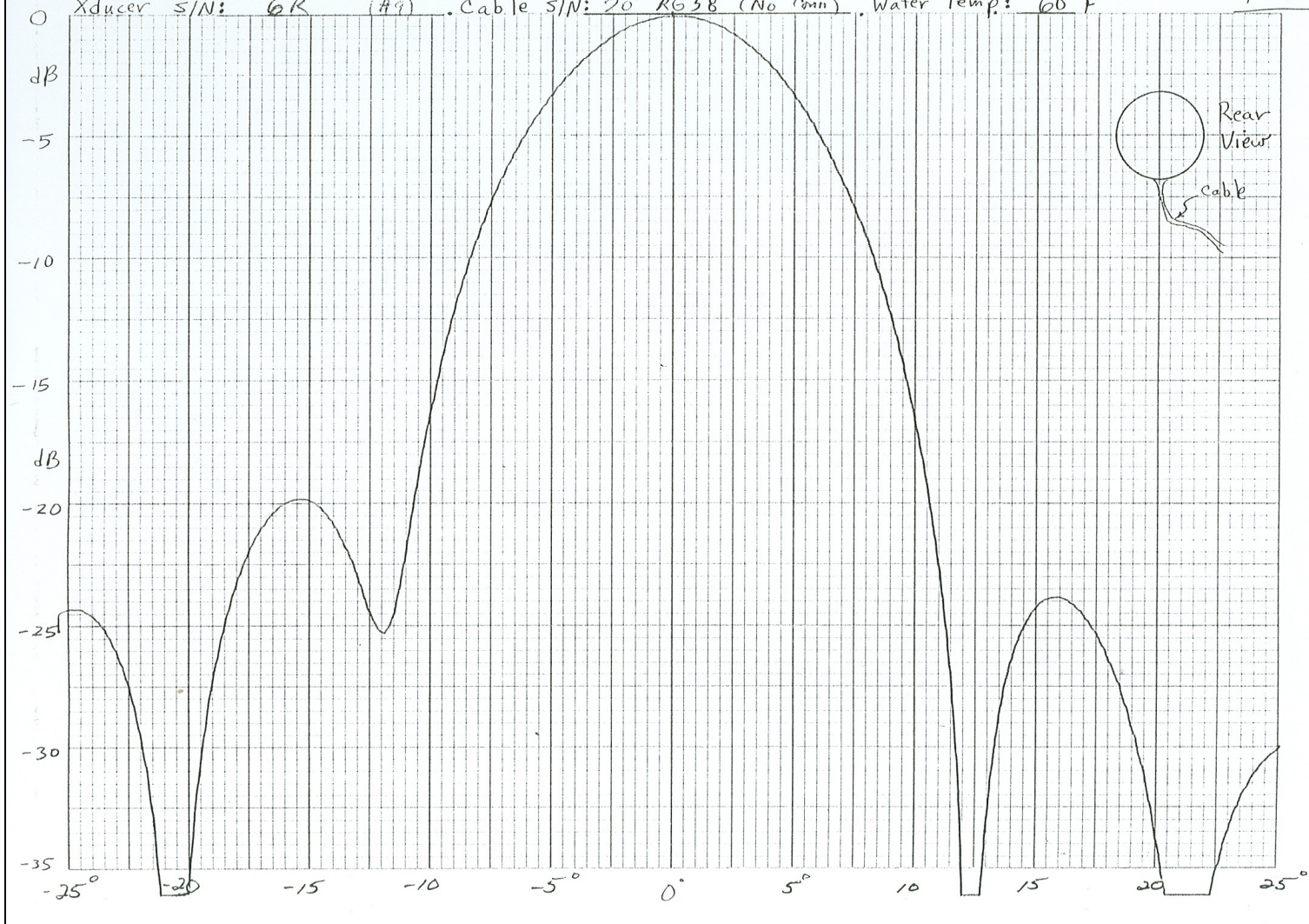
No. XY 1001-SP 2

Freq.: 235 kHz. Separation: 3.416 m. Rec. Sen. \_\_\_\_\_ dBV/uPa. Xmit Sen. \_\_\_\_\_ dB.uPa/V@1 meter

5/20/96

Xducer S/N: 6R (#9). Cable S/N: 20' RG58 (No 3mm). Water Temp: 60 °F

PAS

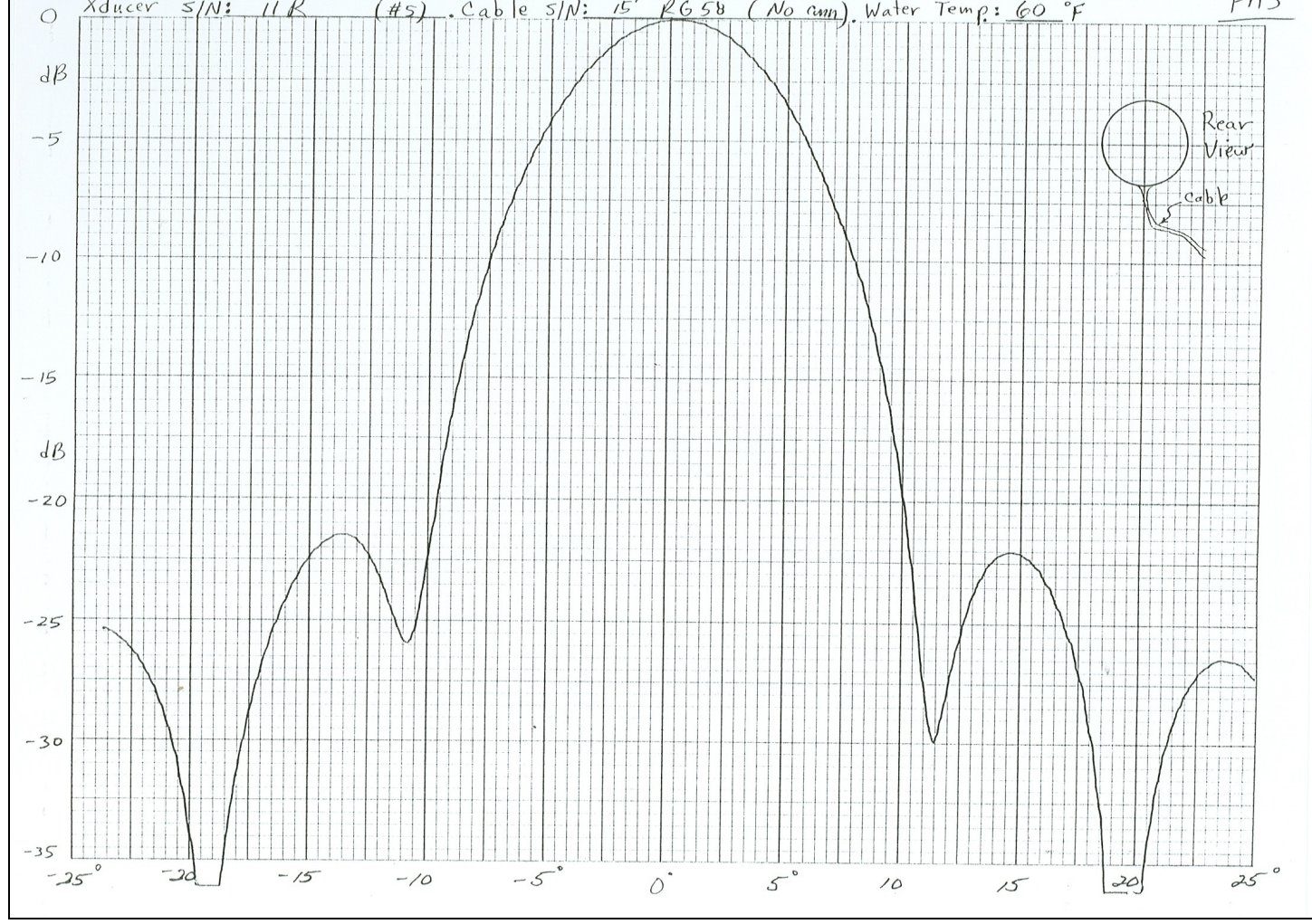


GRAPHIC CONTROLS CORPORATION  
BUFFALO, NEW YORK  
CORPORATED 1954

Mo. XY 1001 - SP 3

Freq.: 235 kHz. Separation: 3.4116 m. Rec. Sen. \_\_\_\_\_ dBV/uPa. Xmit Sen. \_\_\_\_\_ dB.uPa/V @ 1 meter  
Xducer S/N: 11 R (#5). Cable S/N: 15' RG 58 (No run). Water Temp: 60 °F

5/20/96  
PAS



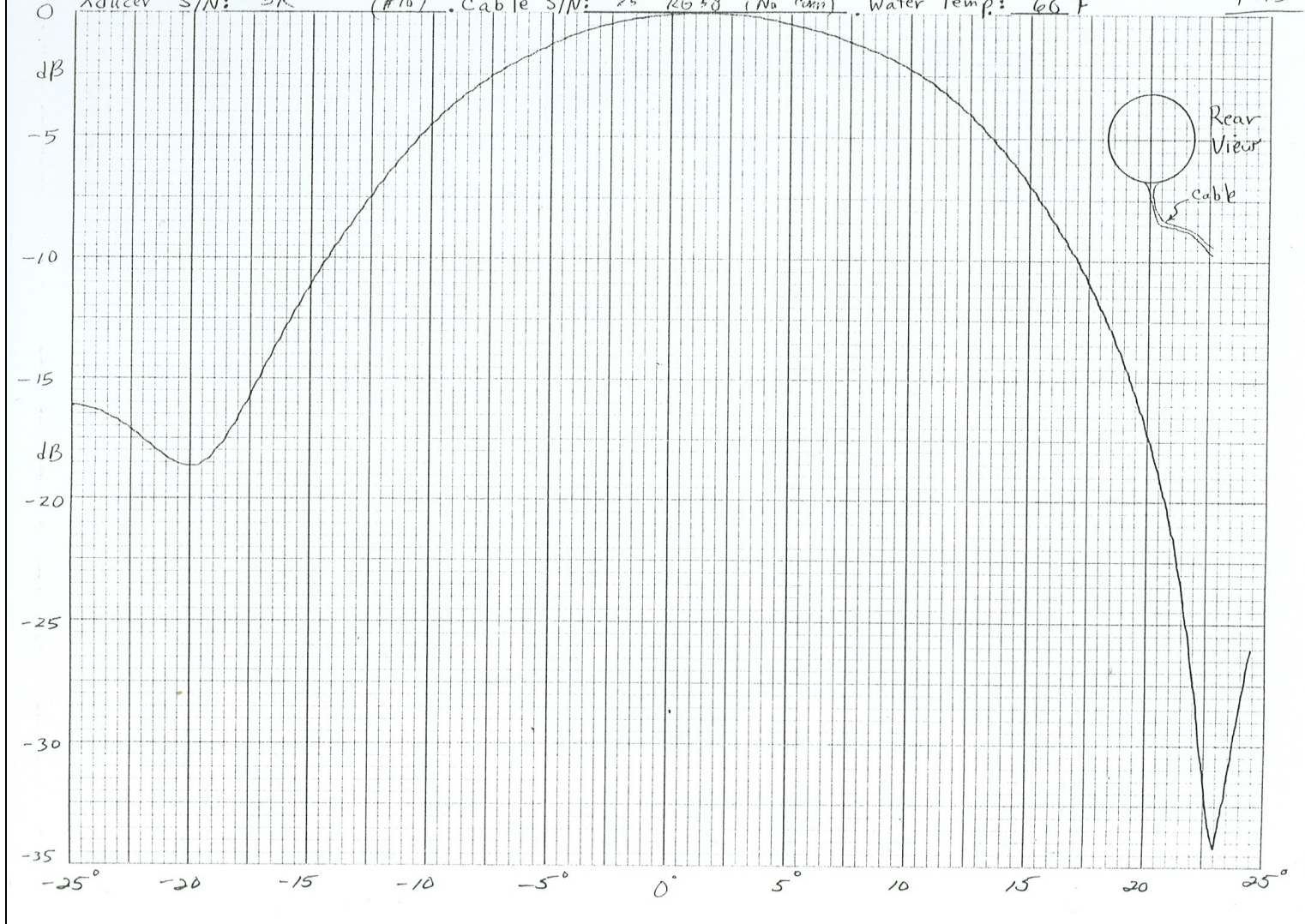
72

GRAPHIC CONTROLS CORPORATION  
BUFFALO, NEW YORK  
4201107 U.S.

no. XY 1001 SP 3

Freq.: 235 kHz. Separation: 3.416 m. Rec. Sen. \_\_\_\_\_ dBV/uPa. Xmit Sen. \_\_\_\_\_ dB.uPa/V @ 1 meter  
Xducer S/N: 3R (#101). Cable S/N: 25' RG 58 (No rms). Water Temp: 66 °F

5/20/96  
PAS



73

Appendix B1.-Page 12 of 18.

GRAINGER CONTROLS CORPORATION  
BUFFALO, NEW YORK  
CORPORATED IN U.S.A.

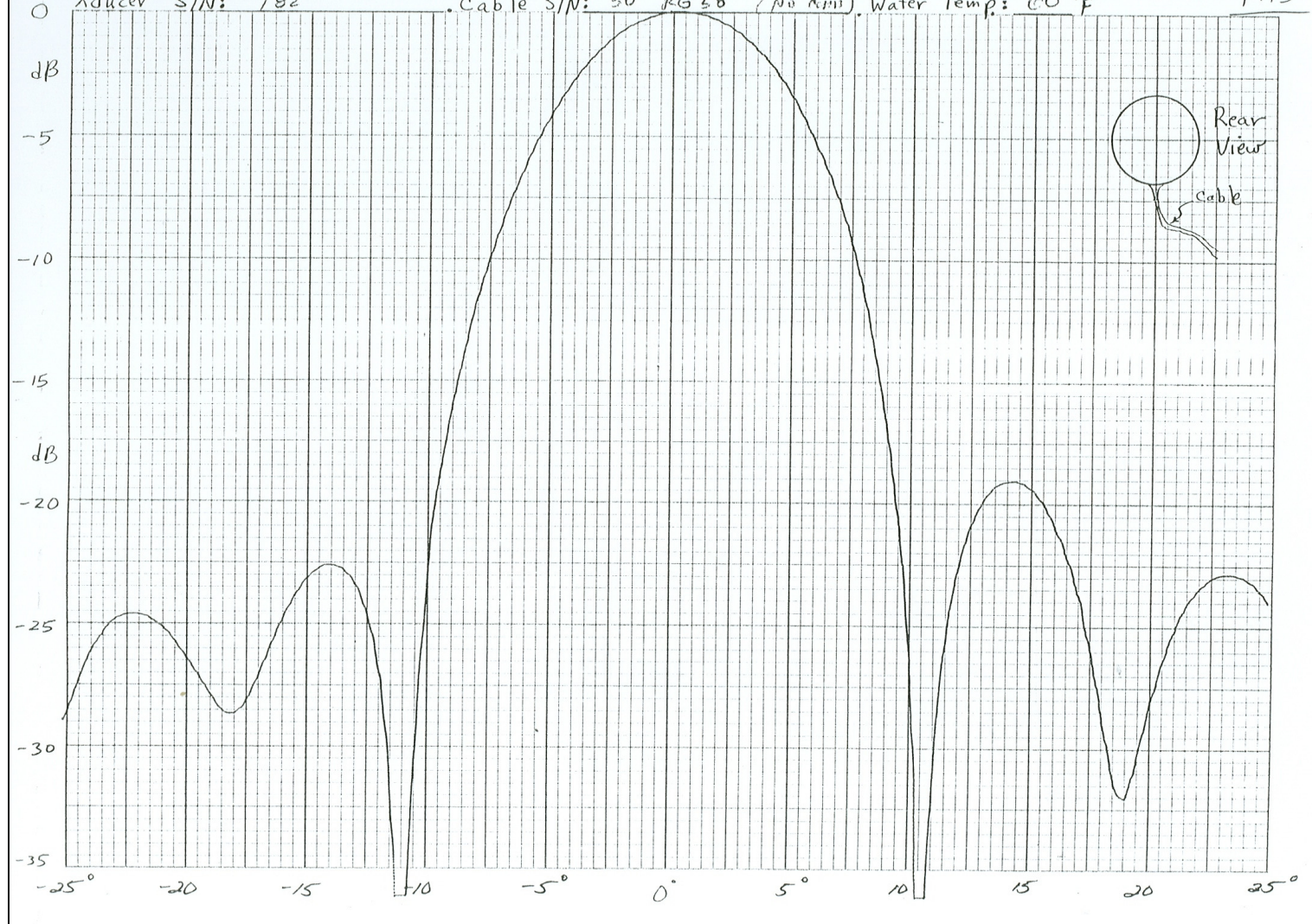
NO. XY 1001-SP 3

5/21/9

Freq.: 235 kHz. Separation: 3.416 m. Rec. Sen. \_\_\_\_\_ dBV/uPa. Xmit Sen. \_\_\_\_\_ dB.uPa/V@1 meter

Xducer S/N: 182. Cable S/N: 30' RG 58 (No Am). Water Temp: 60 °F

PAS



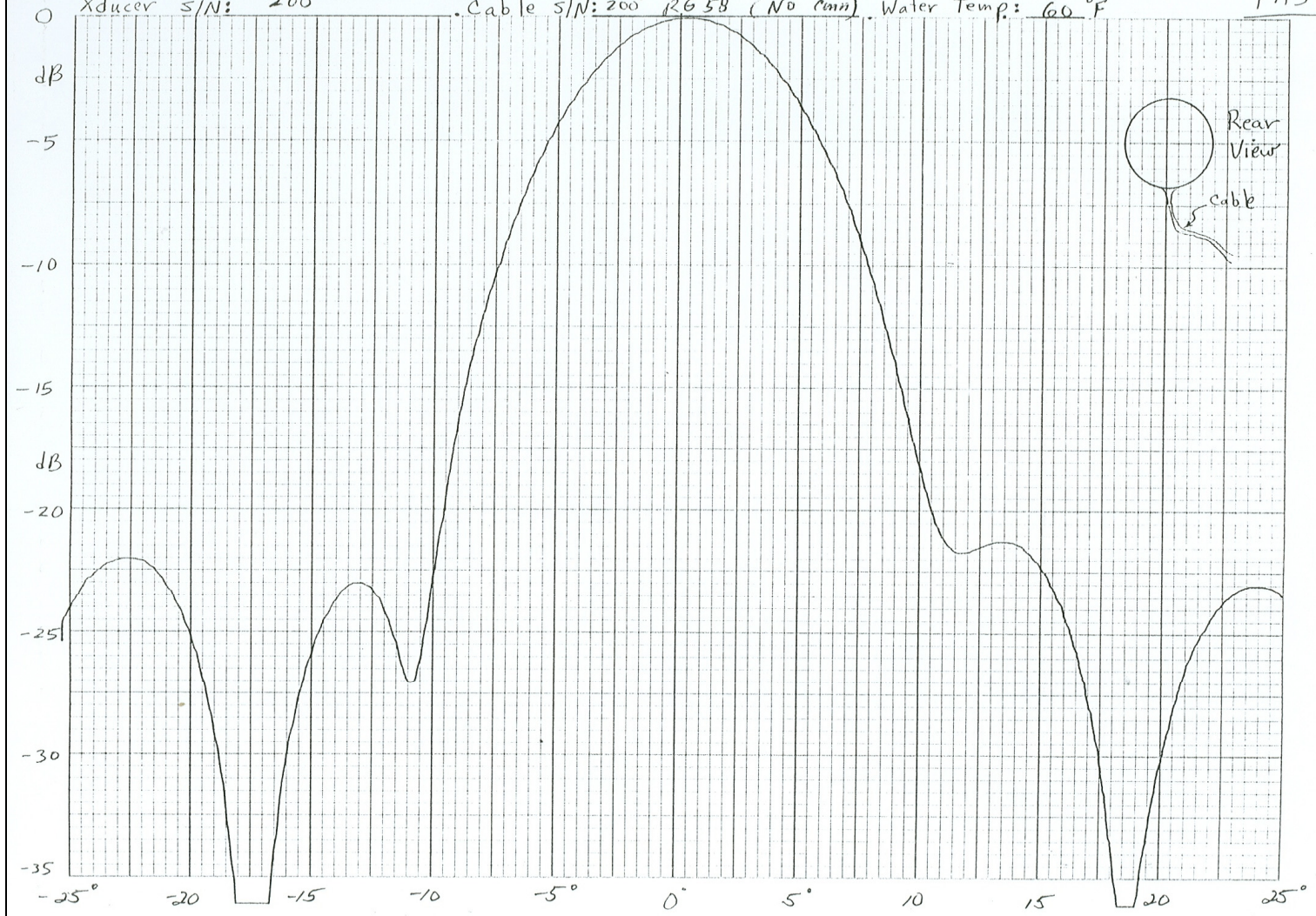
GEORGE CONNORS CORPORATION  
BUFFALO, NEW YORK

NO. XY 1001 - SP 3

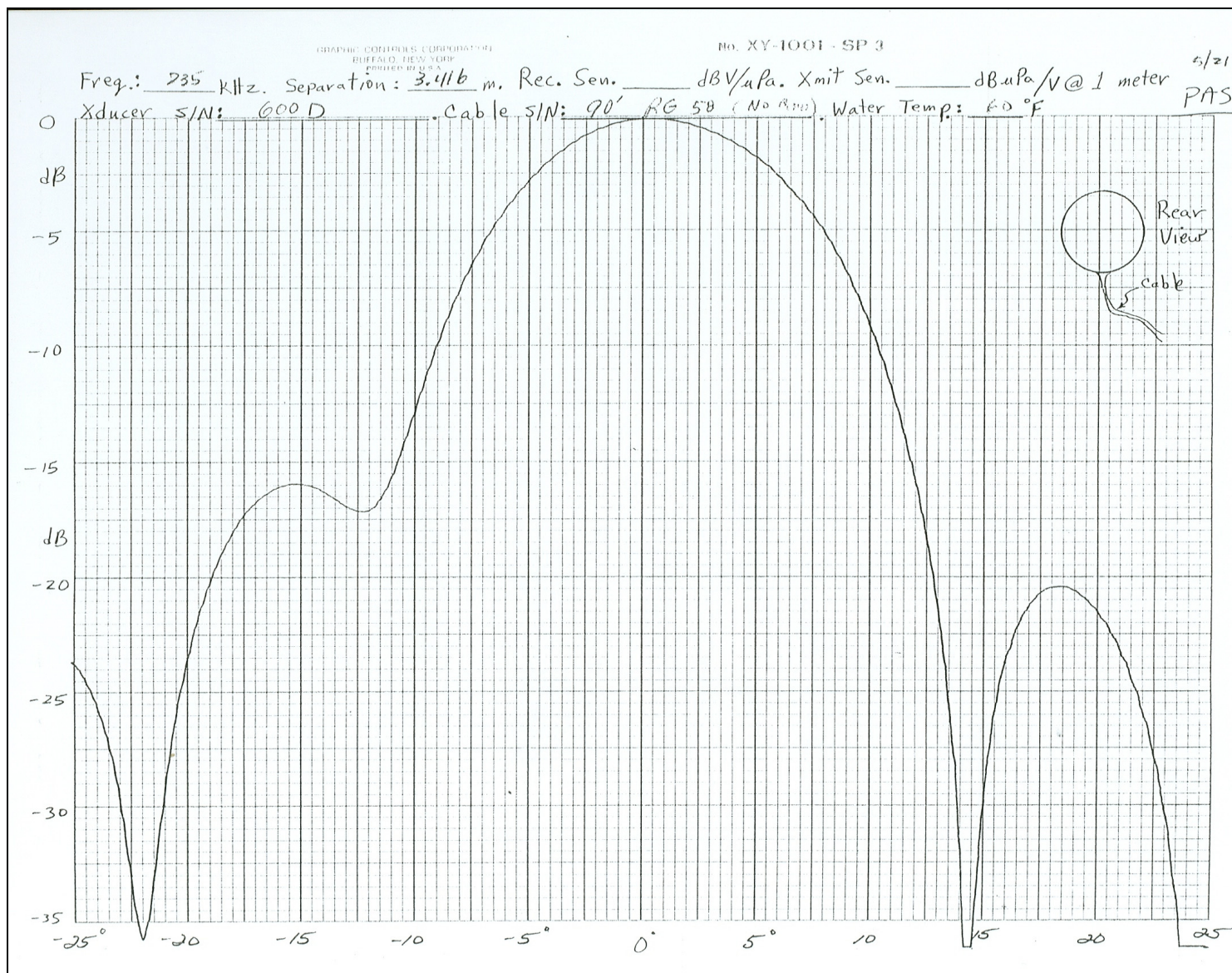
Freq.: 235 kHz. Separation: 3.416 m. Rec. Sen. \_\_\_\_\_ dBV/μPa. Xmit Sen. \_\_\_\_\_ dB.μPa/V @ 1 meter  
Xducer S/N: 200 . Cable S/N: 200' RG 58 (No Conn). Water Temp: 60 °F

5/21/9

PAS

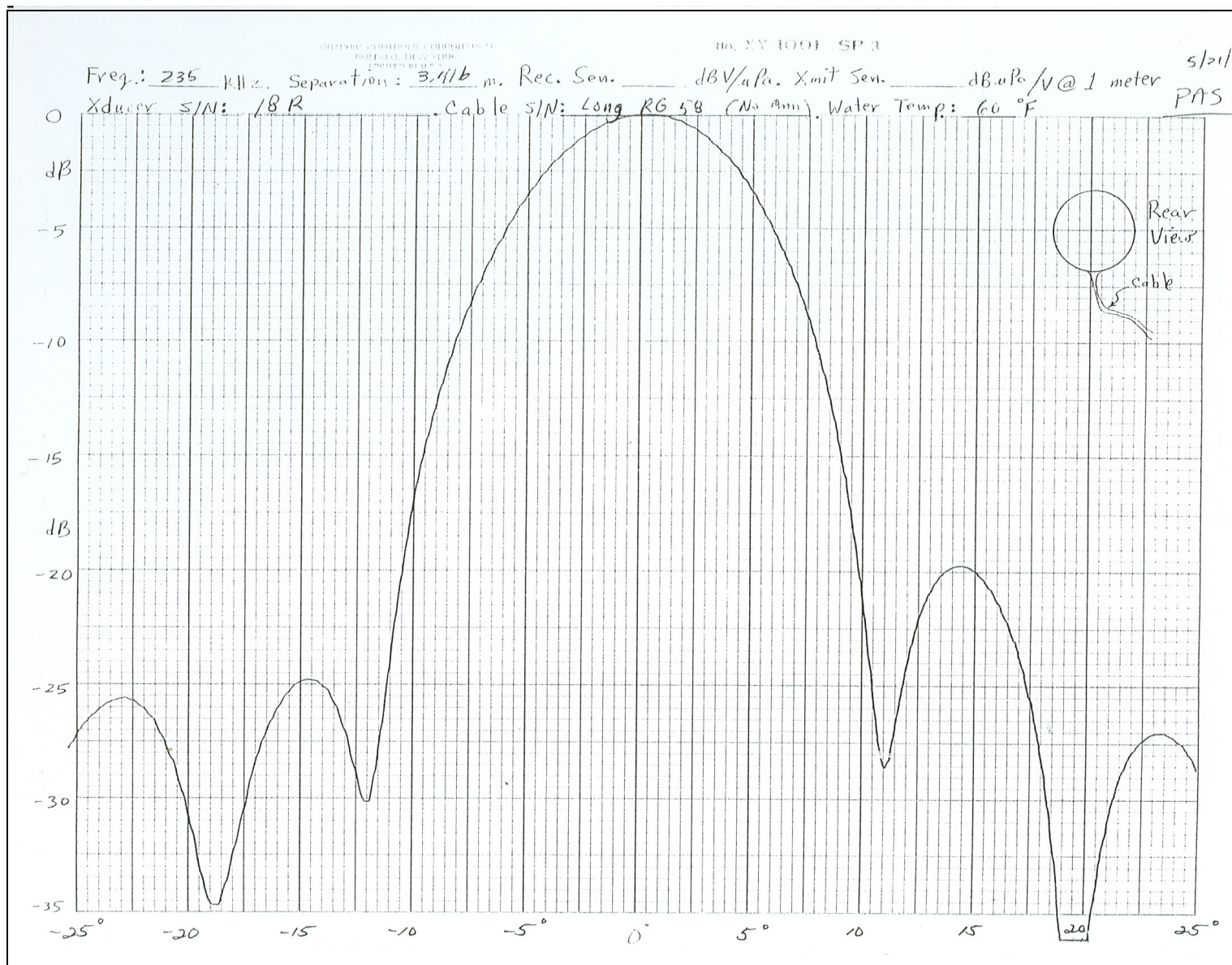


75



Appendix B1.-Page 15 of 18.

77

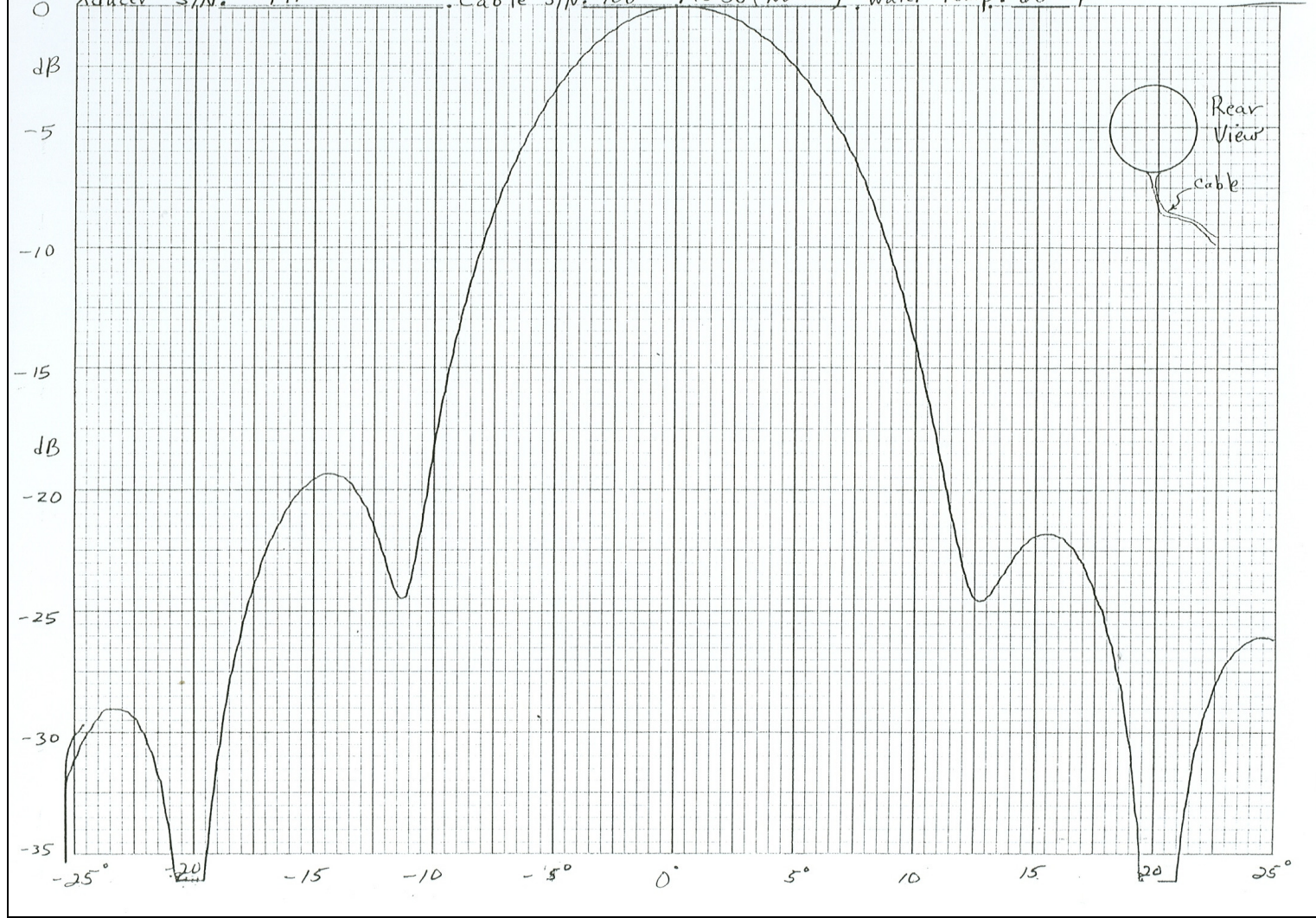


GRAPHIC CONTROLS CORPORATION  
BUFFALO, NEW YORK  
PRINTED IN U.S.A.

No. XY-1001-SP 3

Freq.: 235 KHz. Separation: 3.416 m. Rec. Sen. \_\_\_\_\_ dBV/uPa. Xmit Sen. \_\_\_\_\_ dBuPa/V @ 1 meter  
Xducer S/N: 171. Cable S/N: 100' RG 58 (No conn) Water Temp: 60 °F

5/21/96  
PAS



78

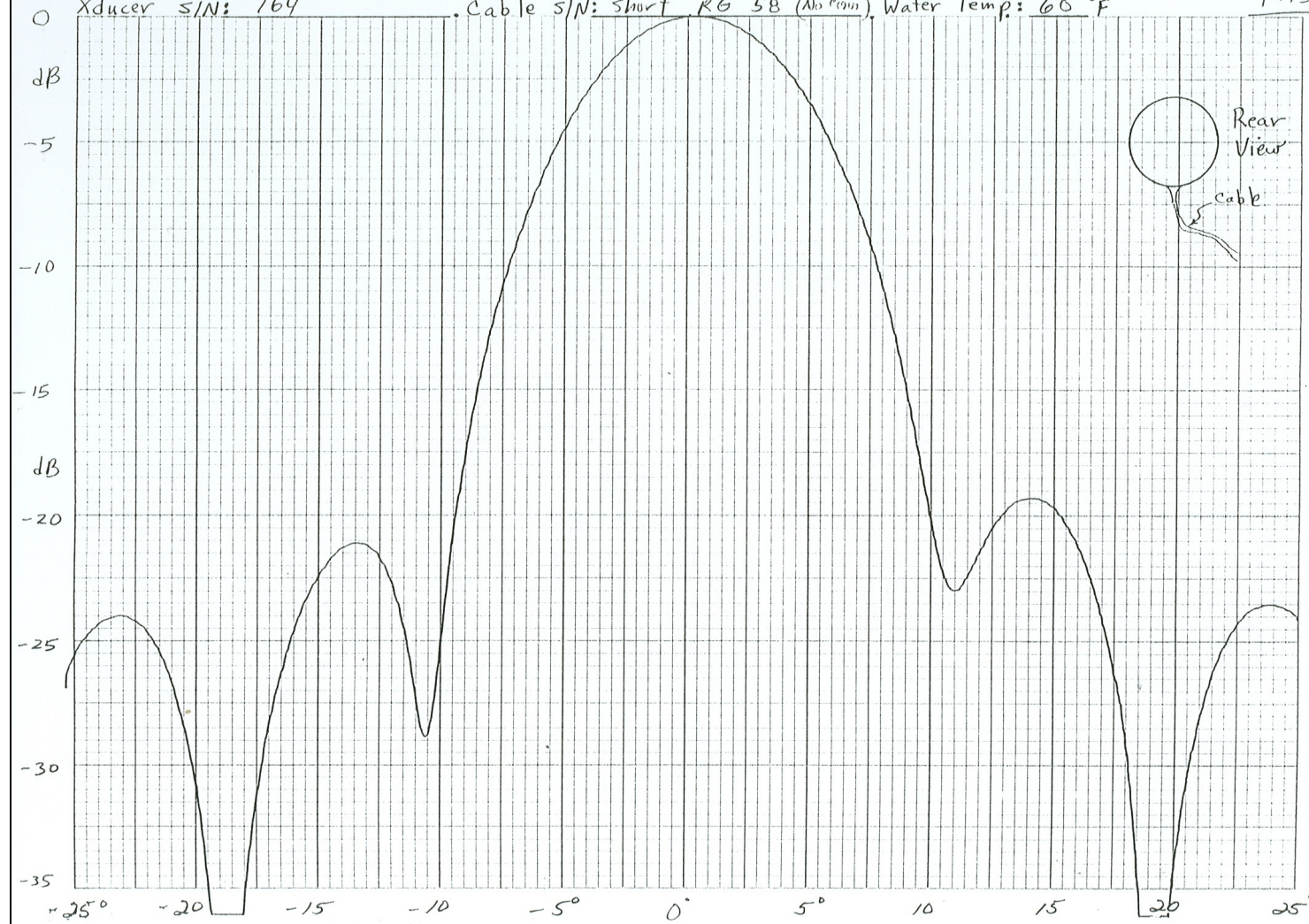
GRAPHIC EQUALIZER  
SHEFFIELD BRIDGE WORKS  
PROFESSOR BRIDGE ST.

No. XY-1001 SP 3

5/21/9

Freq.: 235 kHz. Separation: 3.41 m. Rec. Sen. \_\_\_\_\_ dBV/uPa. Xmit Sen. \_\_\_\_\_ dB.uPa/V @ 1 meter  
Xducer S/N: 164. Cable S/N: short RG 58 (No. 000). Water Temp: 60 °F

PAS



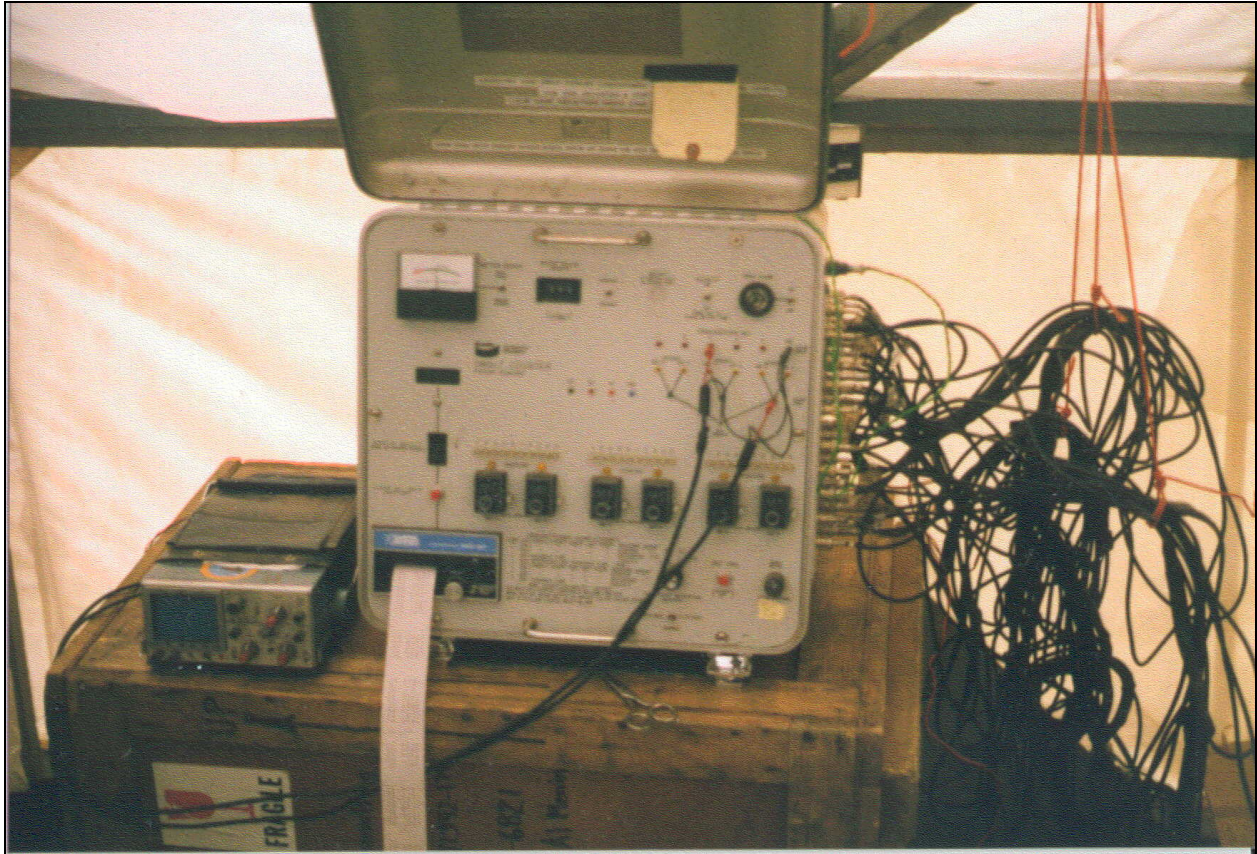
79



## **APPENDIX C**

Appendix C1.–A functional description of the Bendix smolt counter.

---



Prepared by: Edward O. Belcher, Principal Engineer  
Applied Physics Laboratory, University of Washington  
1013 NE 40<sup>th</sup> Street, Seattle WA 98105

Prepared for: Suzanne Maxwell, Sonar Project Coordinator  
Alaska Department of Fish and Game,  
Commercial Fisheries Division  
43961 Kalifornsky Beach Road, Suite B  
Soldotna, AK 99669

---

-continued-

# Bendix Corporation Smolt Counter

## Functional Description

### Table of Contents

1	INTRODUCTION .....	25
2	ARRAYS .....	25
3	TRANSMIT .....	25
3.1	Source level and pulse length .....	25
3.2	Yellow lights .....	25
4	RECEIVE.....	25
4.1	Red lights.....	25
4.2	Receivers .....	25
4.3	Time Varying Gain (TVG) amplifier .....	25
4.4	Constant gain amplifier .....	25
4.5	Bandpass filter .....	25
4.6	Full-wave rectifier .....	25
4.7	Noise threshold.....	25
4.8	Multiplier.....	25
4.9	Integrator .....	25
4.10	Counter .....	25
4.11	Echo Integration .....	25
4.11.1	Maximum Possible Count.....	25
5	CALIBRATION.....	25
5.1	How the smolt simulator relates to TS of a counted fish.....	25
5.2	System Gain Analysis.....	25
6	INITIAL VALIDATION .....	25
7	CURRENT VALIDATION .....	25
7.1	Lab Measurements.....	25
7.2	In-water Measurements .....	25

---

-continued-

## **Introduction**

The Alaska Department of Fish and Game currently uses Bendix 3-Array Smolt Counters on 3 rivers, the Kvichak, Ugashik, and Egegik. The counters estimate the migration of smolt down river and into Bristol Bay. The migrations occur in the May-June timeframe each year. This report provides a functional description of the signal levels and the signal processing that generate the count estimates. The information discussed herein was determined by an interview on May 25, 2000 with Al Menin, the designer of the systems and analysis of the schematics and signal processing. This report is not intended to be an operator's manual, which exists elsewhere.

## **Arrays**

The smolt counter uses 3 arrays of 10 transducers. Figure 1 is a drawing of an array. Table 1 gives exact transducer center-to-center measurements for the Kvichak array. The arrays are placed in the river such that the array lengths are cross-river. The arrays are designated "Inshore", "Middle" or "Center", and "Offshore" with the inshore array closest to the side of the river with the instrumentation tent. In 1999, the distances the arrays were from shore were 48 m, 68 m, and 80 m. These distances vary each year and are recorded as part of the data collection process. The circular-faced transducers look upward, operate at 235 kHz, and are mounted with centers of faces 30 cm apart. The far field begins approximately 20 cm from the transducer face. The Kvichak River transducers were calibrated at the Applied Physics Laboratory, University of Washington in February 2000. The summary of the calibration is shown in Figure 2. These transducers had a nominal 9-degree beamwidth with worst-case sidelobes down a minimum of 17 dB. The average transmit sensitivity was 171.4 dB $\mu$ Pa/V-1m (dB micro-Pascal relative to 1 volt rms referenced 1 m from the source). The average receive sensitivity was -197.7 dBv/ $\mu$ Pa (dB volts rms relative to one micro-Pascal at the face of the transducer).

## **Transmit**

The smolt counter transmits out of 5 transducers simultaneously then pauses to receive the echoes. The pause is on the order of 4 ms to get echoes out to 3 m (the depth of the river). The transmit-listen cycle occurs 6 times as each of the 6 half-arrays is activated. The near-half array of 5 transducers is activated followed by the far-half array. A complete ping cycle occurs when all 6 half-arrays are activated. The ping-cycle rate is controlled by the operator and varies with the velocity of the river in a way to not duplicate counting smolts as they pass with the current. The ping rate is directly proportional with river flow. Al Menin uses information that smolts travel 1.12 ft/s (0.34 m/s) faster than the current.

## *Example Calculation*

The cross-section diameter of the 9°-main-lobe, 3-m from the transducer is approximately 47 cm or 1.55 ft. Smolts need to travel this distance between pings. An equation that calculates an array ping rate (pr) as a function of river velocity (v) including Al's 1.12 ft/s assumption is:

$$pr = (v + 0.34)/(0.47 * h/3) \text{ pings/s}$$

---

-continued-

where:

$v$  = river velocity in m/s; and

$h$  = height of cross-beam measurement (m).

If  $h = 3$  meters and  $v = 1.5$  m/s (5 ft/s) then  $pr = 3.9$  pings/s.

### **Source level and pulse length**

In spring 2000, Al Menin measured the transmit voltage when transducers were connected to the smolt counter. The transmit signal was a square wave at 40 volts p-p (peak-to-peak). This information along with the transmit sensitivity of the transducers allows us to calculate the source level of the smolt counter. The source level (SL) is:

$$SL = 20 \log(V_{p-p}/2.8) + \text{Transmit Sensitivity} =$$

$$20 \log(40/2.8) + 171.4 = 194.5 \text{ dB } \mu\text{Pa-1 m.}$$

The pulse length is 136  $\mu\text{s}$  or 32 cycles at 235 kHz. The theoretical bandwidth of a sinusoidal pulse is approximately the reciprocal of the pulse length or 7.25 kHz. The natural bandwidth of the transducer is the only filtering of the square wave transmit signal.

### **Yellow lights**

The panel of the smolt counter has 6 yellow lights. Each light blinks when its associated half-array transmits.

### **Receive**

Figures 3a and 3b show a block diagram and graphical representation of the signal flow.

### **Red lights**

The panel of the smolt counter has 30 red lights. Each light blinks when the associated transducer receives a signal that exceeds a set threshold. This threshold is approximately 1 dB lower than the count threshold, so a blinking red light does not necessarily indicate a count. These lights were designed to blink when the max range gets close to the river surface and surface returns exceed the red light threshold. The operators are requested to reduce the max range approximately 2 cm less than the range that starts the red light blinking.

### **Receivers**

Immediately after the red-light logic, the receive signals from half-arrays are tied together as they were for transmit. Counts are calculated from the sum-beams of the half arrays. There are 6 receivers, each responsible for one half-array. The following components of the receiver electronics are instrumental in the signal processing:

---

continued-

### **Time Varying Gain (TVG) amplifier**

The TVG has a linear gain between the operator-set min and max ranges. It is designed to compensate for transmission loss from targets within that range. For single targets, the transmission loss is  $40 \log(\text{range})$ . When there is a school of randomly placed fish that extends over the beam cross-section, the appropriate transmission loss is  $20 \log(\text{range})$  because as range increases, more fish are within the beam and that partially offsets the spreading loss. Echo Integration uses the  $20 \log(\text{range})$  TVG option on the echo sounders. Al Menin states that the Bendix Smolt Counter uses a  $20 \log(\text{range})$  TVG.

The 2-way loss for a layer or school of targets that extend beyond the main-lobe of the beam is  $20 \log(\text{range})$ . The TVG should increase 9.5 dB over the range from 1 m to 3 m. Figure 4 shows an ideal  $20 \log(\text{range})$  curve with a best-fit linear curve.

### **Constant gain amplifier**

The receiver has a multistage CMOS amplifier with constant gain to give a linear amplification of the very small returns after the TVG stage.

### **Bandpass filter**

The bandpass filter stage should have a bandwidth of approximately one over the pulse length or 7.25 kHz.

### **Full-wave rectifier**

The full-wave rectifier outputs the absolute value of the input – i.e. the negative components of the input are reflected about the time axis to be positive components.

### **Noise threshold**

During test and calibration, a threshold of 0.2 volts is set such that any rectified value of less than 0.2 volts is not passed forward. This acts as a squelch circuit to zero out any components less than 0.2 volts. Signals less than 0.2 volts are considered noise and are not integrated in the next stage. A squelch threshold is needed or the circuit would continually integrate system noise and give erroneous counts.

### **Multiplier**

After rectification, the signal is multiplied by itself to get a squared output. This is the input to the integrator. The settings of the dead-time pot and the end-range pot enable the multiplier. Received signals after the dead-range (typically 1-m) and before the end-range pass through the enabled multiplier. The multiplier zeros out signals outside of these ranges.

### **Integrator**

This system uses a dual-slope integrator. According to Horowitz and Hill (1989), it is an elegant and popular technique that remains accurate with less demand on exact component values than allowed in other integrator techniques. A current proportional to the integrator input level charges a capacitor for the fixed time associated with the minimum and maximum range of

---

-continued-

interest. The capacitor is discharged at a constant current until the voltage reaches zero. The capacitor accumulates the current proportional to the input level and thus provides an analog integration of the input. During the positive value of the integrator output, a pulse generator is enabled and drives a count proportional to the integrated value. The duration of the pulse train is proportional to the accumulated current and thus is proportional to the integral of the input. The pulse rate was set to 72.8 Hz with the intention that each count represents 5 smolts of average weight of 8.3 grams.

### **Counter**

The number of pulses is accumulated and printed out on paper at an operator-set interval. Separate counts are available for the inshore, center, and offshore arrays. Starting in 2000, a computer interface is available on the counters. The interface allows a PC running Windows 95, 98, or NT to retrieve count data from each array with one-second resolution, display it, and store it on disk.

### **Echo Integration**

The smolt counter performs an analog version of echo integration. Echo integration integrates the mean-squared echo voltage over a range of interest. The integrated value is proportional to fish biomass. Figure 5 shows simulated returns of 10, 100 and 400 smolt echoes from a single transmit pulse detected by one sum-beam. The smolts are uniformly distributed over a range from 1 to 3 meters from the transducer. The phase of each echo is a function of its round-trip distance from the smolt that caused the echo. In this simulation, when only 10 echoes were present, 2 pairs were overlapped. The 100 and 400 echoes were essentially all overlaps.

The returns are amplified, squared and integrated. Figure 6 shows the integrated value of the echoes as a function of the number of echoes in the range segment from 1 m to 3 m. Note that the integration value is linear with respect to the number of echoes. The figure shows 10 independent sets of returns and the average. The integrated value is an unbiased estimate.

### **Maximum Possible Count**

The counters have a maximum count rate. This occurs when there are sufficient echoes to keep the capacitor continuously charged above zero volts over a number of ping cycles. When this occurs the pulse train is continuously on, giving a count of  $72.8 * 5 = 364$  smolts/s/3 m for each array. Note the “3 m” is necessary because the count is over a finite river width of 3 m. The “Bristol Bay Sockeye Salmon Smolt Studies for 1998,” page 97, gives the average placement (in feet) of the arrays from shore from 1989 to 1997 in the Kvichak River. They are 0 (Right Bank shore), 34 (Inshore Limit – Dead zone), 166 (Inshore Array), 235 (Center Array), 301 (Offshore Array), 395 (Offshore Limit Dead Zone), and 427 (Left Bank Shore). Assume all 3 arrays are providing a maximum count. Since the array locations and river width are given in feet, we will interpolate in feet. The 3-m array width is approximate 10 feet. The maximum count *per foot* is  $364/10$  or 36.4 smolt/s/ft. The interpolation is  $((166-34)/2 + (301-166) + (395 - 301)/2) * 36.4$  smolts/s/ft = 9027 smolts/s/river-width = 32.5 million smolts/hour/river-width. In the spring of 2000, the maximum smolt passage on the Kvichak River in a whole day was 23 million smolts.

---

-continued-

### Calibration

The systems are considered calibrated when (1) the pot R22 on page 6 of 8 of the counter schematics is adjusted to provide 0.2 volts DC on pin 2 and (2) gains are adjusted at several places in the counter such that the counter reports 26 counts per transmission when connected to the smolt simulator (page 8 of 8 of the schematics). The smolt simulator outputs a 235 kHz burst square wave 4.62 mv p-p and 136.17 μsec long. The burst occurs 2.04 ms after the transmit pulse. That delay is equivalent to a return from a target approximately 1.5 m above the transducer face. The calibration count is designed to be obtained when the counter settings are set to (a) Dead depth of 1 m, (b) Max depth 1.8 m, and River velocity of 0.999.

The same count of 26 should occur when the simulator is connected to any of the thirty input channels. Normally the counter is allowed to accumulate over at least 10 pings and an average is taken to obtain 26 +/- 0.5 counts.

### The history of 26 counts

After the counter was tweaked for the initial validation (Section 6), Al Menin injected smolt simulator pulses into each channel. The counter counted 26 counts per pulse. That number became the standard for future calibrations.

### How the smolt simulator relates to TS of a counted fish.

As stated above, the smolt simulator injects a single pulse after a fixed delay from the transmit pulse. The single pulse is large enough to give a count of  $26 \times 5 = 130$  smolts. The single large pulse would occur in the field if the smolts were all exactly the same range from the transducer and their echoes added coherently. Figure 7 is an example of 10 pulses added coherently. The linear relationship between echoes and counts occur when the echoes have random arrivals and add incoherently. If the counter is adjusted to give the proper count for incoherent addition, it will give the counts shown in Figure 8 when echoes arrive at the same time and add coherently.

For coherent addition, the counter gives the square of the number of pulses. Thus a single echo with amplitude 10 times the amplitude of a single smolt echo will cause a count of 100. The injected pulse of the smolt simulator must be  $(130)^{1/2} = 11.4$  times the size of a unit smolt echo to give the desired count of  $26 \times 5 = 130$  smolts.

The injected signal amplitude is  $4.62 \times 10^{-3}$  v p-p. Then the calibrated unit smolt echo must be 11.4 times smaller or  $4.05 \times 10^{-4}$  volts p-p. In volts rms dB that would be  $20 \log((4.05 \times 10^{-4})/2.8) \text{ dBv} = -76.8 \text{ dBv}$ . (We are using  $1.2 \times 10^{-4}$  for the scientific notation  $1.2 \times 10^{-4}$ ).

The receive transducer sensitivity,

$$Sr = -198 \text{ dBv}/1\mu\text{Pa}.$$

Then the Echo Level,

$$EL = V_{\text{input}} \text{ dBv} - Sr = -76.8 + 198 = 121 \text{ dB}\mu\text{Pa}.$$

The echo Target Strength,

$$TS = EL - SL + 2 \times TL + TVGE = 121 - 194 + 3.5 + 3.5 = -66 \text{ dB}.$$

---

-continued-

Where:

Source Level SL = 194 dB $\mu$ Pa;

2\*TL = 20 log(1.5)= 3.5 dB; and

TVGE = TVG error for single point target (difference between 20logR and 40logR when R = 1.5 m.

When the counter is calibrated to count 26 counts when connected to the smolt simulator, the counter is adjusted to count smolts with a unit Target Strength estimated to be -66 dB.

### **System Gain Analysis**

If the counter is sensitivity enough to integrate a unit smolt echo, then an input of 4.04e-4 volts p-p when amplified should exceed the 0.2 volts threshold before the multiplier. The system gain would be a little more than 0.2 volts /2.02e-4 volts or 1000 (60 dB). Note the input p-p voltage was converted to zero-peak since the 0.2 volts is after rectification.

The fact that the counter does not count individual smolts but groups of 5 smolts may indicate that a single smolt will not exceed the threshold. This must be tested.

### **Initial Validation**

Al designed the counter based on reports that estimated the number of smolts in a migration, the average size of the smolts, and the period of the migration. This gave him the parameters needed for counter sensitivity, counts as a function of target strength, and the rate it must be able to count and not be overwhelmed.

The validation of the smolt counter occurred by having a fyke net downstream from one of the arrays. When the counter counted 1000 smolts, the fyke net was raised and the fish were counted. This was done 25 times. According to Al Menin, the machine and hand counts correlated well, generally with the counts being within 10% of each other.

### **Current Validation**

#### **Lab Measurements**

The Appendix A indicates measurements that should be made on a counter just after Al Menin calibrates the system.

- Ping rate Vs panel indicator.
- Ratio of inputs in dB to activate the red light / activate the count.
- TVG change in gain as a function of time after transmit.
- Gain of system from input BNC to 0.2 volt threshold point.
- System bandwidth with signal injected at input BNC and measured at input to rectifier.

---

-continued-

- System noise threshold (noise level at 0.2-volt threshold point). Transducers should be attached for this measurement to properly load the inputs.

### **In-water Measurements**

A straightforward way to obtain counter characteristics would be through a set of in-water tests in a benign environment (test tank or lake). Obtain a set of calibrated targets with target strengths as small as a *unit Target Strength* and larger. Before any of the below tests are run, the counter must be calibrated as it is before each season. Remember that a single target N times 6 dB larger than a unit Target Strength will be counted as  $2^{2N}$  smolts. Also remember that single targets will have an acoustic transmission loss of  $40 \log(\text{range})$  and a cloud of targets that extend beyond the cross-section of the sum-beam will have a transmission loss of  $20 \log(\text{range})$ . The TVG of the counter is fixed so it cannot compensate for both cases and you will need to factor in the adjustment in your calculations.

#### *Test 1 Basic sensitivity*

Place a single target with target strength of a unit smolt at different ranges above a transducer. Change the height of the target above the counter from 1 m to 3 m in steps such as 0.5 m and note counter response at each height. Since a count represents 5 smolts, it is likely that 5 or more targets the size of a unit smolt will need to be in the sum-beam between the set min and max ranges, to get a count per transmission.

#### *Test 2 Count as function of TS*

Place targets and distributions of targets with multi-smolt-size target strengths above the sum-beam. Also note how the count may change with different placements of the distribution over the sum-beam

#### *Cross-check counting in the river*

Place video cameras such that bottom and side views of fish can be seen as they pass over the transducer array. Note the correlation between machine counts and visual counts for some visually countable distributions. The video will need to be recorded and time-stamped to be compared with counter data stored on computer. You may also get information on possible missed or duplicated counts due to river flow and ping rate.

---

-continued-

### **Literature Cited**

Crawford, D.L., and B.A. Cross. 1999. Bristol Bay sockeye salmon smolt studies for 1998. Alaska Department of Fish and Game, Division of Commercial Fisheries Management and Development, Regional Information Report 2A99-10, Anchorage.

Horowitz, P. and W. Hill. 1989. The Art of Electronics. Cambridge University Press. Cambridge, UK. 1101 pp.